Nodal antagonists regulate migration of the visceral endoderm along the future anteroposterior axis of the mouse embryo

Masamichi Yamamoto[1], Yukio Saijoh[1], Aitana Perea-Gomez[2,4], Richard R. Behringer[3], Siew-Lan Ang[2,5], Hiroshi Hamada[1] & Chikara Meno[1]

[1]Developmental Genetics Group, Graduate School of Frontier Biosciences, Osaka University, and CREST, Japan Science and Technology Corporation (JST), 1-3 Yamada-oka, Suita, Osaka 565-0871, Japan

[2] IGBMC/CNRS/INSERM, Université Louis Pasteur, 67404 Illkirch Cedex, CU de Strasbourg, France

[3]Department of Molecular Genetics, M.D. Anderson Cancer Center, University of Texas, Houston, Texas 77030, USA

[4]Present address:Institut Jacques Monod, CNRS, Universites Paris 6 et 7, 75251 Paris Cedex 05, France

[5]Division of Developmental Neurobiology, National Institute for Medical Research, The

Ridgeway, Mill Hill, London NW7 1AA, United Kingdom.

Summary

Patterning of the mouse embryo along the anteroposterior (A-P) axis during development requires migration of the distal visceral endoderm (DVE) toward the future anterior side by a mechanism that has remained unknown. Here we show that the signaling molecule Nodal and its antagonists Lefty1 and Cerl are required for migration of the DVE. Whereas Nodal signaling provides the driving force for DVE migration by stimulating the proliferation of visceral endoderm cells, Lefty1 and Cerl determine the direction of migration by asymmetrically inhibiting Nodal activity on the future anterior side.

Establishment of the anteroposterior (A-P) axis is the first overt manifestation of the body plan in the mouse.[1,2] The first morphological sign of A-P patterning is the formation of the primitive streak on the posterior side of the embryo at embryonic day (E) 6.5. At the cellular and molecular levels, however, the patterning events begin much earlier. One day before gastrulation (E5.5), the proximodistal (P-D) axis is established; at this time, the embryo appears radially symmetric, with a group of visceral endoderm (VE) cells that express the homeobox gene *Hex* being present exclusively at the distal end[3]. A few hours later, at E5.7, these Hex-positive distal visceral endoderm (DVE) cells begin to migrate toward the future anterior side, eventually forming the anterior visceral endoderm (AVE) at E6.5. The AVE secretes signaling molecules, including the Nodal antagonists Lefty1 [4] and Cerl [5,6], both of which will inhibit Nodal signaling in the underlying epiblast and restrict Nodal activity to the posterior side of the embryo. Such asymmetry in Nodal signaling specifies the anterior epiblast to form the prospective brain and generates the primitive streak on the posterior side. The entire A-P patterning process can thus be divided into three steps: (1) establishment of the P-D axis, (2) conversion of the P-D axis into the A-P axis by the anterior-directed migration of the DVE, and (3) patterning of the epiblast by the AVE.

Although the mechanism by which the AVE patterns the epiblast has been relatively well characterized[7,8], it has remained unknown how DVE migration is achieved and how the direction of DVE migration is determined. It has been proposed[9] that this anisotropic cell movement may involve differential cell growth, the orientation of cell divisions, or a barrier that prevents posteriorward migration, but this important

issue has not been experimentally addressed. We have now examined the mechanistic basis of DVE migration. Our results suggest that Nodal signaling provides the driving force for DVE migration by stimulating cell proliferation in the VE, whereas Lefty1 and Cerl determine the direction of migration by reducing Nodal activity on the future anterior side.

Expression of Nodal antagonists before DVE migration

We have previously shown that DVE migration does not occur in the most severe phenotype (type B) of embryos that lack the FoxH1 transcription factor[10]. Examination of various types of *FoxH1* mutant embryos for *Hex* and *Nodal* expression revealed an apparent correlation between the level of FoxH1-mediated Nodal signaling in the VE and timing of the onset of DVE migration (Supplementary Figs. S1, S2). This observation suggested that Nodal signaling might promote DVE migration and that asymmetry in Nodal activity may determine the direction of such migration. However, *Nodal* expression is symmetric along the prospective A-P axis at E5.5 and E5.7 [11], the latter being the time when the DVE begins to migrate. We therefore examined in detail the expression domains of the genes for the Nodal antagonists Lefty1 and Cerl at the stages before and after DVE migration (between E5.0 and E6.5).

Expression of *Lefty1* and *Cerl* was not detected at E5.0. The expression of these genes was first apparent at E5.5 in the DVE. Unexpectedly, their expression domains were already shifted toward one side of the embryo before the onset of DVE migration (Fig. 1a, d). From E6.0 to E6.5 (Fig. 1b, c, e, f), the expression domains of *Lefty1* and *Cerl* moved toward the anterior side. These observations suggested that the

expression domains of *Lefty1* and *Cerl* at E5.5 are biased toward the prospective anterior side. This conclusion was confirmed by two-color in situ hybridization. Both *Lefty1* (Fig. 1g) and *Cerl* (Fig. 1i) expression domains at E5.5 were shifted toward the future anterior side of embryos ($n = 8$), whereas the *Hex* expression domain (Fig. 1h, j) was apparent at the distal tip of the same embryos. Such asymmetric expression of *Lefty1* and *Cerl* might thus be expected to generate differential Nodal activity in the DVE along the A-P axis, with lower Nodal activity on the future anterior side.

Asymmetric Nodal inhibition directs DVE migration

To determine whether an asymmetry in Nodal signaling generated by the Nodal antagonists directs DVE migration, we examined the effects of ectopic expression of *Nodal*, *Lefty1*, or *Cerl*, each together with the gene for green fluorescent protein (GFP), in the VE of E5.2 embryos. The DVE was labeled with the dye DiI [3] to trace its migration. Embryos were cultured for 24 h and the positions of GFP-positive and DiI-positive cells were then mapped (Fig. 2a–c). If the test gene did not influence the direction of DVE migration, GFP-positive cells and DiI-positive cells would be expected to be found on random sides of the embryo; the probability of both types of cells being located on the same side would be 25%. In contrast, if the Nodal antagonists were able to direct DVE migration, GFP-positive cells and DiI-positive cells would be located on the same side of the embryo with a frequency of >25%.

Expression of GFP alone did not influence the direction of DVE movement; DiI-labeled cells were thus randomly situated relative to the position of GFP-positive cells, with a colocalization frequency of 26 % ($n = 71$) (Fig. 2d). Ectopic expression of

Lefty1 resulted in the colocalization of GFP-positive cells and DiI-positive cells on the same side in 54% of embryos ($n = 35$; $p < 0.005$ versus GFP alone, chi-square test). Ectopic expression of *Cerl* had a similar effect on DVE migration, with 46% of embryos ($n = 57$, $p < 0.03$) showing same-sided localization of the two types of cells. In embryos ectopically expressing both *Lefty1* and *Cerl*, the DVE migrated toward the side containing the GFP-positive cells in 88% of embryos examined ($n = 57$, $p < 0.0001$).

To determine whether DVE migration depends on the absolute level of, or on a regional difference in, Nodal signaling, we similarly introduced a *Nodal* expression vector into wild-type embryos. DiI and GFP signals were located on the same side in only 4% of such embryos ($n = 85$, $p < 0.0001$) (Fig. 2d), indicating that the DVE migrated away from the side with a higher Nodal activity. The DVE fails to migrate in $FoxH1^{-/-}$ embryos containing one wild-type *Nodal* allele and a *Nodal-lacZ* allele.[10] In such $FoxH1^{-/-}$, $Nodal^{lacZ/+}$ mutant embryos, *Nodal* expression is lost in the VE and distal epiblast and, as in $FoxH1^{-/-}$ type B embryos, that in the proximal epiblast is radially symmetric. If the migration failure in this mutant is due to the loss of *Nodal* expression, restoration of *Nodal* expression would be expected to induce DVE movement. Indeed, whereas DiI-labeled cells remained at the distal tip in 100% of $FoxH1^{-/-}$, $Nodal^{lacZ/+}$ embryos expressing GFP alone ($n = 9$), ectopic expression of *Nodal* repelled the DVE in 100% of such embryos ($n = 4$, $p < 0.0001$ versus those expressing GFP alone) (Fig. 2d).

Nodal antagonists inhibit VE cell proliferation

To determine whether differential cell proliferation contributes to the mechanism of DVE migration, we examined the proliferation of VE cells by labeling embryos with

bromodeoxyuridine (BrdU) at pre- or early gastrulation stages. In wild-type embryos, cell proliferation in the VE was uniform at E5.5 (Fig. 3a). At E5.7, however, when the DVE begins to migrate, cell proliferation was inhibited in the region corresponding to the *Lefty1* and *Cerl* expression domains (Fig. 3b). Inhibition of cell proliferation in the future AVE was manifest at E6.0 (Fig. 3c), and the asymmetry in cell proliferation rate along the A-P axis was maintained in the VE until E6.5 (Fig. 3d, e). This pattern of cell proliferation was reminiscent of the temporal changes in Nodal signaling. To investigate the possible relation between Nodal signaling and cell proliferation, we examined the pattern of BrdU incorporation at E6.5 in various mutants deficient in such signaling. In $Nodal^{lacZ/lacZ}$ embryos[12] ($n = 5$), cell proliferation was markedly impaired in the VE and epiblast (Fig. 3f). In $FoxH1^{-/-}$ embryos, two types of staining pattern were observed. In the type A mutant ($n = 3$), an asymmetric pattern of BrdU incorporation similar to that apparent in the wild type was detected (Fig. 3g), although the staining level was reduced compared with that in wild-type embryos. In the type B mutant ($n = 4$), which expresses *Nodal* only in the proximal epiblast at this stage (Supplementary Fig. S2; data not shown), uniform staining was apparent in the VE overlying the proximal epiblast whereas staining in the DVE was lost (Fig. 3h). Finally, in $FoxH1^{flox/-}$, *Lefty2-cre* embryos ($n = 4$) lacking FoxH1 specifically in the epiblast [10], the distribution of BrdU incorporation was similar to that apparent in wild-type embryos (Fig. 3i). These results indicate that Nodal signaling promotes cell proliferation in the VE and that the asymmetry in proliferation along the A-P axis is due to differential Nodal signaling.

We next examined the effects of ectopic expression of Nodal or Nodal

antagonists on the proliferation of VE cells. The VE of E5.2 embryos was cotransfected unilaterally with a test gene and a GFP expression vector, and the number of GFP-positive cells was counted 12 and 36 h later. The increase in the number of GFP-positive cells during the 24-h period between these two time points was estimated. In embryos transfected with the GFP vector alone (n = 86), the transfected cells duplicated two or three times in about half of the embryos examined and did so more than three times in the remaining embryos (Fig. 4a–d, i). This variability in the number of cell divisions depends on the specific site of transfection, with transfected VE cells on the future anterior side dividing fewer times (average=2.2 times, n= 13) than those on other sides (right side, average=4.0 times, n= 9; left side, average=3.7 times, n= 8; posterior side, average=4.2 times, n= 7). Ectopic expression of both *Lefty1* and *Cerl* in embryos (n = 71) resulted in inhibition of cell proliferation (Fig. 4e, f, i), with transfected cells rarely duplicating more than four times. Conversely, transfection of embryos with a *Nodal* expression vector (n = 61) stimulated cell proliferation (Fig. 4g–i), as reflected by a marked increase in the percentage of embryos in which cells replicated more than four times. These results thus indicate that Nodal signaling promotes, and that Nodal antagonists inhibit, cell proliferation in the VE.

To determine the extent to which asymmetric cell proliferation contributes to DVE migration, we subjected embryos both to unilateral cotransfection of the VE with a GFP vector and an expression vector for wild-type or a dominant negative form of *Cdk2* [13] as well as to labeling of the DVE with DiI (Fig. 4j). Ectopic expression of wild-type *Cdk2* repelled the DVE in 90% of embryos examined (n = 79, $p < 0.008$ versus embryos

expressing GFP alone) whereas that of the dominant negative form of *Cdk2* attracted the DVE in 45% of embryos ($n = 98$, $p < 0.016$), although expression of the wild-type and mutant forms of Cdk2 was less effective in this regard than was that of Nodal or both Nodal antagonists, respectively. We next examined the effect of ectopic expression of *Cdk2* in *FoxH1*$^{-/-}$, *Nodal*$^{lacZ/+}$ embryos. Whereas expression of GFP alone failed to move the DVE, that of wild-type *Cdk2* repelled the DVE in all of the four embryos examined ($p < 0.0001$). DVE migration induced by Cdk2 in the mutant embryos was incomplete (the migration distance was shorter than that in wild-type embryos), possibly because the small population of proliferating cells was not sufficient for complete migration of the DVE or because Nodal signaling has relevant effects other than that on cell proliferation. These data suggest that inhibition of cell proliferation by Nodal antagonists directs the DVE to migrate toward the future anterior side.

Impaired A-P patterning without Lefty1 and Cerl

To confirm the role of Nodal antagonists in A-P patterning, we analyzed mutant mice lacking Lefty1 or Cerl. *Lefty1*$^{-/-}$ [14] and *Cerl*$^{-/-}$ [6 15 16] embryos undergo normal gastrulation, whereas *Cerl*$^{-/-}$, *Lefty1*$^{-/-}$ embryos develop multiple primitive streaks[8], suggestive of functional redundancy between *Lefty1* and *Cerl*. We first examined expression of the AVE marker *Hex* (Fig. 5a, b, h, i). The *Hex* expression domain was expanded slightly in *Cerl*$^{-/-}$ and *Lefty1*$^{-/-}$ mutants (data not shown) and markedly in the *Cerl*$^{-/-}$, *Lefty1*$^{-/-}$ double mutant (Fig. 5b, i), in which cells positive for *Hex* transcripts occupied the entire anterior half of the VE at E6.5 ($n = 4$). These results reveal a new role for the Nodal antagonists in A-P patterning; these molecules thus restrict the size or location of the

AVE, perhaps by inhibiting the proliferation of AVE cells.

We next examined DVE migration in the *Lefty1* and *Cerl* mutants by monitoring *Hex* expression. Although the *Lefty1*$^{-/-}$ or *Cerl*$^{-/-}$ embryos did not manifest obvious migration defects (data not shown), migration of the DVE was delayed in *Cerl*$^{-/-}$, *Lefty1*$^{-/-}$ embryos. The *Hex* expression domain, which is normally located on the anterior side at E6.0 (Fig. 5a), thus remained in the distal region of the double mutant at this time (Fig. 5h).

The loss of the Nodal antagonists also affected the proliferation of VE cells. In wild-type embryos at E6.0 and E6.5, the extent of BrdU incorporation into the VE was greater on the posterior side and gradually decreased toward the anterior side (Fig. 3c-e; Fig. 5c, d). The asymmetry in BrdU incorporation between the anterior and posterior VE was less obvious in *Lefty1*$^{-/-}$ ($n = 4$) (Fig. 5q) and *Cerl*$^{-/-}$ ($n = 5$) (Fig. 5u) embryos. In *Cerl*$^{-/-}$, *Lefty1*$^{-/-}$ embryos at E6.0 ($n = 5$) (Fig. 5j) and E6.5 ($n = 4$) (Fig. 5k), however, BrdU incorporation was apparent at a high level throughout the entire VE, with the exception of a small region of the AVE. We also examined *Nodal* expression in the various mutant embryos at E6.5. In the wild type, *Nodal* expression in the epiblast at this stage is greater in the posterior region[2] (Fig. 5e–g). In the single mutants lacking *Lefty1* ($n = 3$) (Fig. 5r–t) or *Cerl* ($n = 5$) (Fig. 5v–x), *Nodal* expression was down-regulated in the posterior epiblast but was up-regulated in the VE. Increased *Nodal* expression was more evident in the double mutant ($n = 4$) (Fig. 5l–n); *Nodal* expression in the epiblast was thus uniform in the distal region (Fig. 5n) but was asymmetric in the proximal region (Fig. 5m). In addition, *Nodal* expression was up-regulated throughout

the VE (Fig. 5l–n).

Although DVE migration was delayed in *Cerl*$^{-/-}$, *Lefty1*$^{-/-}$ embryos (n = 12) (Fig. 5o), the DVE cells did migrate anteriorly (Fig. 5i). Furthermore, although the extent of VE cell proliferation was greatly increased in the double mutant, a small BrdU-negative region was apparent in the AVE (Fig. 5j, k). These observations suggest the existence of an additional Nodal antagonist (or antagonists) that partially compensates for the lack of Lefty1 and Cerl. An obvious candidate for such a molecule was Lefty2. *Lefty2* is not expressed in the VE of wild-type embryos[4], but, unexpectedly, it was expressed in a portion of the AVE of *Cerl*$^{-/-}$, *Lefty1*$^{-/-}$ embryos (n = 5) (Fig. 5p) that corresponded to the BrdU-negative region (Fig. 5k). It is therefore likely that ectopic expression of *Lefty2* partially compensates for the loss of Lefty1 and Cerl and thereby reduces the severity of the A-P patterning defects in *Cerl*$^{-/-}$, *Lefty1*$^{-/-}$ embryos. Ectopic activation of *Lefty2* in *Cerl*$^{-/-}$, *Lefty1*$^{-/-}$ embryos likely results from the increased Nodal activity in the DVE and AVE, given that *Lefty2* is not induced in the AVE of *Lefty1*$^{-/-}$ embryos (n = 4) (data not shown).

Discussion

How does differential Nodal activity drive DVE migration? Several lines of evidence indicate that differential cell proliferation in the VE along the future A-P axis acts as the driving force of DVE migration: (1) Asymmetry in cell proliferation in the VE was apparent as early as E5.7, when the DVE begins to migrate. A faster rate of cell growth on the prospective posterior side of the embryo was also suggested by previous observations[17]. (2) Ectopic expression of wild-type or dominant negative forms of Cdk2

mimicked the actions of Nodal and of Lefty1 plus Cerl, respectively, in the DVE migration assay. (3) Asymmetry in VE cell proliferation along the A-P axis was lost in mutants in which DVE migration is impaired. Cell proliferation was thus markedly compromised in the entire VE of *FoxH1*$^{-/-}$ type B embryos, in which the DVE does not migrate.

Although our data implicate differential cell proliferation in DVE migration, they do not necessarily exclude other possibilities. For instance, DVE cells may receive a signal that induces their anteriorward movement. Several mechanisms of cell migration are operative during development. During gastrulation in *Xenopus* or zebra fish, for example, cells dorsalized by the organizer are conveyed toward the anterior side by cell intercalation, a process that is known as convergent extension and which requires noncanonical Wnt signaling that regulates cell planar polarity. Extension of the animal cap in response to Activin (Nodal), which is reminiscent of convergent extension, is also triggered by the induction of Wnt11 [18,19]. If Nodal signaling in the VE induces expression of Wnt or a Wnt antagonist, it would generate differential Wnt activity across the DVE and the latter may then migrate by a mechanism similar to convergent extension.

The ectopic expression of both *Lefty1* and *Cerl* had a greater effect on DVE migration than did the expression of either Nodal antagonist alone. Furthermore, A-P patterning defects were apparent only in the absence of both Lefty1 and Cerl, although VE cell proliferation was mildly affected in *Lefty1*$^{-/-}$ and *Cerl*$^{-/-}$ single mutants. Lefty1 and Cerl are thought to antagonize Nodal signaling by different mechanisms. Whereas

Lefty1 blocks the Nodal signal through competitive binding to the Nodal receptor[20], Cerl inhibits Nodal activity by binding to Nodal itself[21]. Inhibition at both levels might thus be necessary to suppress Nodal signaling fully. Alternatively, Cerl may inhibit signaling by other molecules, such as Wnt or bone morphogenetic protein, as has been suggested previously[6,21]. Mice deficient in β-catenin also show defects in DVE migration[22], suggesting that a canonical pathway of Wnt signaling contributes to this process, either directly or indirectly. In this regard, Wnt antagonists such as Dkk-1 [23] also might participate in DVE migration.

The direction of DVE migration appears to be determined by the anteriorly shifted expression domains of *Lefty1* and *Cerl*, which raises the question of the origin of the information responsible for the asymmetric expression of these genes. Cell-labeling experiments have linked polarity of the blastocyst to later P-D polarity of the egg cylinder[24]. VE descendants of the inner cell mass located near the polar body thus tend to be localized in the DVE, whereas those of cells located opposite to the polar body tend to contribute to the proximal VE. Prospective Lefty1$^+$, Cerl$^+$ VE cells might be specified early, and the global cell movement of the VE may bring such cells to the distal end with a slight dislocation toward the future anterior side. Epiblast-derived Nodal would then act on these VE cells and induce the expression of *Lefty1* and *Cerl*, given that the expression of these genes in the VE is known to be induced by Nodal signaling either directly or indirectly[25,26]. *Hex* is widely expressed in the VE at E5.0 but its expression becomes restricted to the DVE at E5.5. It is not known how *Hex* expression is regulated during this period, but distally located cells may escape from an

inhibitory signal derived from the proximal region, resulting in the symmetric distribution of Hex^+ cells in the distal region. Although this simple model does not require additional cues for formation of the A-P axis, other mechanisms are also possible. For example, if an asymmetric positional cue is already established in the epiblast before E5.5, *Lefty1* and *Cerl* expression could be induced by this asymmetric signal. Although expression of *Lefty1* and *Cerl* in the VE requires Nodal signaling either directly or indirectly[25,26], *Nodal* expression in the epiblast at E5.0 and E5.5 appears radially symmetric. In either case, analysis of the transcriptional regulation of *Lefty1* and *Cerl* may clarify the mechanisms responsible for their shifted expression domains.

The necessity to establish polarity of *Nodal* expression along the A-P axis is conserved among vertebrates, although different strategies appear to be adopted to achieve this end. In *Xenopus* and zebra fish[27,28], the expression of Nodal-related proteins in the vegetal hemisphere or marginal zone is induced by maternal factors; this expression is later extinguished by a negative signaling loop involving Lefty (Antivin) in the zebra fish[29], whereas the expression on the dorsal side is increased by β-catenin signaling[27] in addition to the Nodal positive signaling loop[30,31]. In the chick, *Nodal* expression is induced by Vg1 and Wnt in the posterior marginal zone[32], whereas the expression in the periphery of the blastoderm is suppressed by Cerl produced in the hypoblast[33]. A positional cue such as that generated by cortical rotation in *Xenopus*[34] or by gravity in the chick[35] does not appear to contribute to mouse development. Instead, the mouse embryo may have developed a dynamic system involving *Nodal–Lefty/Cerl* positive and negative signaling loops that make use of a subtle change generated in the

VE.

Methods

Introduction of expression vectors into the VE

E5.2 embryos were dissected from the uterus and the parietal endoderm membrane was reflected. The introduction of expression vectors [36] into the VE and labeling of the DVE with DiI were performed with a Leica micromanipulator. Liposomes composed of the expression vectors and Lipofectamine2000 (Invitrogen) were injected into the VE with an injection pipette by a method to be described in detail elsewhere (C.M., et al, unpublished). Embryos were cultured for 24 h under a humidified atmosphere of 5% CO_2 at 37 C in dishes containing Dulbecco's modified Eagle's medium supplemented with 75% rat serum. They were then examined with a Leica compound fluorescence microscope equipped with rhodamine and GFP2 optics[3]. In most injected embryos, the GFP signal was detected only in the VE; those in which GFP was apparent in the epiblast were discarded.

BrdU labeling of embryos

Labeling of proliferating cells with BrdU was performed as described previously[37]. In brief, pregnant mice were injected intraperitoneally with BrdU (100 mg per kilogram of body mass) at E5.5, E5.7, E6.0, E6.2, or E6.5 and killed 25 min thereafter. The embryos were recovered, fixed with Bouin's solution, and exposed consecutively to antibodies to BrdU (MBL, Nagoya, Japan), biotinylated secondary antibodies and an ABC-horseradish peroxidase system (VECTOR Laboratories). The genotype of each embryo

was determined by the polymerase chain reaction with DNA obtained from the ectoplacental cone.

Two-color whole-mount in situ hybridization

Mouse embryos were staged on the basis of their morphology. Two-color whole-mount in situ hybridization was performed with one RNA probe labeled with digoxygenin and the other labeled with fluorescein according to a standard procedure. After the first staining, alkaline phosphatase was inactivated by incubation at 70 C for 30 min. The second staining was performed with INT/BCIP solution (Roche), because the reaction product can be later decolorized by exposure to methanol.

References

1. Beddington, R. S. & Robertson, E. J. Anterior patterning in mouse. *Trends Genet* **14**, 277-84 (1998).
2. Beddington, R. S. & Robertson, E. J. Axis development and early asymmetry in mammals. *Cell* **96**, 195-209 (1999).
3. Thomas, P. Q., Brown, A. & Beddington, R. S. Hex: a homeobox gene revealing peri-implantation asymmetry in the mouse embryo and an early transient marker of endothelial cell precursors. *Development* **125**, 85-94 (1998).
4. Meno, C. et al. Two closely-related left-right asymmetrically expressed genes, lefty-1 and lefty-2: their distinct expression domains, chromosomal linkage and direct neuralizing activity in Xenopus embryos. *Genes Cells* **2**, 513-24 (1997).
5. Belo, J. A. et al. Cerberus-like is a secreted factor with neutralizing activity expressed in the anterior primitive endoderm of the mouse gastrula. *Mech Dev* **68**, 45-57 (1997).
6. Belo, J. A. et al. Cerberus-like is a secreted BMP and nodal antagonist not essential for mouse development. *Genesis* **26**, 265-70 (2000).
7. Kimura, C. et al. Visceral endoderm mediates forebrain development by suppressing posteriorizing signals. *Dev Biol* **225**, 304-21 (2000).
8. Perea-Gomez, A. et al. Nodal antagonists in the anterior visceral endoderm prevent the formation of multiple primitive streaks. *Dev Cell* **3**, 745-56 (2002).
9. Tam, P. P., Gad, J. M., Kinder, S. J., Tsang, T. E. & Behringer, R. R. Morphogenetic tissue movement and the establishment of body plan during development from blastocyst to gastrula in the mouse. *Bioessays* **23**, 508-17 (2001).
10. Yamamoto, M. et al. The transcription factor FoxH1 (FAST) mediates Nodal signaling during anterior-posterior patterning and node formation in the mouse. *Genes Dev* **15**, 1242-56 (2001).
11. Norris, D. P. & Robertson, E. J. Asymmetric and node-specific nodal expression patterns are controlled by two distinct cis-acting regulatory elements. *Genes Dev* **13**, 1575-88 (1999).
12. Collignon, J., Varlet, I. & Robertson, E. J. Relationship between asymmetric nodal expression and the direction of embryonic turning. *Nature* **381**, 155-8

(1996).

13. Belachew, S. et al. Cyclin-dependent kinase-2 controls oligodendrocyte progenitor cell cycle progression and is downregulated in adult oligodendrocyte progenitors. *J Neurosci* **22**, 8553-62 (2002).
14. Meno, C. et al. lefty-1 is required for left-right determination as a regulator of lefty-2 and nodal. *Cell* **94**, 287-97 (1998).
15. Simpson, E. H. et al. The mouse Cer1 (Cerberus related or homologue) gene is not required for anterior pattern formation. *Dev Biol* **213**, 202-6 (1999).
16. Shawlot, W., Min Deng, J., Wakamiya, M. & Behringer, R. R. The cerberus-related gene, Cerr1, is not essential for mouse head formation. *Genesis* **26**, 253-8 (2000).
17. Wiley, L. M. & Pedersen, R. A. Morphology of mouse egg cylinder development in vitro: a light and electron microscopic study. *J Exp Zool* **200**, 389-402 (1977).
18. Heisenberg, C. P. et al. Silberblick/Wnt11 mediates convergent extension movements during zebrafish gastrulation. *Nature* **405**, 76-81 (2000).
19. Wallingford, J. B. et al. Dishevelled controls cell polarity during Xenopus gastrulation. *Nature* **405**, 81-5 (2000).
20. Sakuma, R. et al. Inhibition of Nodal signalling by Lefty mediated through interaction with common receptors and efficient diffusion. *Genes Cells* **7**, 401-12 (2002).
21. Piccolo, S. et al. The head inducer Cerberus is a multifunctional antagonist of Nodal, BMP and Wnt signals. *Nature* **397**, 707-10 (1999).
22. Huelsken, J. et al. Requirement for beta-catenin in anterior-posterior axis formation in mice. *J Cell Biol* **148**, 567-78 (2000).
23. Glinka, A. et al. Dickkopf-1 is a member of a new family of secreted proteins and functions in head induction. *Nature* **391**, 357-62 (1998).
24. Weber, R. J., Pedersen, R. A., Wianny, F., Evans, M. J. & Zernicka-Goetz, M. Polarity of the mouse embryo is anticipated before implantation. *Development* **126**, 5591-8 (1999).
25. Brennan, J. et al. Nodal signalling in the epiblast patterns the early mouse embryo. *Nature* **411**, 965-9 (2001).
26. Yamamoto, M. et al. Nodal signaling induces the midline barrier by activating Nodal expression in the lateral plate. *Development* **130**, 1795-804 (2003).

27. De Robertis, E. M., Larrain, J., Oelgeschlager, M. & Wessely, O. The establishment of Spemann's organizer and patterning of the vertebrate embryo. *Nat Rev Genet* **1**, 171-81 (2000).

28. Schier, A. F. Axis formation and patterning in zebrafish. *Curr Opin Genet Dev* **11**, 393-404 (2001).

29. Chen, Y. & Schier, A. F. Lefty proteins are long-range inhibitors of squint-mediated nodal signaling. *Curr Biol* **12**, 2124-8 (2002).

30. Cheng, A. M., Thisse, B., Thisse, C. & Wright, C. V. The lefty-related factor Xatv acts as a feedback inhibitor of nodal signaling in mesoderm induction and L-R axis development in xenopus. *Development* **127**, 1049-61 (2000).

31. Meno, C. et al. Mouse Lefty2 and zebrafish antivin are feedback inhibitors of nodal signaling during vertebrate gastrulation. *Mol Cell* **4**, 287-98 (1999).

32. Skromne, I. & Stern, C. D. Interactions between Wnt and Vg1 signalling pathways initiate primitive streak formation in the chick embryo. *Development* **128**, 2915-27 (2001).

33. Bertocchini, F. & Stern, C. D. The hypoblast of the chick embryo positions the primitive streak by antagonizing nodal signaling. *Dev Cell* **3**, 735-44 (2002).

34. Miller, J. R. et al. Establishment of the dorsal-ventral axis in Xenopus embryos coincides with the dorsal enrichment of dishevelled that is dependent on cortical rotation. *J Cell Biol* **146**, 427-37 (1999).

35. Eyal-Giladi, H., Goldberg, M., Refael, H. & Avner, O. A direct approach to the study of the effect of gravity on axis formation in birds. *Adv Space Res* **14**, 271-9 (1994).

36. Mizushima, S. & Nagata, S. pEF-BOS, a powerful mammalian expression vector. *Nucleic Acids Res* **18**, 5322 (1990).

37. Hayashi, Y., Koike, M., Matsutani, M. & Hoshino, T. Effects of fixation time and enzymatic digestion on immunohistochemical demonstration of bromodeoxyuridine in formalin-fixed, paraffin-embedded tissue. *J Histochem Cytochem* **36**, 511-4 (1988).

Supplementary information accompanies the paper on **www.nature.com/nature.**

Acknowledgements We thank E. Robertson for *Nodal*^{lacZ} mutant mice; R. Beddington for the *Hex* probe; V. Gallo for expression vectors for Cdk and dominant negative Cdk; and N. Mine and Y. Ohnishi for help in improving the lipofection procedure. This work was supported by grants from the Ministry of Education, Science, Sports, and Culture of Japan (to C.M. and H.H.), a grant from CREST (Core Research for Evolutional Science and Technology) of the Japan Science and Technology Corporation (to H.H.), a grant from NIH (to R.R.B.), and a grant from Association pour la Recherche sur le Cancer and by funds from the INSERM, the CNRS and the Hopital Universitaire de Strasbourg (to S.-L.A.). M.Y. is a recipient of a fellowship from the Japan Society for the Promotion of Science for Japanese Junior Scientists.

Competing interests statement: The authors declare that they have no competing financial interests.

Correspondence and requests for materials should be addressed to H.H. (hamada@fbs.osaka-u.ac.jp).

Figure Legends

Figure 1 Asymmetric expression of *Lefty1* and *Cerl* before DVE migration. Expression of *Lefty1* (**a–c**) and *Cerl* (**d–f**) was examined in wild-type mouse embryos at the indicated stages of development. Expression of *Lefty1* (amber) and *Hex* (blue) (**g**) or of *Cerl* (amber)and *Hex* (blue) (**i**) was simultaneously examined in the same E5.5 embryos by two-color in situ hybridization; the *Hex* expression domains alone (**h, j**) were visualized after removal of the amber staining by treatment of the embryos shown in **g** and **i**, respectively, with methanol. Amber arrowheads indicate the borders of *Lefty1* (**g**) or *Cerl* (**i**) expression domains; blue arrowheads indicate those of *Hex* expression domains (**h, j**). Lateral views are shown for each embryo, with the anterior side on the left.

Figure 2 Ectopic expression of *Lefty1* or *Cerl* directs DVE migration. **a**, Experimental strategy. An effector gene, together with a GFP expression vector, was introduced into VE cells on the lateral side of E5.2 mouse embryos, and the DVE was labeled with DiI. The embryos were then cultured for 24 h, after which the fates of GFP-labeled cells (green) and DiI-labeled cells (red) were examined. The egg cylinder was divided into four quarters; localization of DiI-labeled cells in the same quarter or in a different quarter relative to the position of GFP-positive cells was categorized as "same side" or "different side", respectively. **b, c**, Two representative embryos showing localization of GFP-positive cells and DiI-positive cells on different sides (**b**) or on the same side (**c**). **d**, Summary of the effects of ectopic expression of the indicated genes on DVE migration.

The numbers of embryos showing each localization pattern are indicated. Host embryos were wild type with the exception of those in rows 6 and 7, which were *FoxH1*$^{-/-}$, *Nodal*$^{lacZ/+}$. "DiI at distal" (green) indicates a pattern in which the DVE remains at the distal end without migration.

Figure 3 Patterns of VE cell proliferation in wild-type and various mutant embryos. The pattern of BrdU incorporation was determined in wild-type (WT) embryos at the indicated stages (**a–e**) as well as in the indicated mutants at E6.5 (**f–i**). Lateral views are shown for each embryo, with the anterior side on the left. Arrowheads indicate regions negative for BrdU labeling. The square region in **b** is expanded in **b'**. A section indicated by the horizontal bar of the embryo in **c** is shown in **c'**; BrdU-positive or -negative nuclei in the VE are shown by closed black and red arrowheads, respectively (**c'**).

Figure 4 Nodal antagonists inhibit and Nodal promotes VE cell proliferation. **a–h**, The VE of E5.2 wild-type embryos was transfected unilaterally with a GFP expression vector either alone or together with a test gene, as indicated. The numbers of GFP-positive cells were counted 12 and 36 h after transfection. Both differential interference contrast (**a–h**) and GFP fluorescence (**a'–h'**) images of embryos are shown. **i**, Summary of the percentages of embryos in which GFP-positive cells replicated the indicated numbers of times during the 24-h period of analysis for the three groups of embryos described in **a–h**. **j**, Effects of ectopic expression of wild-type (WT) *Cdk2* or of a

dominant negative (DN) form of *Cdk2* on DVE migration. Host embryos were wild type (rows 1–3) or *FoxH1*$^{-/-}$, *Nodal*$^{lacZ/+}$(row 4) and were analyzed as described in Figure 2a. The numbers of embryos showing localization of DiI on the same side or on a different side relative to that of GFP are indicated.

Figure 5 A-P patterning defects in the absence of Lefty1 and Cerl. *Cerl*$^{+/-}$, *Lefty1*$^{+/-}$ (a), wild-type (b–g), *Cerl*$^{-/-}$, *Lefty1*$^{-/-}$ (h–n, p), *Lefty1*$^{-/-}$ (q–t), and *Cerl*$^{-/-}$ (u–x) embryos were examined for *Hex* expression (a, b, h, i), BrdU incorporation (c, d, j, k, q, u), *Nodal* expression (e–g, l–n, r–t, v–x), and *Lefty2* expression (p) at the indicated stages. Lateral views are shown for each embryo with the anterior side on the left, with the exception that anterior views are shown in b and i. The planes of transverse sections (f, g, m, n, s, t, w, x) are indicated by the horizontal bars in e, l, r, and v. Patterns of the *Hex* expression domain are summarized for *Cerl*$^{+/-}$, *Lefty1*$^{+/-}$ and *Cerl*$^{-/-}$, *Lefty1*$^{-/-}$ embryos at E6.0 in o. The numbers of embryos showing each pattern are indicated. Green, the expression domain remains at the distal tip; light blue, it was shifted toward the anterior side; medium blue, it reached half way toward the junction between embryonic and extraembryonic regions; dark blue, it reached the junction.

Figure 6. Model for A-P determination by Nodal antagonists.
In the wild-type embryo at E5.5, Nodal signals in the epiblast and overlying VE regulate cell proliferation of VE in a symmetric manner (Step 1; green arrows represent putative migration force generated by cell proliferation). Nodal antagonists (*Lefty1 and Cerl*) in

DVE whose expression domains are already inclined toward the prospective anterior side start to inhibit the Nodal signals in the region adjacent to the DVE (step 2). Cell proliferation will be inhibited in the VE regions that have received the Nodal antagonists (step 3). This would generate higher migration force on the posterior side and induce the DVE to migrate toward the anterior side (step 4). Migration of the DVE toward the anterior side further establishes A-P asymmetries in Nodal signaling and cell proliferation (step 5).

Supplementary Information

Figure S1 Delayed migration of the DVE in *FoxH1* mutant embryos. Expression of *Hex* was examined by whole-mount in situ hybridization in wild-type (**a–e**), *FoxH1*$^{+/-}$ (**f–j**), *FoxH1*$^{-/-}$ type A (**k–o**), and *FoxH1*$^{flox/-}$, *Lefty2-cre* (**p–t**) embryos at the indicated stages of development. Lateral views are shown for each embryo, with the anterior side on the left. The numbers of embryos showing each pattern of *Hex* expression are indicated in **u** through **x**, respectively, according to the following color code: orange, *Hex* expression not detected; green, expression domain located at the distal tip; light blue, expression domain shifted toward the anterior side; medium blue, expression domain reached half way toward the junction between embryonic and extraembryonic regions; dark blue, expression domain reached the junction. In wild-type embryos (**a–e**, **u**), *Hex* is expressed at the distal tip at E5.5 and the expression domain begins to move toward the future anterior side at E5.7. In some (5/14) *FoxH1*$^{+/-}$ embryos (**f–j**, **v**), DVE migration was delayed, so that *Hex* was still expressed at the distal tip at E5.7. The DVE had moved to the anterior side at E6.0 in all *FoxH1*$^{+/-}$ embryos examined, however. Migration of the DVE was further delayed in the least severe form (type A) of *FoxH1*$^{-/-}$ embryos (**k–o**, **w**); *Hex* expression was thus apparent at the distal tip as late as E6.0 and the expression domain had begun to move at E6.2. The DVE did not migrate from the distal region in the most severe form (type B) of *FoxH1*$^{-/-}$embryos[10]. In *FoxH1*$^{flox/-}$, *Lefty2-cre* embryos (**p–t**, **x**), which lack FoxH1 specifically in the epiblast, the *Hex* expression domain appeared to move normally. These results suggest that the level of FoxH1-mediated Nodal signaling in the VE regulates migration of the DVE.

Figure S2 *Nodal* expression in *FoxH1* mutant embryos. *Nodal* expression was examined by whole-mount in situ hybridization in wild-type (**a–d**), *FoxH1*$^{+/-}$ (**e–h**), *FoxH1*$^{-/-}$ type A (**i–l**), *FoxH1*$^{-/-}$ type B (**m–p**), and *FoxH1*$^{flox/-}$, *Lefty2-cre* (**q–t**) embryos at the indicated stages. Lateral views are shown for each embryo, with the anterior side on the left. In wild-type embryos, *Nodal* is expressed throughout the epiblast and overlying VE at E5.5, with the expression domain gradually shifting to the posterior side of the epiblast between E5.7 and E6.2. In *FoxH1*$^{+/-}$ embryos, although the localization of *Nodal* expression appeared normal, the level of expression was reduced compared with that in the wild type, consistent with the delay in DVE migration. In *FoxH1*$^{-/-}$ type A embryos, *Nodal* expression was detected throughout the epiblast but was lost in the VE between E5.5 and E6.0; expression in the epiblast shifted toward the proximal and posterior side with a delay at E6.2. In *FoxH1*$^{-/-}$ type B embryos, *Nodal* expression was undetectable until E5.7 as a result of failure to augment such expression in the epiblast; *Nodal* expression increased in the proximal epiblast and overlying VE at E6.0 but was radially symmetric. In *FoxH1*$^{flox/-}$, *Lefty2-cre* embryos, which lack *FoxH1* expression in the epiblast, expression of *Nodal* in the VE appeared relatively normal, whereas that in the distal epiblast had disappeared or waned and the asymmetric expression in the proximal epiblast was delayed as in *FoxH1*$^{-/-}$ embryos.

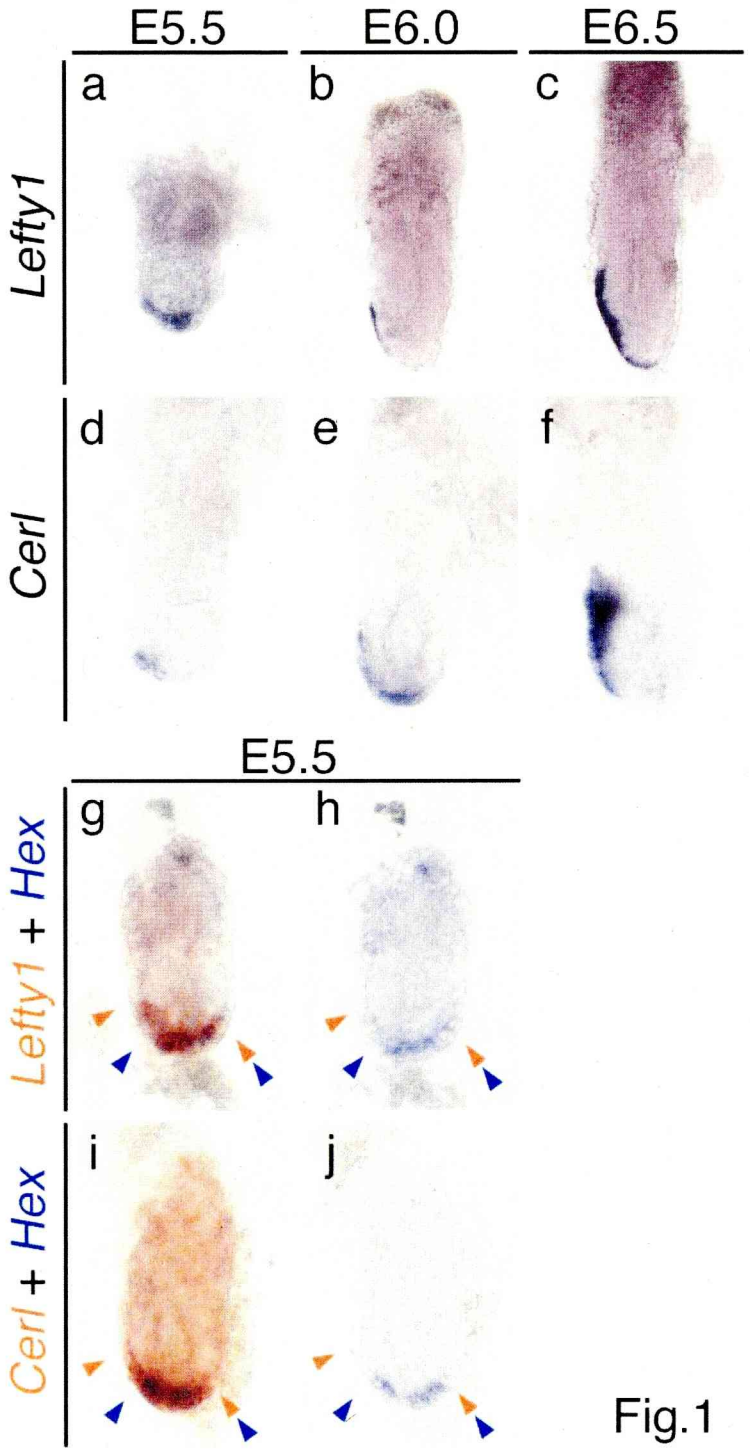

Fig.1

Fig.2

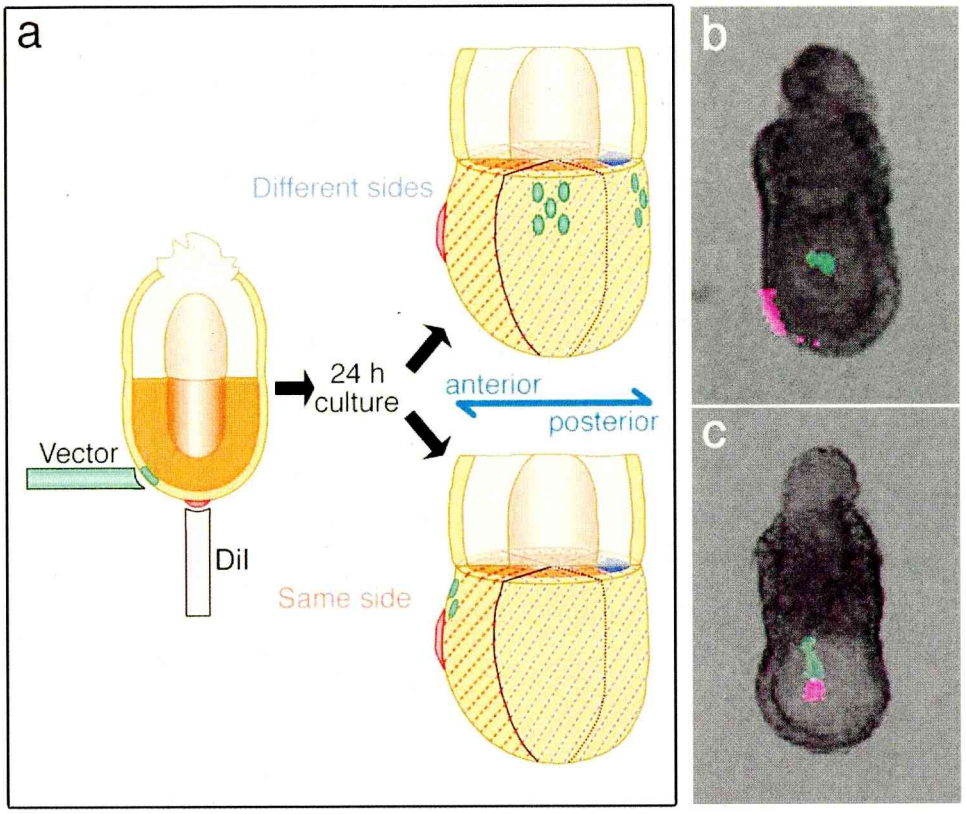
a
Different sides
24 h
culture
anterior
posterior
Vector
DiI
Same side
b
c

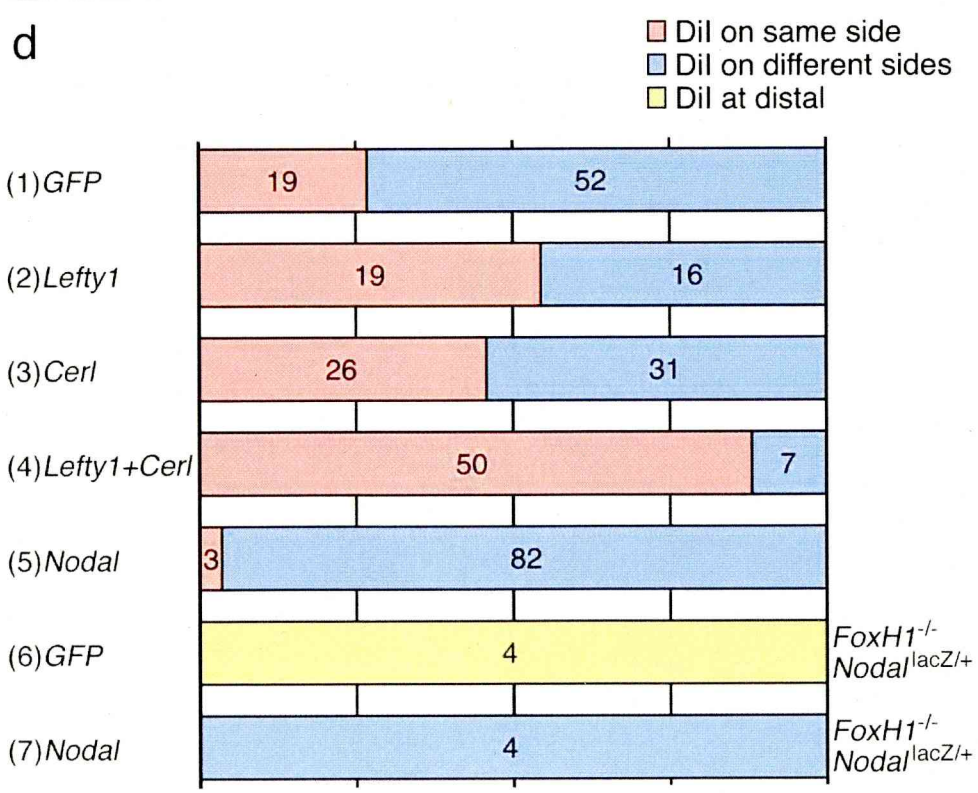
d
DiI on same side
DiI on different sides
DiI at distal
(1)GFP
19
52
(2)Lefty1
19
16
(3)Cerl
26
31
(4)Lefty1+Cerl
50
7
(5)Nodal
3
82
(6)GFP
4
FoxH1-/-
NodallacZ/+
(7)Nodal
4
FoxH1-/-
NodallacZ/+

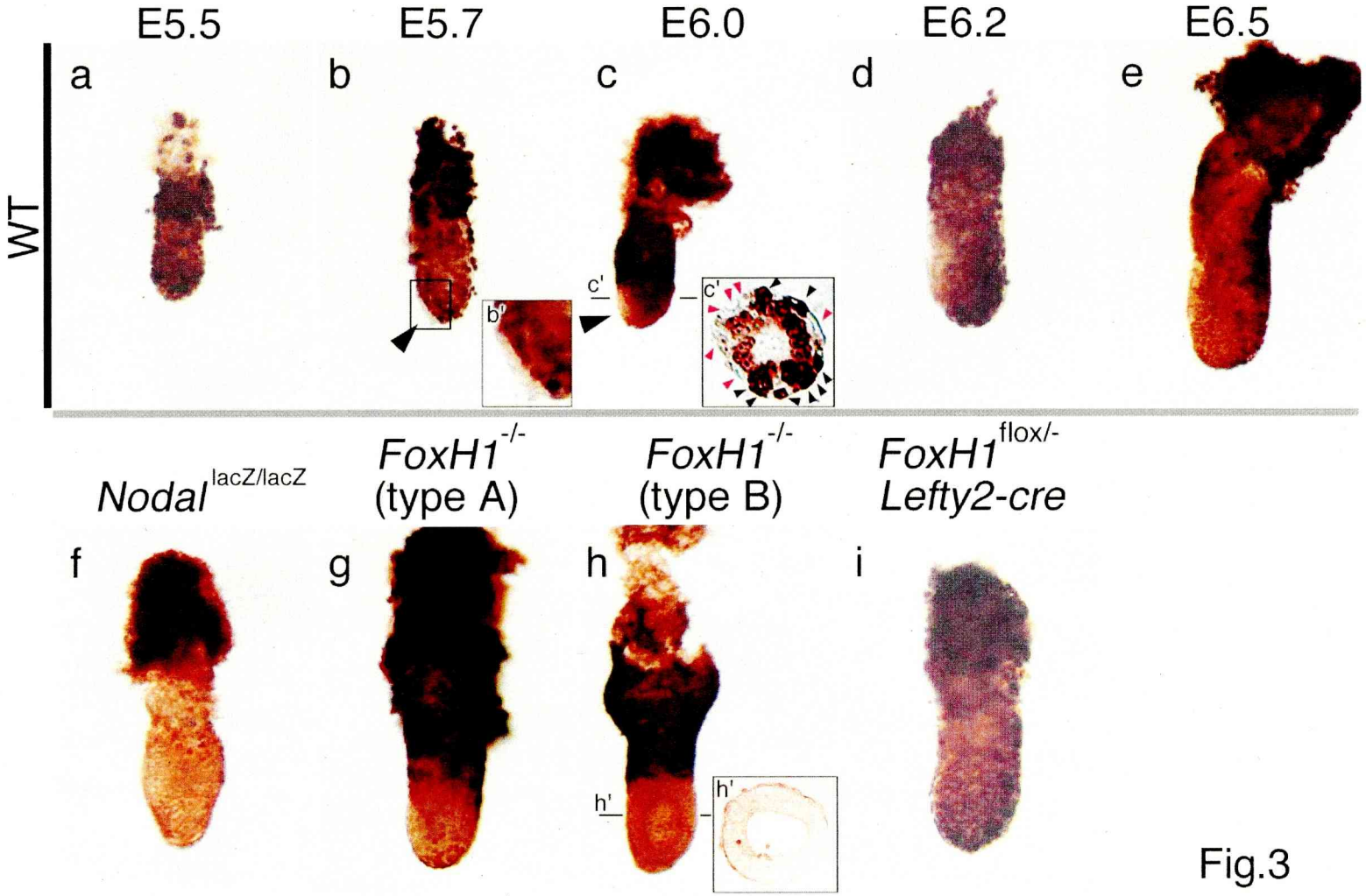
E5.5
E5.7
E6.0
E6.2
E6.5
WT
a
b
c
d
e
b'
c'
c'
Nodal lacZ/lacZ
FoxH1 -/- (type A)
FoxH1 -/- (type B)
FoxH1 flox/- Lefty2-cre
f
g
h
i
h'
h'

Fig.3

Fig.4

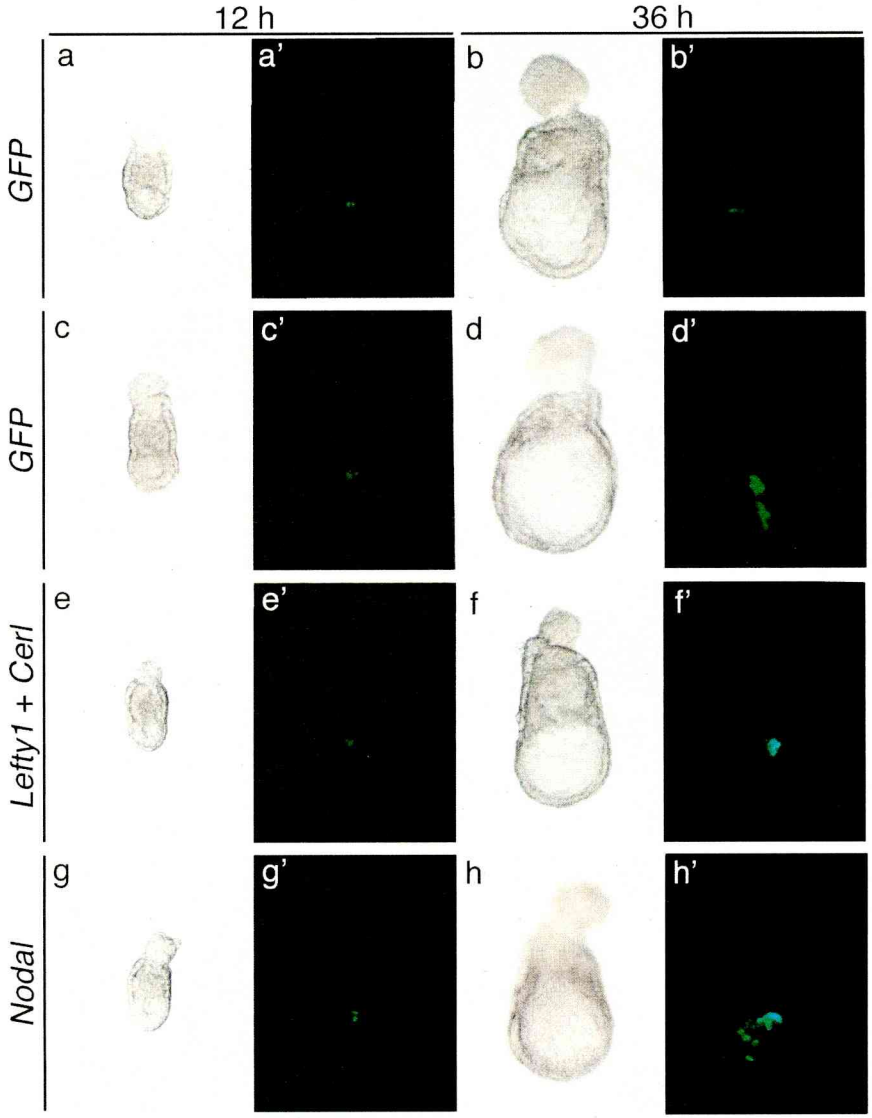
12 h
36 h
a
a'
b
b'
c
c'
d
d'
e
e'
f
f'
g
g'
h
h'
GFP
GFP
Lefty1 + Cerl
Nodal

i

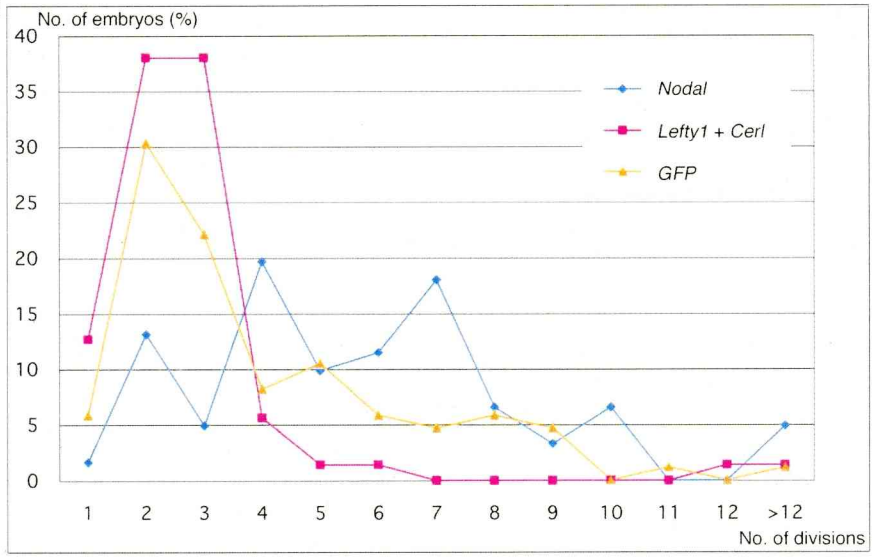
No. of embryos (%)
40
35
30
25
20
15
10
5
0
Nodal
Lefty1 + Cerl
GFP
1
2
3
4
5
6
7
8
9
10
11
12
>12
No. of divisions

j

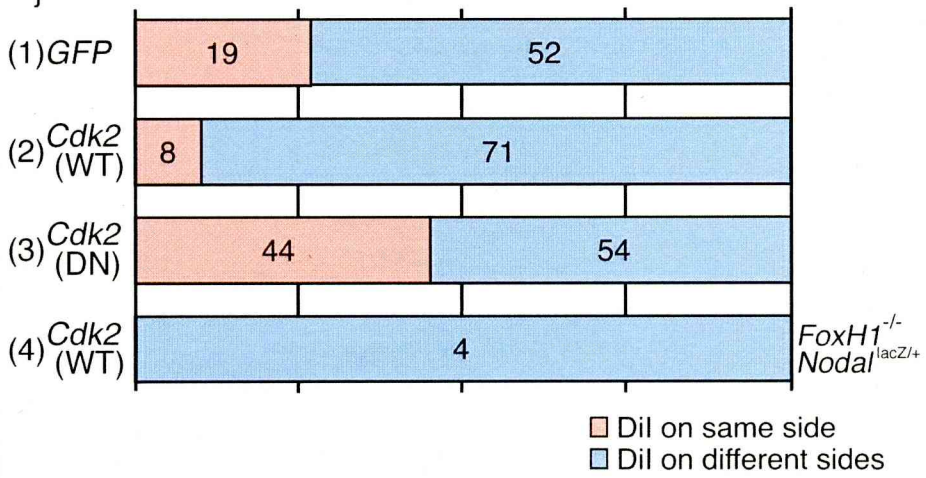
(1) GFP
19
52
(2) Cdk2 (WT)
8
71
(3) Cdk2 (DN)
44
54
(4) Cdk2 (WT)
4
FoxH1-/-
Nodal lacZ/+
DiI on same side
DiI on different sides

Fig.5

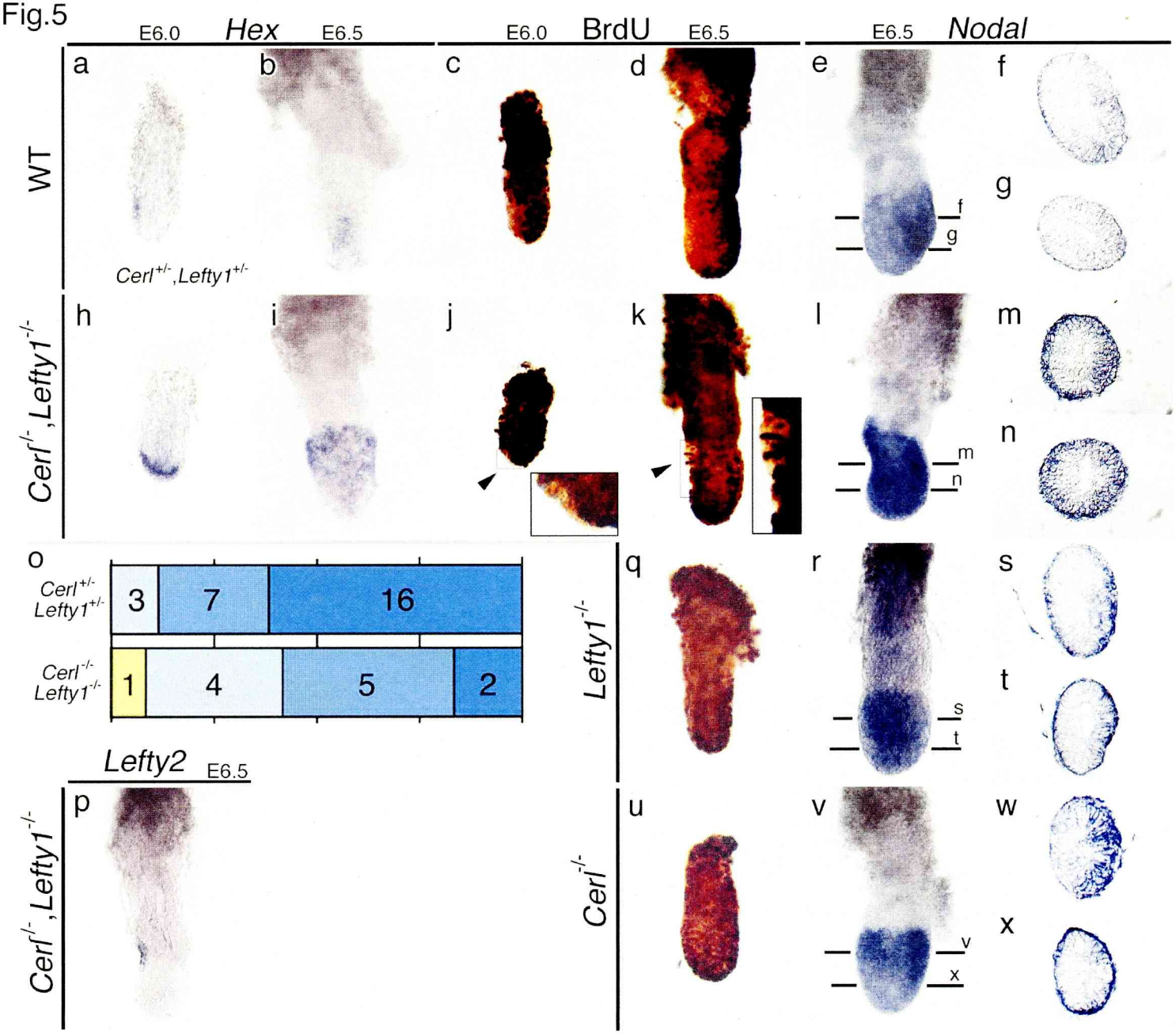
E6.0
Hex
E6.5
E6.0
BrdU
E6.5
E6.5
Nodal
WT
Cerl+/-,Lefty1+/-
Cerl-/-,Lefty1-/-
Lefty1-/-
Cerl-/-
Lefty2
E6.5
a
b
c
d
e
f
g
h
i
j
k
l
m
n
o
p
q
r
s
t
u
v
w
x
Cerl+/-
Lefty1+/-
Cerl-/-
Lefty1-/-
3
7
16
1
4
5
2

Fig.6

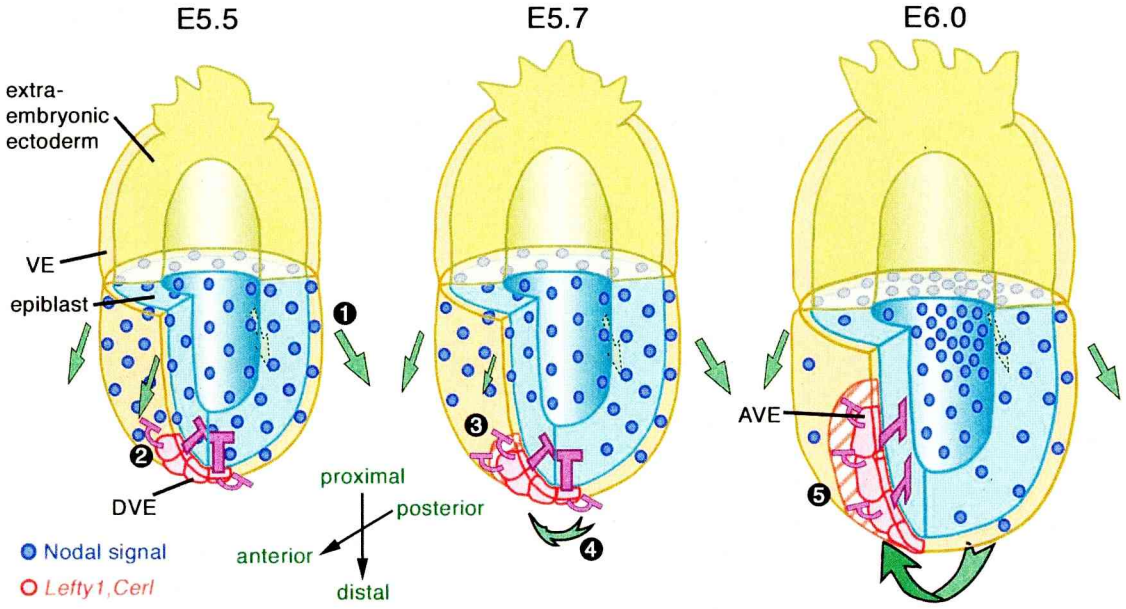
E5.5
E5.7
E6.0
extra-
embryonic
ectoderm
VE
epiblast
DVE
AVE
1
2
3
4
5
proximal
posterior
anterior
distal
Nodal signal
Lefty1,Cerl

Fig.S1

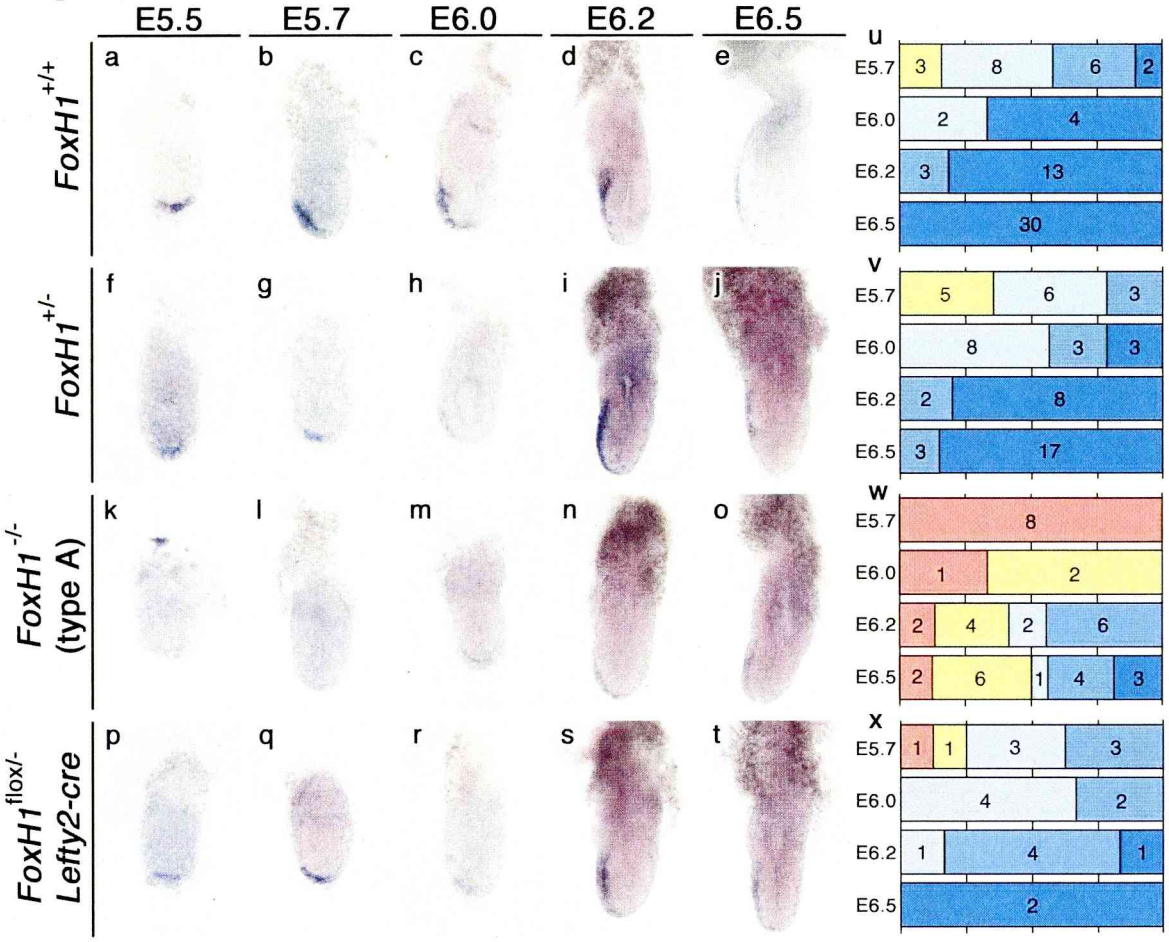
E5.5
E5.7
E6.0
E6.2
E6.5
FoxH1+/+
FoxH1+/-
FoxH1-/- (type A)
FoxH1flox/- Lefty2-cre
a
b
c
d
e
f
g
h
i
j
k
l
m
n
o
p
q
r
s
t
u
E5.7 3 8 6 2
E6.0 2 4
E6.2 3 13
E6.5 30
v
E5.7 5 6 3
E6.0 8 3 3
E6.2 2 8
E6.5 3 17
w
E5.7 8
E6.0 1 2
E6.2 2 4 2 6
E6.5 2 6 1 4 3
x
E5.7 1 1 3 3
E6.0 4 2
E6.2 1 4 1
E6.5 2

Fig.S2

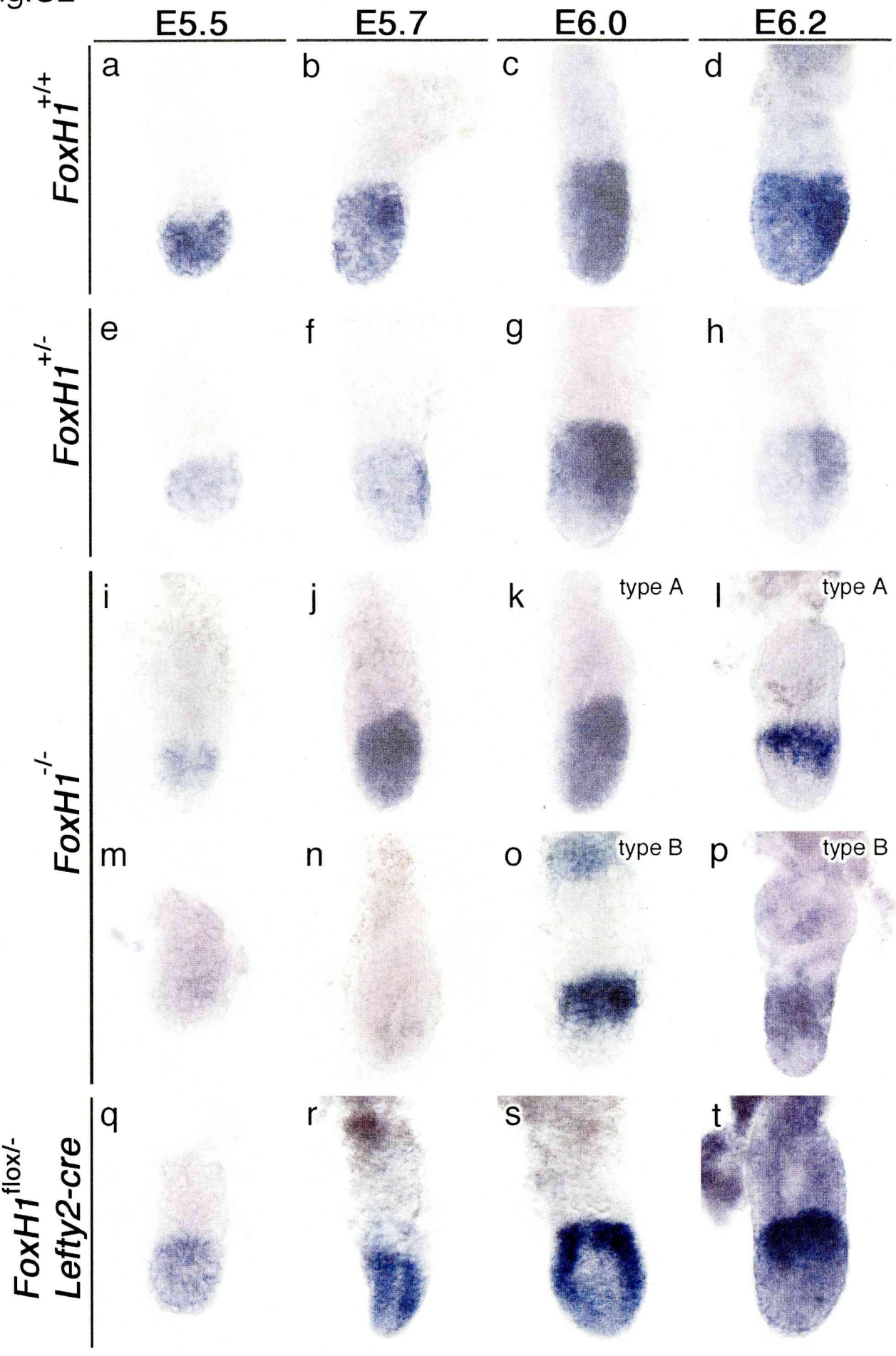
E5.5
E5.7
E6.0
E6.2
FoxH1+/+
FoxH1+/-
FoxH1-/-
FoxH1flox/-
Lefty2-cre
a
b
c
d
e
f
g
h
i
j
k
type A
l
type A
m
n
o
type B
p
type B
q
r
s
t

MIME-Version: 1.0
Date: Fri, 16 Jan 2004 21:58:13 UT
To: hamada@fbs.osaka-u.ac.jp
Subject: Decision on manuscript 2003-09-09716B
From: n.dewitt@naturesf.com
Status:

Content-Disposition: inline
Content-Length: 2336
Content-Transfer-Encoding: binary
Content-Type: text/plain

January 16, 2004

Dear Professor Hamada

We are pleased to inform you that your manuscript, "Nodal antagonists regulate migration of the visceral endoderm along the future anteroposterior axis of the mouse embryo", has now been accepted for publication in Nature.

Before your manuscript is typeset, our subeditors will change the text to ensure it is intelligible to our wide readership and to conform with house style. We look particularly carefully at the titles of all papers to ensure that they are relatively brief and that indexing is accurate.

The subeditor may send you the edited text for your approval. Once the edited text is typeset you will receive a PDF by email with a request to return a corrected version within 48 hours. If, when you receive your proof, you are unable to meet this deadline, please inform us at proofs@nature.com immediately.

our publication policies (see
http://www.nature.com/nature/submit/policies/index.html). In particular your manuscript must not be published elsewhere and there must be no announcement of the work to any media outlet until the publication date (the day on which it is uploaded onto our web site).

An online order form for reprints is at
http://www.nature.com/nature/submit/finalsubmission/form.html. Please note

reprints using the form appropriate to their geographical
region.

We welcome the submission of potential cover material (including a short caption of around 40 words) related to your manuscript; suggestions should be sent to Nature Editorial production department in London, either as hard copies or as electronic files (the image should be 300 dpi at 210 x 297 mm in either TIFF or JPEG format).

A description of some of Nature 寰泛 benefits for authors, including information about our press service, is attached to this
letter.

With kind regards

Natalie DeWitt
Senior Editor
Nature

The transcription factor FoxH1 (FAST) mediates Nodal signaling during anterior-posterior patterning and node formation in the mouse

Masamichi Yamamoto, Chikara Meno, Yasuo Sakai, Hidetaka Shiratori, Kyoko Mochida, Yayoi Ikawa, Yukio Saijoh, and Hiroshi Hamada

Division of Molecular Biology, Institute for Molecular and Cellular Biology, Osaka University; CREST, Japan Science and Technology Corporation, Osaka 565-0871, Japan

GENES & DEVELOPMENT 15:1242–1256 © 2001 by Cold Spring Harbor Laboratory Press ISSN 0890-9369/01 $5.00; www.genesdev.org

The transcription factor FoxH1 (FAST) mediates Nodal signaling during anterior-posterior patterning and node formation in the mouse

Masamichi Yamamoto, Chikara Meno, Yasuo Sakai, Hidetaka Shiratori, Kyoko Mochida, Yayoi Ikawa, Yukio Saijoh, and Hiroshi Hamada[1]

Division of Molecular Biology, Institute for Molecular and Cellular Biology, Osaka University; CREST, Japan Science and Technology Corporation, Osaka 565-0871, Japan

FoxH1 (FAST) is a transcription factor that mediates signaling by transforming growth factor-β, Activin, and Nodal. The role of FoxH1 in development has now been investigated by the generation and analysis of FoxH1-deficient (*FoxH1*$^{-/-}$) mice. The *FoxH1*$^{-/-}$ embryos showed various patterning defects that recapitulate most of the defects induced by the loss of Nodal signaling. A substantial proportion of *FoxH1*$^{-/-}$ embryos failed to orient the anterior-posterior (A-P) axis correctly, as do mice lacking Cripto, a coreceptor for Nodal. In less severely affected *FoxH1*$^{-/-}$ embryos, A-P polarity was established, but the primitive streak failed to elongate, resulting in the lack of a definitive node and its derivatives. Heterozygosity for *nodal* renders the *FoxH1*$^{-/-}$ phenotype more severe, indicative of a genetic interaction between *FoxH1* and *nodal*. The expression of *FoxH1* in the primitive endoderm rescued the A-P patterning defects, but not the midline defects, of *FoxH1*$^{-/-}$ mice. These results indicate that a Nodal-FoxH1 signaling pathway plays a central role in A-P patterning and node formation in the mouse.

[*Key Words*: anterior-posterior patterning; FoxH1; gastrulation; Nodal; node]

Received January 30, 2001; revised version accepted March 28, 2001.

Factors related to transforming growth factor-β (TGF-β) control multiple aspects of early development in vertebrates. One such factor, Nodal (Zhou et al. 1993), is a potent signaling molecule that is required for specification of the anterior-posterior (A-P) axis, formation of the primitive streak, and left-right patterning (Schier and Shen 2000). In general, TGF-β–related factors initiate intracellular signaling by interacting with type I and type II receptors on the cell surface, which in turn activate intracellular effectors known as Smad proteins (Massague 1998). The activated Smad proteins then translocate to the nucleus, where they interact with transcription factors and thereby regulate the expression of target genes. Although the Nodal signaling pathway remains to be fully characterized, genetic evidence suggests that ALK4 (ActRIB) functions as a type I receptor and that ActRIIA and ActRIIB serve as type II receptors in this pathway. Nodal activity is modulated by extracellular cofactors that belong to the EGF-CFC family of proteins (Gritsman et al. 1999), as well as by inhibitors that belong to the Lefty (Meno et al. 1999) and Cerberus families (Piccolo et al. 1999). Intracellular effectors of Nodal signaling most likely include Smad2, Smad3, and Smad4; consistent with this notion, Smad2 mutant mice exhibit early patterning defects that can be explained by a lack of Nodal signaling in the extraembryonic endoderm (Nomura and Li 1998; Waldrip et al. 1998; Heyer et al. 1999).

The transcription factor FoxH1 (FAST) also mediates Nodal signaling. This protein is a winged-helix transcription factor that was initially identified in *Xenopus* as a transducer of Activin signaling (Chen et al. 1996). Thus, FAST-1 (the FoxH1 ortholog in *Xenopus*) forms a complex with Smad2 and Smad4 in response to Activin and activates a set of genes that includes *Mix1* and *goosecoid* (Chen et al. 1997; Watanabe and Whitman 1999). However, recent studies have revealed that, in cultured mammalian cells or frog animal caps, this transcription factor also mediates signaling by TGF-β (Labbe et al. 1998; Zhou et al. 1998; Liu et al. 1999) and Nodal (Saijoh et al. 2000). In particular, FoxH1 appears to induce asymmetric expression of *lefty2* in response to Nodal signaling (Osada et al. 2000; Saijoh et al. 2000). In the mouse, *FoxH1* is expressed in early embryos (until the early somite stage) but is rapidly down-regulated as *nodal* expression disappears (Weisberg et al. 1998; Saijoh et al.

[1]**Corresponding author.**
E-MAIL hamada@imcb.osaka-u.ac.jp; FAX 81-6-6878-9846
Article and publication are at http://www.genesdev.org/cgi/doi/10.1101/gad. 883901.

2000). The expression patterns of *nodal* and *FoxH1* thus appear to overlap with each other. Together, these observations have implicated FoxH1 in Nodal signaling.

Both Smad2 and Smad3 interact with a large number of transcription factors, including TCF, NF-κB, Mix, and Gli (Whitman 1998). It has therefore remained possible that Nodal signaling is mediated in vivo by the interaction of Smad proteins with transcription factors other than FoxH1. Different transcription factors also may mediate Nodal signaling in different cell types. To determine the role of FoxH1 in Nodal signaling, we have therefore generated and characterized mutant mice that lack this transcription factor. The mutant embryos were shown to die early during embryonic development and to show various patterning defects that can be explained by a deficiency in Nodal signaling. Our results indicate that FoxH1 indeed mediates Nodal signaling during A-P patterning and node formation.

Results

Embryonic mortality of FoxH1$^{-/-}$ *mice*

To investigate the role of FoxH1 in development, we generated mutant mice that lack this transcription factor. The *FoxH1* gene is closely linked to *KIF-C2* in the reverse orientation; indeed, these two genes share a common 3′ untranslated region (Liu et al. 1999). We therefore determined to remove exon 1 of *FoxH1*, leaving *KIF-C2* intact (Fig. 1A). A targeting vector was designed to insert a Frt-flanked *neo* gene and a loxP site into the 5′ upstream region of *FoxH1* and to insert an additional loxP site into intron 1. Two embryonic stem (ES) cell lines (F94, F128) that had undergone homologous recombination were obtained (Fig. 1B), and the F94 ES cells were used to generate chimeric mice. Exon 1 of *FoxH1* and the *neo* gene were excised by crossing the chimeric animals with transgenic mice expressing the Cre recombinase (Sakai and Miyazaki 1997), resulting in the production of *FoxH1*$^{+/-}$ offspring (Fig. 1C). To generate a flox (flanked by loxP) allele (*FoxH1*^{flox}), we treated F128 ES cells with a Flp expression vector. One resulting clone, F128-10, from which *neo* had been correctly excised, was used to generate mice with the *FoxH1*^{flox} allele (Fig. 1C). Most of the analyses described in the present study focused on *FoxH1*$^{-/-}$ mice.

Both *FoxH1*$^{+/-}$ mice and *FoxH1*$^{flox/-}$ heterozygous mice appeared normal and fertile. Genotype analysis at weaning of progeny produced from intercrosses of *FoxH1*$^{+/-}$ heterozygotes revealed the absence of homozygous mutant animals, indicating that *FoxH1*$^{-/-}$ mutants die during embryonic development. The *FoxH1*$^{-}$ allele

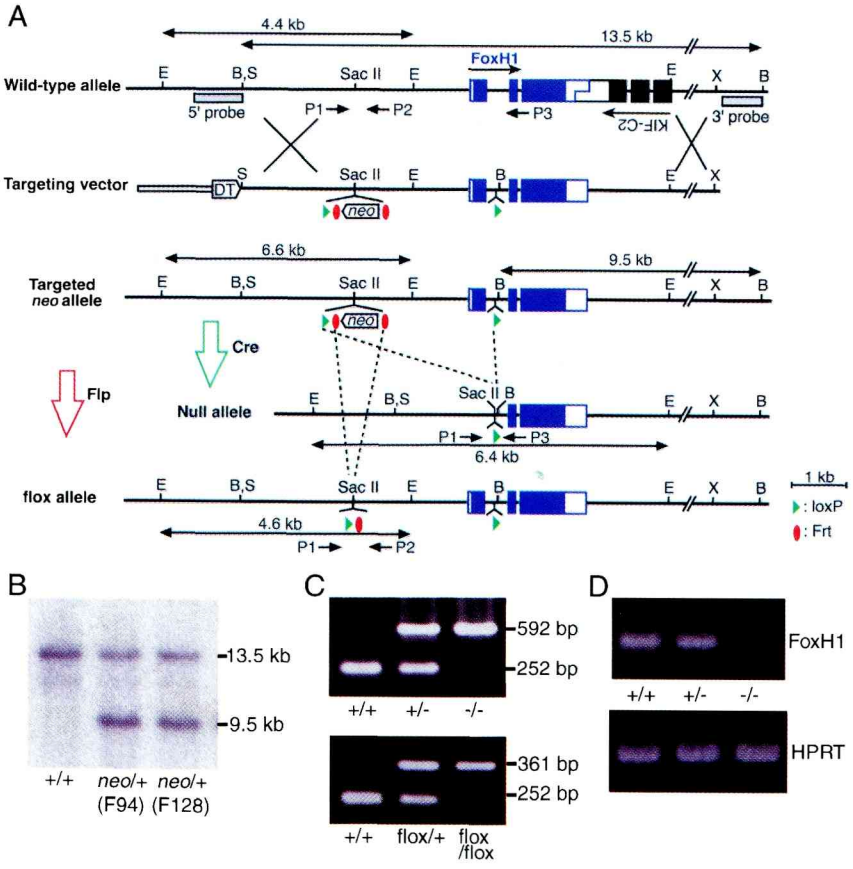

Figure 1. Generation of *FoxH1*$^{-/-}$ mice. (*A*) Targeting strategy. The genomic organization of *FoxH1* is shown at the top of the panel. The *KIF-C2* gene is closely linked to *FoxH1* in the opposite orientation. Homologous recombination between the wild-type *FoxH1* allele (exons are shown as purple solid boxes) and the targeting vector generates a *neo* insertional allele (*FoxH1*^{neo}). A null allele (*FoxH1*$^{-}$) was created by subsequent Cre-mediated deletion of the indicated region located between loxP sites. A flox allele (*FoxH1*^{flox}) was generated by Flp-mediated deletion of the *neo* cassette located between Frt sites. B indicates *Bam*HI; E, *Eco*RI; S, *Sac*I; X, *Xho*I; DT, diphtheria toxin resistance cassette. (*B*) Southern blot analysis of two correctly targeted ES cell clones (F94, F128). Genomic DNA was digested with *Eco*RI and subjected to hybridization with the 3′ probe indicated in *A*. The sizes of hybridized fragments are shown in kilobases. (*C*) PCR analysis of offspring obtained from intercrosses either of *FoxH1*$^{+/-}$ heterozygotes (*upper* panel) or of *FoxH1*$^{flox/+}$ heterozygotes (*lower* panel). PCR was performed with a mixture of the three primers (P1, P2, P3) shown in *A* or with a mixture of P1 and P2 (*upper* and *lower* panels, respectively). The sizes of PCR products are shown in base pairs. (*D*) Expression of *FoxH1* and *Hprt* mRNA in E7.5 wild-type and *FoxH1* mutant embryos was examined by RT-PCR. Note that *FoxH1* mRNA was not detected in the *FoxH1*$^{-/-}$ embryo.

lacking the exon 1 is probably a null allele because *FoxH1*-related RNA was not detected in *FoxH1*$^{-/-}$ embryos by in situ hybridization with a full-length *FoxH1* anti-sense probe (data not shown) or by reverse transcription–polymerase chain reaction (RT-PCR; Fig. 1D).

Variable pattern defects in FoxH1$^{-/-}$ *embryos*

To characterize the embryonic lethality of the homozygous *FoxH1* null allele, we analyzed between embryonic day 7.0 (E7.0) and E11.5 litters produced from heterozygote intercrosses. *FoxH1*$^{-/-}$ embryos showed a variable phenotype that could be classified into three types. Embryos with the type I (least severe) phenotype show marked axial defects, lacking a definitive node and notochord. Embryos with the type II (intermediate) phenotype completely lack anterior structures but possess posterior structures with midline defects. Embryos with the type III (most severe) phenotype lack structures derived from the embryo proper as a result of A-P patterning defects; they thus resemble *Cripto* mutant embryos (Ding et al. 1998).

The three types of *FoxH1*$^{-/-}$ embryos were distinguishable morphologically at E8.5 (Fig. 2). Type I embryos (65/

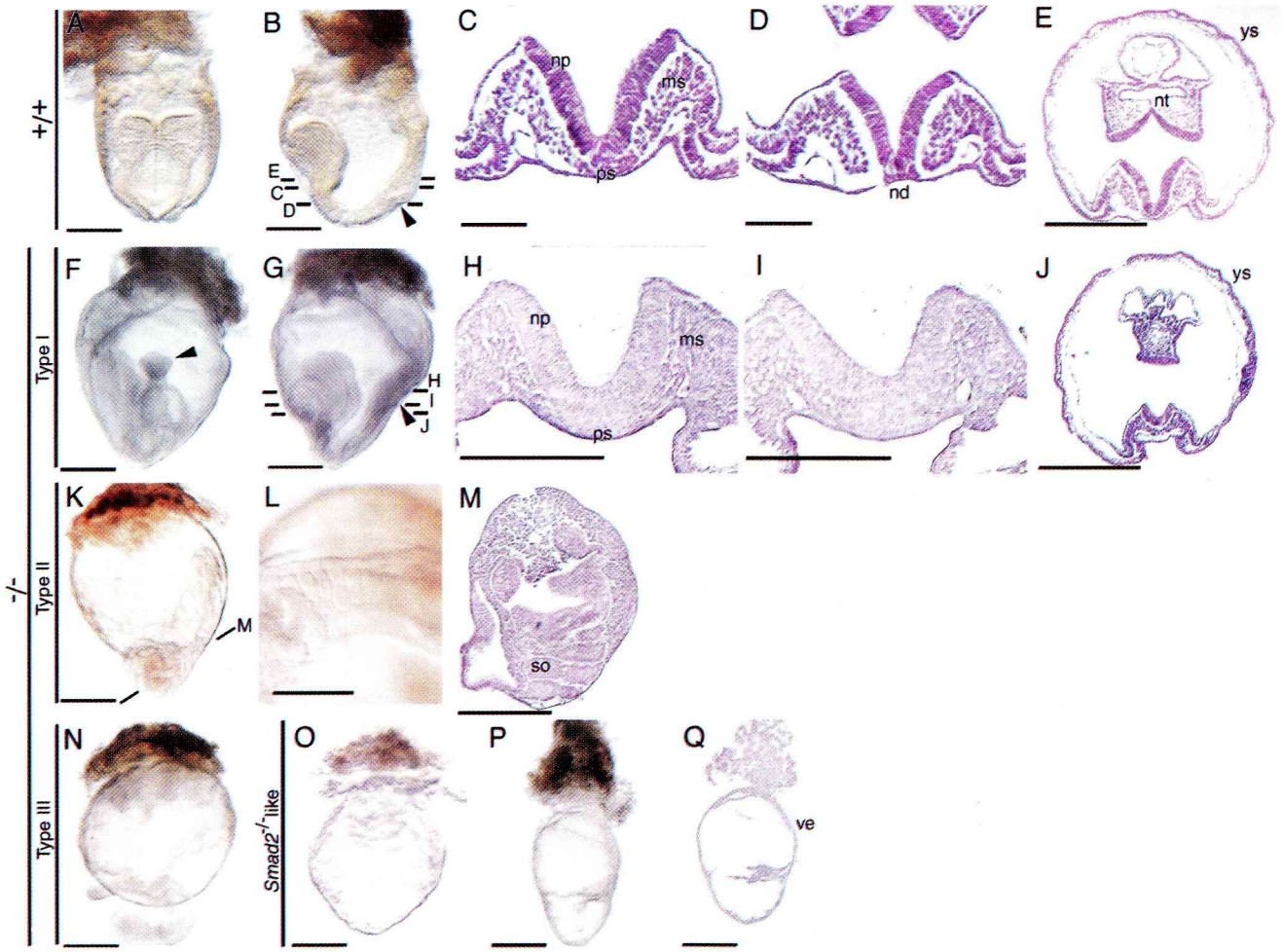

Figure 2. Three types of *FoxH1*$^{-/-}$ embryos at E8.5 (*A–N*). Typical morphologies of wild-type (+/+) embryos and of three types of *FoxH1*$^{-/-}$ mutant embryos at E8.5. Anterior views are shown in *A*, *F*, and *N*, whereas lateral views are shown in *B*, *G*, and *K*. The arrowhead in *B* indicates the position of the node. Although the type I embryo lacks a node, the corresponding position is indicated by the arrowhead in *G*. The arrowhead in *F* denotes a fused single head, which is characteristic of type I mutant embryos. A close-up ventral view of the type II embryo in *K* is shown in *L*, highlighting the fused somites. Sections of the wild-type and type I embryos are shown in *C–E* and *H–J*, respectively. The plane of each section is indicated in *B* and *G*. Sections *C* and *H* are at the level of the primitive streak. Sections *D* and *I* are at the level of the node. Transverse sections were all oriented with anterior to the top. The type I embryo possesses a primitive streak (*H*) but lacks a node (*I*) and axial tissues (*J*). Fused somites of a type II embryo are apparent in the section shown in *M*. The embryos shown in *O–Q* are rare examples of the most severe (*Smad2*$^{-/-}$-like) phenotype observed for *FoxH1*$^{-/-}$ embryos at E8.5 (*O*) or E7.5 (*P,Q*). A frontal section of the embryo in *P* is shown in *Q*. Endoderm cells are abnormal in that those in the embryonic region are columnar, an extraembryonic characteristic (*P,Q*). The embryonic ectoderm is absent, but mesoderm-like cells are present inside (*Q*). ms indicates mesoderm; nd, node; np, neural plate; nt, notochord; ps, primitive streak; so, somites; and ys, yolk sac. Scale bars indicate 500 μm with the exception of those in *C*, *D*, *H*, and *I*, which represent 100 μm.

152 of *FoxH1*$^{-/-}$ embryos, 43%) showed a single, narrow-fused head structure, or pinheadlike morphology (Fig. 2F,G). In transverse sections, the primitive streak was detected (Fig. 2H), but midline structures such as the node, prechordal plate, notochordal plate–notochord, and floor plate were missing (Fig. 2I,J). The neural plate was unfolded and markedly thickened (Fig. 2I,J), and ectopic ingression of mesoderm was apparent between the neural plate and the primitive endoderm (Fig. 2J). Somites had formed, but they were fewer in number than in wild-type embryos and were fused in the midline. Type II mutant embryos (31/152 of *FoxH1*$^{-/-}$ embryos, 20%) showed severe anterior truncation; they completely lacked anterior structures, such as the head fold, and instead manifested accumulation of cells in the distal region (occasionally, a beating heart–like structure was observed). Extraembryonic tissues such as the amnion and allantois, which were absent in type III embryos, were properly formed (Fig. 2K). The posterior portion of the embryo was formed but showed severe midline defects. Thus, several somites had formed, but they were fused across the midline (Fig. 2K–M). Type III embryos (52/152 of *FoxH1*$^{-/-}$ embryos, 34%) showed no signs of development of the embryo proper and showed a balloon-like morphology at this time (Fig. 2N). The embryo proper was recognized as a small cell mass located outside the yolk sac. In contrast, the yolk sac appeared relatively normal; it consisted of endodermal and mesothelial layers and contained blood islands. However, other components of extraembryonic tissue, such as the chorion, amnion, and allantois, were not observed, suggesting that the A-P axis was not properly formed. Rare embryos (4/152 of *FoxH1*$^{-/-}$ embryos, 3%) showed relatively normal extraembryonic components with no embryo proper (Fig. 2O–Q) and therefore resembled *Smad2* mutant embryos (Waldrip et al. 1998).

Three types of *FoxH1*$^{-/-}$ embryos were also distinguishable on the basis of their morphology at E7.5. At this stage, mutant embryos showed various degrees of constriction at the extraembryonic-embryonic junction (Fig. 3). Mutant embryos that showed this constriction also manifested histological anomalies. In normal embryos, endoderm cells in the extraembryonic region are cuboidal and contain apical vacuoles, whereas those in the embryonic region are squamous. In the mutant embryos with the most marked constriction, however, endoderm cells in both the embryonic and extraembryonic regions are cuboidal and contain apical vacuoles (Fig.

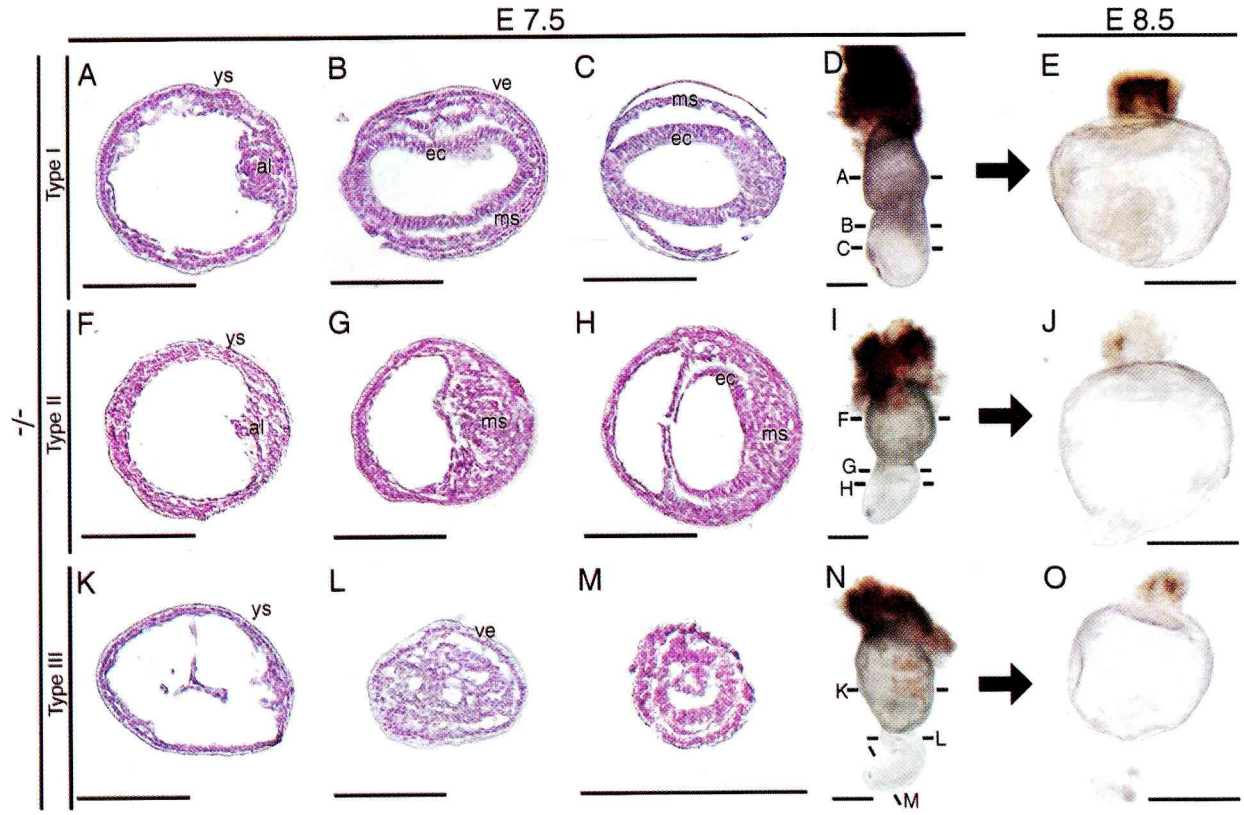

Figure 3. Morphology of *FoxH1*$^{-/-}$ embryos at E7.5 and their subsequent development in vitro. Three types of *FoxH1*$^{-/-}$ embryos at E7.5 showed no (*D*), mild (*I*), or severe (*N*) constriction at the extraembryonic-embryonic junction. Transverse sections at the level of the extraembryonic region (*A,F,K*), the proximal embryonic region (*B,G,L*), and the distal embryonic region (*C,H,M*) are shown for each type of embryo. Embryos recovered at E7.5 were cultured in vitro for an additional 24 h (*E,J,O*). Embryos that showed no (*D*), mild (*I*), or severe (*N*) constriction at E7.5 developed the type I (*E*), type II (*J*), and type III (*O*) morphologies, respectively. Scale bars indicate 200 μm with the exception of those in *E*, *J*, and *O*, which represent 500 μm. al indicates allantois; ec, embryonic ectoderm; ms, mesoderm; ve, visceral endoderm; ys, yolk sac.

3K–M). Furthermore, whereas the mesoderm layer was present in the extraembryonic region (Fig. 3K), the normal organized structure of the ectoderm and mesoderm was not apparent in the embryonic region (Fig. 3L,M). Such histological anomalies were not detected in *FoxH1*$^{-/-}$ embryos that did not show a constriction (Fig. 3A–C). Mutant embryos in which the constriction was apparent but not pronounced showed relatively organized structures, although mesodermal cells accumulated near the junction between the embryonic and extraembryonic regions (Fig. 3F–H).

To determine the relation between the defects apparent at E7.5 and those observed at E8.5, embryos were recovered at E7.5 and allowed to develop in vitro for an additional 24 h. Embryos showing a severe constriction at E7.5 (Fig. 3N) developed the type III morphology after culture in vitro (Fig. 3O). Those showing a mild constriction (Fig. 3I) developed the type II morphology (Fig. 3J). Finally, *FoxH1*$^{-/-}$ embryos showing no constriction at E7.5 (Fig. 3D) developed the type I morphology (Fig. 3E). Therefore, embryos at stages earlier than E8.5 will hereafter also be referred to as type I, II, or III, accordingly.

Impaired orientation of the A-P axis in type III FoxH1$^{-/-}$ *embryos*

The constriction at the extraembryonic-embryonic junction of type III (and, to a lesser extent, of type II) *FoxH1*$^{-/-}$ embryos at E7.5 is reminiscent of the constriction that is a characteristic feature of *HNF3β/FoxA2* (Ang and Rossant 1994; Weinstein et al. 1994), *Lim1* (Shawlot and Behringer 1995), *Otx2* (Acampora et al. 1995; Matsuo et al. 1995; Ang et al. 1998), and *nodal* (Varlet et al. 1997) mutants, all of which show defects in anterior specification caused by impaired function of the anterior visceral endoderm (AVE). We therefore examined type III (and type II) embryos for several AVE markers.

In normal embryos at E5.5, two AVE marker genes, *Hex* and *lefty1*, are initially expressed in the visceral endoderm at the distal tip (Thomas and Beddington 1996; Thomas et al. 1998; data not shown). The visceral endoderm cells expressing these genes subsequently migrate anteriorly to form the AVE by E6.5. Thus, *Hex*, *Cer-l*, *Hesx1*, and *lefty1* are all expressed in the AVE at E6.75 (Fig. 4A,D,H,N). In contrast, *Brachyury* is initially expressed in the proximal epiblast, but its expression domain subsequently moves to the posterior side at E6.5 and marks the primitive streak (Fig. 4A). These complementary cell movements establish A-P polarity.

In type III *FoxH1*$^{-/-}$ embryos, however, *Hex*-expressing cells remained in the distal region at E6.75, with no evidence of movement toward the future anterior side (Fig. 4B). *Cer-l* (Fig. 4E), *Hesx1* (Fig. 4I), and *Lim-1* (data not shown) were also expressed in the visceral endoderm at the distal tip at this time, indicating that the AVE is incorrectly formed in the distal region. Conversely, the *Brachyury* expression domain failed to move to the posterior side, remaining in the proximal epiblast (Fig. 4B,E,I,O). *Otx2* expression in the visceral endoderm was maintained in the mutant embryo (Fig. 4L). The expression of *lefty1* in the visceral endoderm was abolished in the type III mutants (Fig. 4O), indicating that *lefty1* expression in the endoderm may normally be induced by a Nodal-FoxH1 signaling pathway.

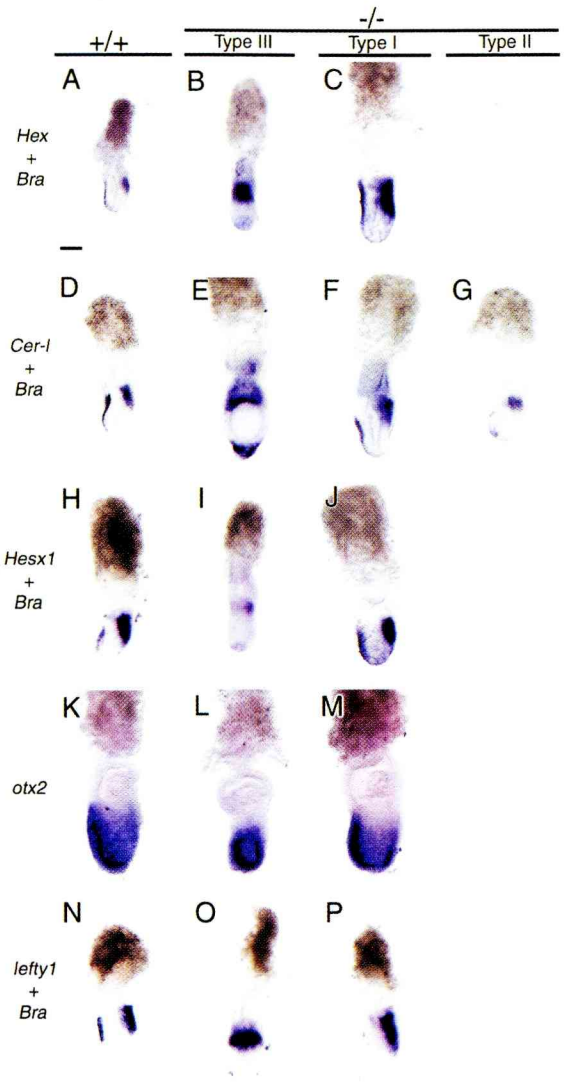

Figure 4. Misorientation of the A-P axis in type III *FoxH1*$^{-/-}$ embryos. Expression of various AVE marker genes was examined by whole-mount in situ hybridization in wild-type (+/+) embryos and in each of the three types of *FoxH1*$^{-/-}$ mutant embryos at E6.75. Probes were specific for *Hex* (*A–C*), *Cer-l* (*D–G*), *Hesx-1* (*H–J*), *Otx2* (*K–M*) or *lefty1* (*N–P*) transcripts. The probe for *Brachyury* was also included in the indicated samples. Lateral views are shown for each embryo, with the anterior side on the left. Scale bars: 200 μm.

We also examined the type III embryo at E7.25. Whereas *Brachyury* expression remained in the proximal epiblast (Fig. 5C), expression of *goosecoid*, which marks the anterior primitive streak at this stage, was lost (Fig. 5I). *FoxA2* expression, which also marks the anterior primitive streak, was absent, but its expression in the visceral endoderm was maintained (Fig. 5L,M). Furthermore, expression of *lefty2*, a marker for the nascent me-

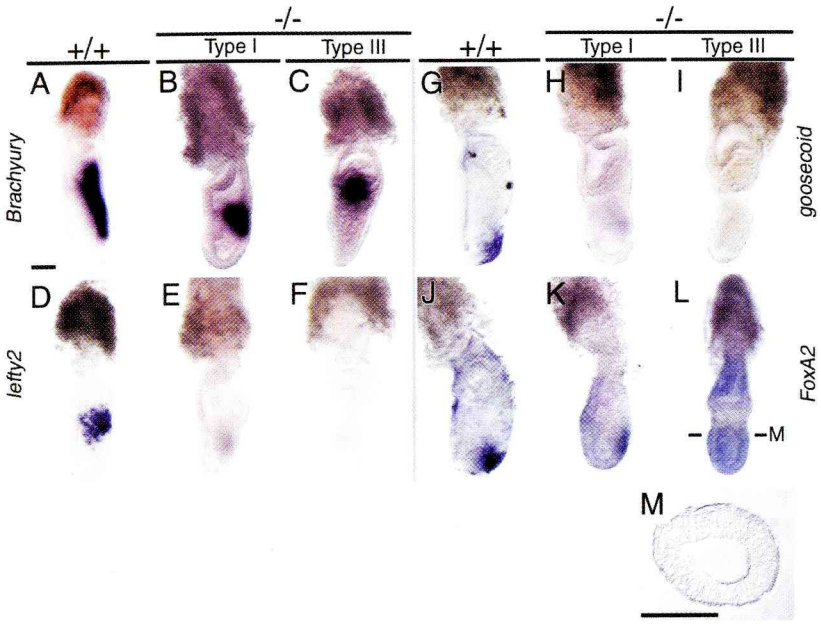

Figure 5. Defective morphogenesis of the primitive streak in *FoxH1*$^{-/-}$ embryos. Expression of various marker genes for the primitive streak was examined by whole-mount in situ hybridization in wild-type (+/+) embryos as well as in type II and type I *FoxH1*$^{-/-}$ embryos at E7.25. Probes were specific for *Brachyury* (*A–C*), *lefty2* (*D–F*), *goosecoid* (*G–I*), or *FoxA2* (*J–L*) transcripts. Lateral views are shown for each embryo, with the anterior side on the left. A transverse section at the plane indicated in (*L*) are shown in (*M*). *FoxA2* expression was maintained in the endoderm of the type III mutant embryo. Scale bars: 200 μm.

soderm, was also absent (Fig. 5F), indicating the lack of the primitive streak. *Otx2*, which is initially expressed before gastrulation throughout the epiblast and becomes restricted to the anterior third of the embryo by E7.5 (Ang et al. 1994), was widely expressed in the ectoderm layer of type III embryos at E7.5 (data not shown). These results indicate that proximal-distal (P-D) polarity is properly established in the type III mutants but that this polarity is not converted to the A-P axis. Incorrect orientation of the A-P axis is likely caused by impaired movement of the distal visceral endoderm. Consistent with this notion, sagittal sections of type III embryos (such as the one shown in Fig. 4E) revealed a marked accumulation of endoderm-like cells at the distal tip (data not shown). These defects are highly similar to those of *Cripto* mutants (Ding et al. 1998), but with one important difference: Anterior neural fates (*Bf1*- and *En1*-expressing cells) are induced in the distal region of *Cripto* mutants (Ding et al. 1998) but not in the corresponding region of type III *FoxH1*$^{-/-}$ embryos (data not shown). The visceral endoderm cells at the distal end are enlarged in *Cripto* mutants (Ding et al. 1998), whereas massive endoderm cells accumulate in type III *FoxH1*$^{-/-}$ mutants (Fig. 4E).

Type II embryos show similar but less severe phenotypes at this stage of development. The expression of *Cer-l* in the visceral endoderm at E6.75 was down-regulated; the expression domain of this gene was apparent on the future anterior side but was located closer to the distal tip than in wild-type embryos (Fig. 4G). These results indicate that A-P patterning is partially impaired and that the AVE is not fully functional in type II embryos, which likely explains why they lack anterior structures. In contrast, type I embryos showed normal expression patterns for *Brachyury* (Fig. 4C,F,J,P), *Hex* (Fig. 4C), *Cer-l* (Fig. 4F), *Hesx1* (Fig. 4J), and *Otx2* (Fig. 4M) but had lost *lefty1* expression in the AVE (Fig. 4P).

Failure of primitive streak elongation and lack of the node in type I FoxH1$^{-/-}$ *mutants*

Histological examination indicated that type I *FoxH1*$^{-/-}$ embryos lack a definitive node, prechordal plate, and notochordal plate–notochord (Fig. 2H–J). To confirm these observations, we examined the expression at E8.5 of *Shh*, *Brachyury*, and *HNF3β* genes that are normally expressed in the node and its derivatives at this stage (Fig. 6A,C,E,I). In type I mutants, the expression of *Shh* (Fig. 6B,D) and *HNF3β* (Fig. 6J) was completely lost, and only sparse expression of *Brachyury* was apparent at the anterior midline (Fig. 6F), indicating a deficiency of node-derived tissues. Type I embryos develop a single fused-head structure (pinhead) and specifically lack the most rostral portion, the forebrain. Thus, *Six3* expression, which is a marker for the forebrain (Fig. 6L), was abolished in type I mutants (Fig. 6M), whereas *Otx2* expression, which marks the forebrain and midbrain (Fig. 6N), was detected in these mutants (Fig. 6O). In normal embryos, *Fgf8* is expressed in the forebrain, midbrain-hindbrain junction, and posterior streak at this stage (Fig. 6C; Crossley and Martin 1995). In type I embryos, however, *Fgf8* expression in the most anterior region was not apparent, although the other expression domains were preserved (Fig. 6H). The lack of the forebrain is likely because of the absence of the prechordal plate, insufficient function of the AVE, or both. Truncation of anterior structures is more severe in type II embryos. Thus, Otx2 expression (Fig. 6P) and HNF3β expression in the midline (Fig. 6K) are absent.

To investigate the mechanisms by which the absence of FoxH1 results in the failure of node formation, we examined the primitive streak of type I embryos at earlier stages. During normal gastrulation, *Brachyury* is expressed in the entire primitive streak, and its expression domain extends anteriorly with the extension of the

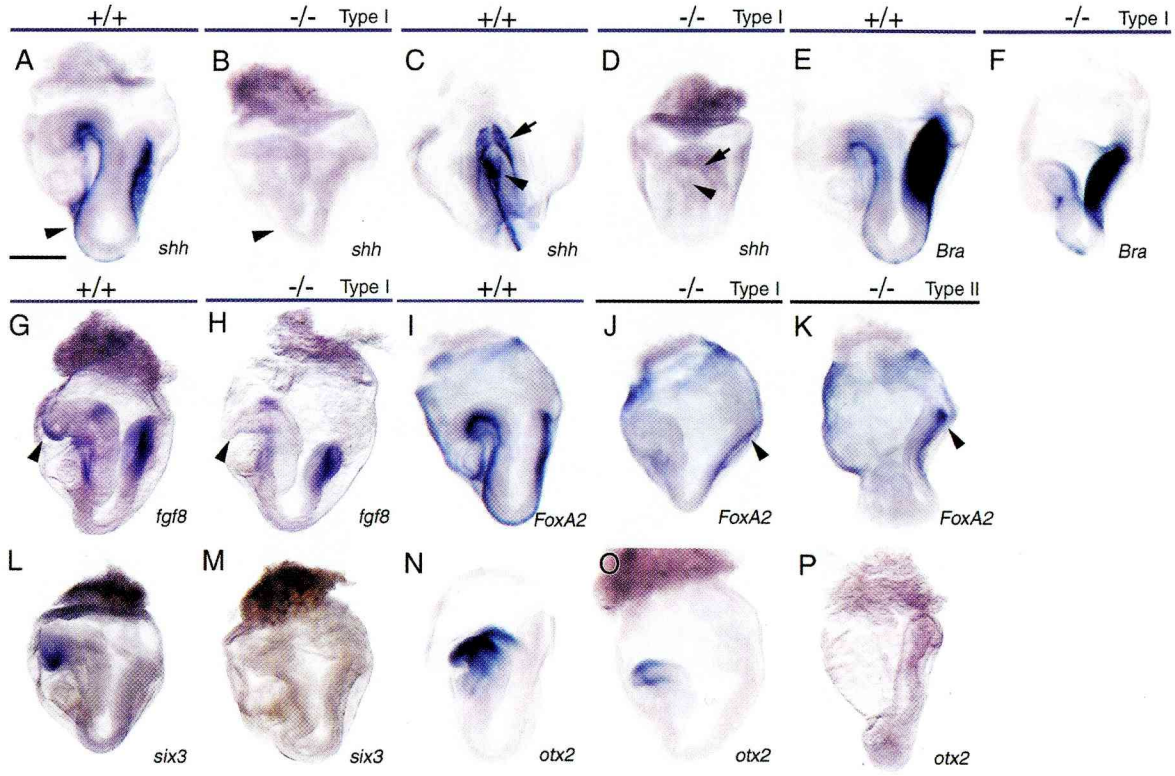

Figure 6. Midline defects in type I *FoxH1*$^{-/-}$ embryos. Expression of various midline markers and forebrain markers in wild-type (+/+) and *FoxH1*$^{-/-}$ mutant embryos was examined at E8.5 by whole-mount in situ hybridization. Probes were specific for *Shh* (*A–D*), *Brachyury* (*E,F*), *Fgf8* (*G,H*), *FoxA2* (*I–K*), *Six3* (*L,M*), or *Otx2* (*N–P*) transcripts. All mutant embryos are type I with the exception of those shown in *K* and *P*, which are type II. Lateral views are shown for each embryo with the anterior side on the left, except that posterior views are shown for *C* and *D*. The arrowheads in *A* and *B* indicate the notochord. The arrowheads and arrows in *C* and *D* indicate the node and definitive endoderm, respectively. The arrowhead in *G* indicates an *Fgf8* expression domain in the forebrain, which was lost in *H*. In type II (*K*) and type I (*J*) mutant embryos, *FoxA2* expression is absent in the definitive endoderm but is apparent in the yolk sac (arrowheads). Scale bars: 500 μm.

streak (Fig. 5A; Kispert and Herrmann 1994). In type I mutants, the *Brachyury* expression domain was localized to the posterior side, but it failed to elongate anteriorly or distally (Fig. 5B). The expression of *goosecoid* and *FoxA2*, which marks the anterior primitive streak at this stage in normal embryos (Fig. 5G,J; Sasaki and Hogan 1993; Ang and Rossant 1994; Weinstein et al. 1994), was also examined. In the mutant embryos, *goosecoid* expression was greatly reduced and observed in the posterior-proximal region of the embryo proper (Fig. 5H). The expression of *FoxA2* was also down-regulated and detected in the proximal region of the embryo proper (Fig. 5K), indicating that the anterior primitive streak was not properly specified. The expression of *lefty2*, which marks nascent mesoderm generated from the primitive streak (Fig. 5D; Meno et al. 1997), was also markedly down-regulated in type I mutants (Fig. 5E). Given that *lefty2* expression is induced by a Nodal-FoxH1 signaling pathway, at least in the lateral plate at the early somite stage (Saijoh et. al. 2000), this down-regulation of *lefty2* may result directly from the loss of Nodal signaling. Together, these results indicate that formation of the primitive streak is initiated in type I embryos, but the anterior portion of the streak is not properly specified, resulting in node agenesis.

Genetic interaction between FoxH1 *and* nodal

The expression of *nodal* is induced by a Nodal-FoxH1 signaling pathway, at least in certain aspects of development, such as left-sided expression of this gene in the lateral plate at the early somite stage (Osada et al. 2000; Saijoh et al. 2000). Expression of *nodal* in the posterior-distal ectoderm during gastrulation also may be regulated by a FoxH1-dependent enhancer (Norris and Robertson 1999). We therefore examined *nodal* expression in *FoxH1*$^{-/-}$ embryos with the use of in situ hybridization. In wild-type embryos, this gene is initially expressed throughout the epiblast and in the underlying primitive endoderm at E5.5, but its expression in the epiblast becomes progressively restricted to the posterior region (Fig. 7A; Varlet et al. 1997). The expression of *nodal* disappears from the AVE at E6.75, but it is maintained in the lateral and posterior portions of visceral endoderm. It disappears from the posterior ectoderm and the visceral endoderm at E7.25 and then begins in the prospective

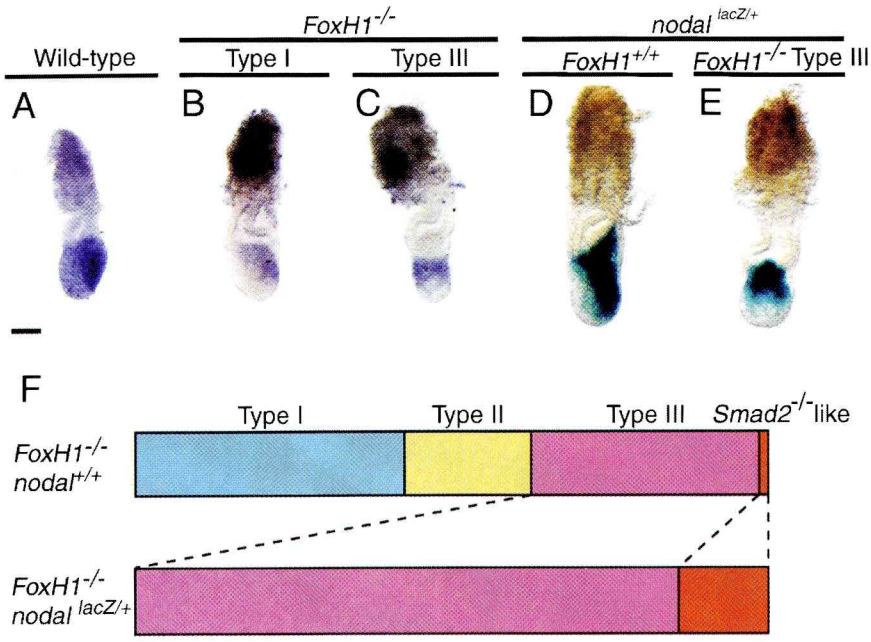

Figure 7. Genetic interaction between *FoxH1* and *nodal*. The expression of *nodal* in wild-type (*A*), type I *FoxH1*$^{-/-}$ (*B*), and type III *FoxH1*$^{-/-}$ (*C*) embryos was examined at E7.0 by whole-mount in situ hybridization. In type I embryos, *nodal* expression was greatly reduced and was confined to the proximal posterior ectoderm (*B*). In type III embryos (*C*), *nodal* expression was down-regulated and remained at the rim of the proximal epiblast. The frequencies of type III, type II, type I, and *Smad2*$^{-/-}$-like phenotypes were also determined for *FoxH1*$^{-/-}$,*nodal*$^{+/+}$ (*upper bar*) and *FoxH1*$^{-/-}$,*nodal*$^{lacZ/+}$ (*lower bar*) embryos at E8.5 (*F*). The total numbers of the embryos examined are 152 and 28 for *FoxH1*$^{-/-}$,*nodal*$^{+/+}$ and *FoxH1*$^{-/-}$,*nodal*$^{lacZ/+}$, respectively. Most *FoxH1*$^{-/-}$,*nodal*$^{lacZ/+}$ embryos showed the type III morphology. Staining for β-galactosidase activity is also shown for *FoxH1*$^{+/+}$,*nodal*$^{lacZ/+}$ (*D*) and *FoxH1*$^{-/-}$,*nodal*$^{lacZ/+}$ (*E*) embryos at E7.0. Scale bars: 200 μm.

node. In type III *FoxH1*$^{-/-}$ embryos, however, *nodal* expression was down-regulated and remained at the rim of the proximal epiblast at E7.0, without being shifted to the posterior side (Fig. 7C). In type I embryos, the abundance of *nodal* mRNA was also reduced (Fig. 7B); the *nodal* expression site was shifted to the posterior side but was localized more proximally than in wild-type embryos. The down-regulation of *nodal* apparent in *FoxH1*$^{-/-}$ embryos indicates that the expression of this gene in the epiblast is maintained by a positive autoregulatory loop that includes FoxH1.

We also examined the potential genetic interaction between *FoxH1* and *nodal* by crossing *FoxH1* and *nodal*^{lacZ} mutants (Collignon et al. 1996). Double heterozygotes (*FoxH1*$^{+/-}$,*nodal*$^{lacZ/+}$) appeared normal and were crossed with *FoxH1*$^{+/-}$ mice. The phenotype of the resulting *FoxH1*$^{-/-}$, *nodal*$^{lacZ/+}$ embryos was more severe than that of *FoxH1*$^{-/-}$, *nodal*$^{+/+}$ embryos (Fig. 7F). Thus, most (24/28, 86%) of the *FoxH1*$^{-/-}$, *nodal*$^{lacZ/+}$ embryos examined at E8.5 were type III, manifesting A-P patterning defects; the remaining embryos (4/28, 14%) resembled *Smad2* mutant embryos, similar to the *FoxH1*$^{-/-}$ mutant shown in Figure 2O. As expected, *nodal* expression, which was monitored on the basis of the activity of the *nodal*^{lacZ} allele, remained in the proximal epiblast at E7.0 in all *FoxH1*$^{-/-}$, *nodal*$^{lacZ/+}$ embryos examined (Fig. 7E).

Rescue of A-P patterning defects, but not midline defects, in FoxH1$^{-/-}$ *embryos by expression of FoxH1 in extraembryonic tissues*

We next examined whether FoxH1 is required in the epiblast lineage or in the extraembryonic lineage, including the primitive endoderm. The *FoxH1* gene was specifically deleted from the epiblast with the use of the *FoxH1*^{flox} allele and transgenic mice that express Cre in the epiblast and its derivatives but not in the primitive endoderm. The Cre-expressing transgenic mice harbor *lefty2-Cre*, a fusion construct comprising the *Cre* gene linked to the 5.5-kb upstream region of *lefty2* (Fig. 8A). When linked to the *lacZ* gene, the 5.5-kb upstream region of *lefty2* confers expression in the nascent mesoderm at E6.5 to E7.0 and in the left lateral plate mesoderm at E8.25 (Saijoh et al. 1999). However, one *lefty2-Cre* transgenic line (21B) showed epiblast-specific expression of *Cre* between E5.5 and E8.0 (*lefty2* is not expressed in the epiblast). Thus, crossing of line 21B animals with mice that harbor a Cre-sensitive *lacZ* reporter gene (Sakai and Miyazaki 1997) yielded embryos harboring both *lefty2-Cre* and the *lacZ* reporter gene that showed β-galactosidase activity throughout the epiblast lineage but not in the extraembryonic tissues, including the primitive endoderm, both at E6.5 (Fig. 8B,C) and E7.0 (Fig. 8D,E).

We crossed *FoxH*$^{+/-}$ animals harboring the *Cre* transgene with *FoxH1*$^{flox/flox}$ mice and genotyped the resulting embryos by PCR analysis of yolk sac DNA. *FoxH1*$^{flox/-}$, *lefty2-Cre* embryos were first examined at E8.5; most (15/16, 94%) of these embryos showed the type I phenotype, having a single fused head (Fig. 8J–L). We also examined *FoxH1*$^{flox/-}$, *lefty2-Cre* embryos at an earlier stage (E7.0). Again, they (3/3) showed the type I morphology, showing normal *Cer-l* expression in the AVE region (Fig. 8N); type III embryos showing *Cer-l* expression at the distal end (such as the one shown in Fig. 4B) were not detected (0/3) at this stage. Unexpectedly, *lefty1* expression in the visceral endoderm was lost in the epiblast-specific *FoxH1* mutant embryos (Fig. 8P), indicating that the expression of *lefty1* is induced by

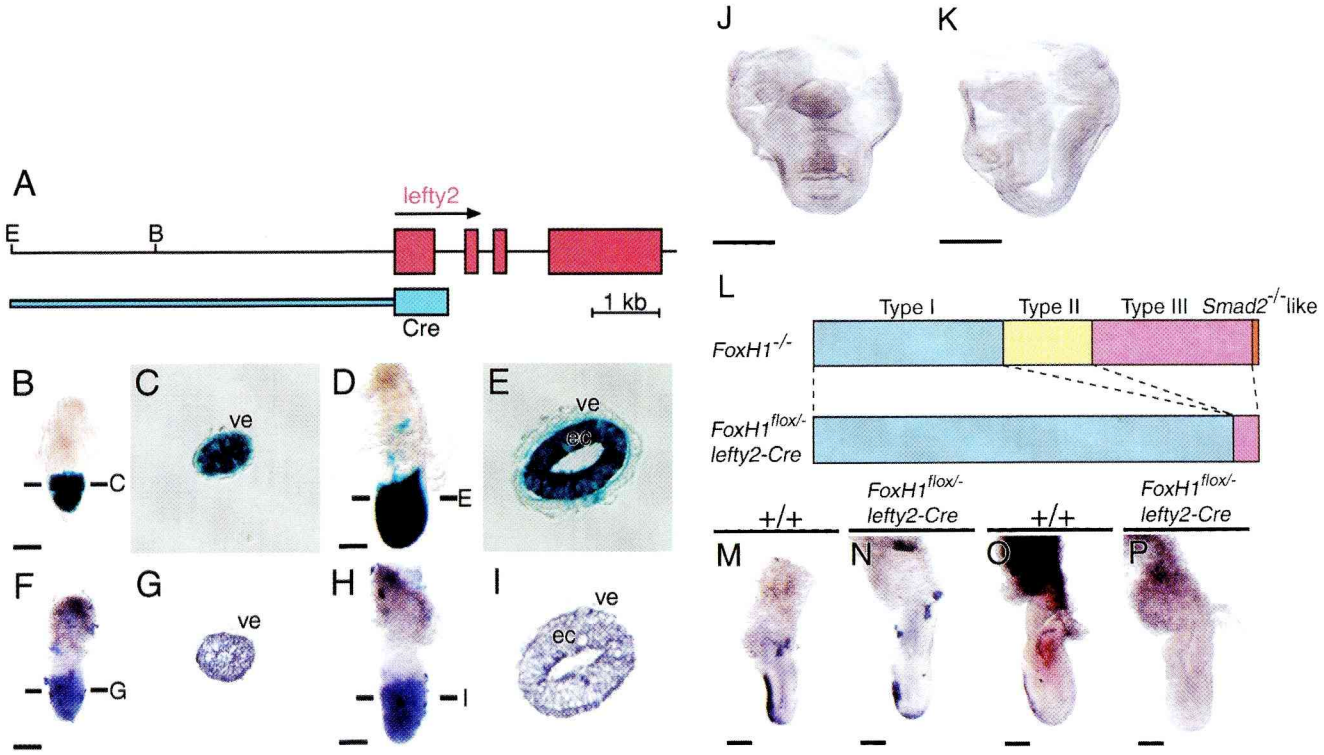

Figure 8. Midline defects but normal A-P patterning in embryos with epiblast-specific deletion of *FoxH1*. The structure of the *lefty2-Cre* transgene, in which *Cre* is linked to the 5.5-kb upstream region of mouse *lefty2*, is shown in *A*. Mice harboring this transgene (line 21B) were crossed with mice that express *lacZ* in response to Cre. Embryos containing both *lefty2-Cre* and the *lacZ* reporter gene were stained for β-galactosidase activity at E6.5 (*B,C*) and E7.0 (*D,E*); transverse sections at the planes indicated in *B* and *D* are shown in *C* and *E*, respectively. At both stages, staining is apparent in the epiblast but is absent from the remaining portions of the embryo. Expression of *FoxH1* was examined in the wild-type embryos by whole-mount in situ hybridization at E6.5 (*F,G*) and E7.0 (*H, I*); transverse sections at the planes indicated in *F* and *H* are shown in *G* and *I*, respectively. A $FoxH1^{flox/-}$ embryo harboring the *lefty2-Cre* transgene examined at E8.5 showed typical type I morphology, with a fused head (*J,K*). Anterior and lateral views of the same embryo are shown in *J* and *K*, respectively. The frequencies of type III, type II, type I, and $Smad2^{-/-}$-like phenotypes are shown for $FoxH1^{-/-}$ (*upper bar*) and $FoxH1^{flox/-}$ *lefty2-Cre* (*lower bar*) embryos at E8.5 (*L*); most of the $FoxH1^{flox/-}$, *lefty2-Cre* embryos showed the type I morphology. The total number of the $FoxH1^{flox/-}$, *lefty2-Cre* embryos examined is 16. Expression of *Cer-l* (*M,N*) and *lefty1* (*O,P*) was examined in wild-type (+/+) and $FoxH1^{flox/-}$, *lefty2-Cre* embryos at E7.0; the $FoxH1^{flox/-}$, *lefty2-Cre* embryos showed a normal *Cer-l* expression pattern (*N*) but had lost *lefty1* expression in the AVE (*P*). Scale bars indicate 200 μm with the exception of those in *J* and *K*, which represent 500 μm. ec indicates embryonic ectoderm; ve, visceral endoderm.

FoxH1-dependent signals (most likely, Nodal signals) derived from the epiblast. Type II embryos were not detected at either E8.5 or E7.0. These results indicate that the presence of FoxH1 in the primitive endoderm is able to rescue the A-P patterning defects of type III and type II embryos but not the anterior primitive streak defects of type I embryos.

We also examined chimeric embryos that were generated by injecting $FoxH1^{+/+}$ ES (ROSA26) cells into $FoxH1^{-/-}$ blastocysts (Fig. 9). Among such chimeras with extensive colonization of ROSA26 ES cells, about a half of them (5/9) showed severe A-P patterning defects characteristic of type III phenotype (Fig. 9J,K). In the remaining chimeric embryos, midline defects were mostly rescued (Fig. 9E–I). Thus, the node and notochordal plate were formed (data not shown), and somites on the both sides were separated by the midline (Fig. 9I). The neural plate was folded along the A-P axis (Fig. 9G), but the most rostral part of the neural plate remained unfolded (Fig. 9H). Therefore, injection of wild-type ES cells could rescue midline defects but failed to rescue A-P patterning defects.

These results indicate that FoxH1 in the primitive endoderm is required for A-P patterning, whereas FoxH1 in the epiblast is essential for primitive streak formation. The expression pattern of *FoxH1* is consistent with this notion; *FoxH1* was expressed both in the visceral endoderm and in the epiblast, but not in the extraembryonic region, of wild-type embryos at E6.5 to E7.0 (Figs. 8F–I). Therefore, among the nonepiblast tissues, it is most likely in the visceral endoderm that FoxH1 plays a role in A-P patterning.

Discussion

Our analysis of *FoxH1* mutant mice indicates that FoxH1 is the major transcriptional transducer of Nodal signaling in early development. This transcription factor

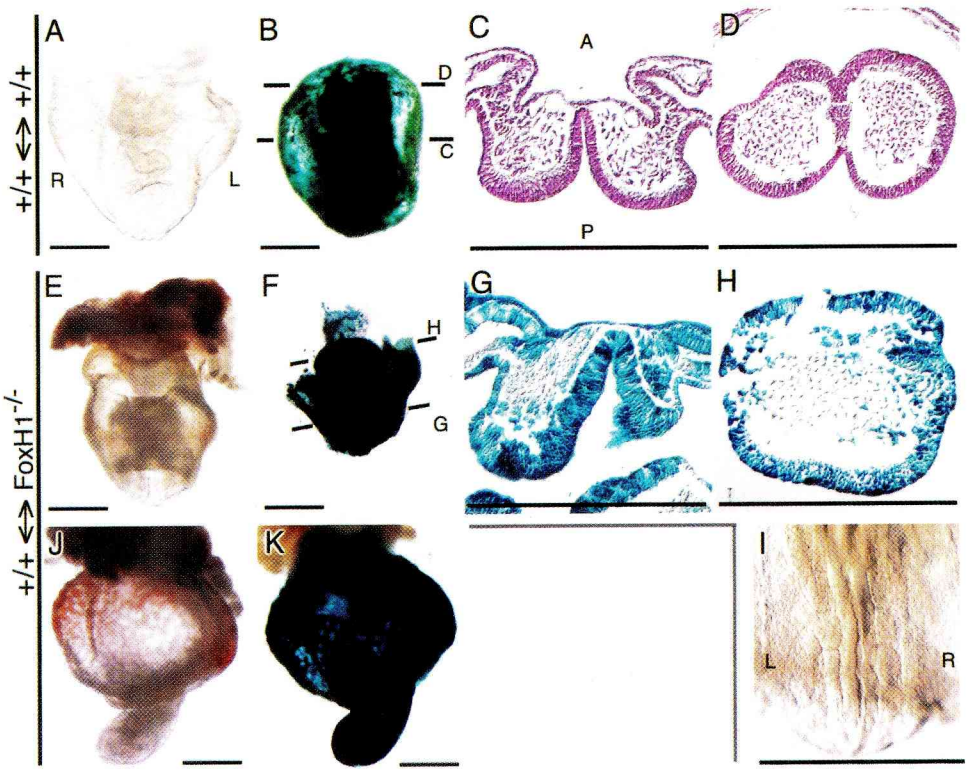

Figure 9. Rescue of midline defects but not A-P patterning defects by wild-type embryonic cells in wild-type (↔) *FoxH1*$^{-/-}$ chimeric embryos. Wild-type (↔) *FoxH1*$^{+/+}$ (*A–D*) and wild-type (↔) *FoxH1*$^{-/-}$ (*E–K*) chimeric embryos were recovered at E8.5. Whole-mount views of the chimeric embryos with extensive colonization of wild-type ES cells are shown before (*A,E,I,J*) or after (*B,F,K*) X-Gal staining. They are all anterior views except that a ventral view is shown in *I*. Hematoxylin and eosine-stained sections of a wild-type (↔) *FoxH1*$^{+/+}$ chimeric embryo at the levels of the trunk and forebrain are shown in *C* and *D*, respectively. Corresponding sections of X-Gal stained wild-type (↔) *FoxH1*$^{-/-}$ chimeric embryo are shown in *G* and *H*. About a half of the wild-type (↔) *FoxH1*$^{-/-}$ embryo shown in *E–I*, midline defects were rescued (*E,G,I*) whereas the forebrain remained abnormal (*H*). The neural plate, except for the most rostral part (*H*), was folded normally (*G*). The remaining wild-type (↔) *FoxH1*$^{-/-}$ embryos (*J,K*) showed severe A-P patterning defects characteristic of type III phenotype. Scale bar indicates 500μm.

appears to play multiple roles: Its activity in the primitive endoderm and in the epiblast is essential for A-P patterning and for node formation, respectively. A zebrafish mutant (*schumalspur*, or *sur*) that is deficient in FoxH1 has been described recently (Pogoda et al. 2000; Sirotkin et al. 2000). This mutant lacks an organizer and shows defects in dorsal axial structures that are equivalent to the defects observed in type I *FoxH1*$^{-/-}$ mice.

FoxH1-dependent signals in visceral endoderm are required for orienting the A-P axis

The A-P axis is established by three sequential steps: (1) graded expression of several genes along the P-D axis of the embryo, (2) movement of the distal visceral endoderm toward the anterior end of the embryo, and (3) specification of the underlying epiblast to an anterior identity by AVE-derived signals (Beddington and Robertson 1998, 1999; Kimura et al. 2000).

In type III *FoxH1*$^{-/-}$ embryos, the P-D axis is established properly in the egg cylinder structure, but the distal visceral endoderm fails to migrate anteriorly. Epiblast-specific deletion of *FoxH1* indicated that FoxH1 in the visceral endoderm is essential for cell movement. The FoxH1-dependent signals may be provided by Nodal, a notion that is supported by previous observations by other researchers. Thus, type III *FoxH1* mutants show A-P patterning defects similar to those of mouse mutants that lack Cripto (Ding et al. 1998), which functions as a coreceptor for Nodal (Sakuma et al., in prep.). Furthermore, chimeric embryos consisting of wild-type epiblast and *ALK4*$^{-/-}$ endoderm (Gu et al. 1998) fail to undergo gastrulation and show defects similar to those of type III *FoxH1* mutants (ALK4 is most likely a type I receptor for Nodal; R. Sakuma, Y. Ohnishi, C. Meno, and H. Hamada, in prep.). The mechanism by which FoxH1-dependent signals (Nodal signals) promote the anterior-directed migration of the distal visceral endoderm remains unknown. One possibility is that Nodal activity may be distributed unevenly along the future A-P axis in the region of the distal visceral endoderm, and this differential Nodal activity may generate differences in cell proliferation or in the orientation of cell division.

Formation of the anterior neural structures requires one additional step: stabilization of anterior identity by signals derived from the prechordal plate (Rhinn et al.

1998; Shawlot et al. 1999; Tam and Steiner 1999). The absence of the forebrain in type I *FoxH1*$^{-/-}$ embryos may result from the lack of the prechordal plate, which comprises axial mesoderm cell populations derived from the anterior streak. Consistent with this conclusion, epiblast-specific deletion of *FoxH1* was sufficient to give rise to type I embryos lacking the forebrain. However, impairment of AVE function can also induce a similar phenotype, as evident in chimeric *nodal*$^{-/-}$ embryos that show extensive colonization of wild-type ES cells (Varlet et al. 1997). Therefore, the absence of the forebrain in type I embryos might also result from dysfunction of the AVE. Indeed, the forebrain was also impaired in chimeric embryos in which the visceral endoderm is composed of *FoxH1*$^{-/-}$ cells.

In an accompanying paper, Hoodless et al. (2001) also report *FoxH1* mutant mice, which showed similar phenotype. However, there was a difference in the degrees of the A-P patterning defects. In their mutant mice, the prospective AVE cells can move anteriorly, although this migration may be delayed. Thus, their mutants do not show A-P patterning defects at later stages. The most likely reason for this difference is genetic background. Our mutant mice have a 129/B6 mixed background, whereas their mutant mice have a 129/CD-1 mixed background. Genetic interaction between *FoxH1* and *nodal* indicates that both FoxH1-dependent and independent pathways mediate Nodal signaling during A-P patterning. Perhaps, FAST-independent pathway can complement the absence of FoxH1 in some genetic backgrounds but not in others.

Role of FoxH1 in formation and patterning of the primitive streak

Despite extensive studies in various vertebrates, little is known of the mechanism by which formation of the primitive streak is initiated in the mouse. The observations that mice with mutations in *nodal* or in genes for its putative receptors, such as *ActRIB* (*ALK4*), *ActRIIA*, and *ActRIIB*, fail to gastrulate (Conlon 1994; Gu et al. 1998; Song et al. 1999) indicate that Nodal signals are essential for this process. However, type I and type II *FoxH1*$^{-/-}$ embryos formed the primitive streak, and posterior development was relatively normal in these animals, suggesting that FoxH1 is dispensable for streak formation. Nodal signaling is thus likely mediated by transcription factors other than FoxH1 during streak formation.

The primitive streak is initially formed in a small region near the extraembryonic-embryonic junction and elongates distally during gastrulation. The streak is patterned along the A-P axis, and cells derived from this structure are allocated to various mesodermal lineages, depending on their stage and position. For instance, cells derived from the early streak contribute predominantly to extraembryonic mesoderm, and the anterior portion of the mid-to-late primitive streak contributes to the node (Lawson et al. 1986; Tam and Beddington 1987). However, little is known of the mechanisms that underlie these patterning events.

The primitive streak of type I *FoxH1*$^{-/-}$ mutants failed to elongate and lacked the anterior portion. The truncation of the streak in these embryos is likely because of down-regulation of *nodal* expression in the posterior ectoderm. Thus, *nodal* expression was abolished in the distal-posterior epiblast and was markedly reduced in the proximal-posterior region of the epiblast in the type I mutants. These observations on *nodal* expression are consistent with the results of recent studies on the transcriptional regulation of *nodal* (Adachi et al. 1999; Norris and Robertson 1999). The expression of *nodal* in the ectoderm is controlled by at least two enhancers: The FoxH1-dependent enhancer (referred to as ASE) induces expression in the posterior ectoderm, whereas the other enhancer induces expression in the proximal epiblast. The lack of FoxH1 would therefore be expected to reduce *nodal* expression in the posterior ectoderm. In conclusion, FoxH1 is not essential for the initiation of primitive streak formation. However, it plays an important role in elongation and patterning of the streak; specifically, it maintains *nodal* expression in the anterior portion of the streak by acting as a component of a Nodal autoregulatory loop.

In other vertebrates, such as *Xenopus* and the chicken, the organizer is induced by synergistic stimulation by Wnt and Nodal-Activin–like signals (Harland and Gerhart 1997). In frog and zebrafish, a Nodal-FoxH1 pathway induces the expression of organizer-associated genes (Toyama et al. 1995; Watanabe and Whitman 1999). Furthermore, *FoxH1* mutants (*sur*) in zebrafish fail to form a gastrula organizer (Pogoda et al. 2000; Sirotkin et al. 2000). These observations and our analysis of *FoxH1* mutant mice indicate that a Nodal-FoxH1 signaling pathway plays a conserved role in organizer formation in vertebrates.

FoxH1 mediates Nodal signaling during early mouse development

FoxH1 was initially identified as a mediator of Activin signaling (Chen et al. 1996). In cultured cells or frog animal caps, FoxH1 interacts with Smad2 (or Smad3) and Smad4 and mediates signaling by TGF-β and TGF-β–related factors such as Activin and Nodal (Chen et al. 1996; Labbe et al. 1998; Weisberg et al. 1998; Zhou et al. 1998; Liu et al. 1999; Saijoh et al. 2000). However, our data now indicate that FoxH1 plays the major role in mediating Nodal signaling during early development of the mouse. *FoxH1*$^{-/-}$ mice showed various patterning defects that have been observed previously in mutant mice lacking other components of the Nodal signaling pathway. Thus, type III *FoxH1*$^{-/-}$ embryos manifested A-P patterning defects similar to those apparent in *Cripto* mutants (Ding et al. 1998). In addition, similar to *Cripto*$^{-/-}$ mice (Ding et al. 1998) and *Smad2*$^{-/-}$ chimeric mice (Tremblay et al. 2000), type II and type I *FoxH1*$^{-/-}$ embryos lacked definitive endoderm. Furthermore, the phenotype of type I *FoxH1*$^{-/-}$ embryos was similar to

that of chimeric *nodal*$^{-/-}$ embryos with a small contribution of wild-type ES cells (Varlet et al. 1997). Genetic interaction was apparent between *FoxH1* and *nodal*. Consistent with the suggestion that expression of *nodal* and *lefty2* is induced by a Nodal-FoxH1 pathway (Saijoh et al. 2000), we showed that *nodal* expression was initiated but down-regulated in type III and type I *FoxH1*$^{-/-}$ embryos and that *lefty2* expression was markedly reduced in the type III and type I mutants. The expression of *lefty1* in the visceral endoderm also may be induced by a Nodal-FoxH1 pathway, given that expression of this gene in this region was lost in type III *FoxH1*$^{-/-}$ embryos and epiblast-specific *FoxH1* mutant embryos.

Despite the similarities between the phenotypes of *FoxH1*$^{-/-}$ mutants and mutants lacking other components of the Nodal signaling pathway, substantial differences are also apparent. In *Cripto* mutants, the AVE incorrectly formed at the distal tip acts on the underlying epiblast and induces anterior neural fates in the absence of streak-derived tissues (Ding et al. 1998). In contrast, such anterior neural identity was not induced in type III *FoxH1*$^{-/-}$ mutants. This apparent discrepancy is not easily reconciled, but one possible explanation is that Cripto plays a role in addition to functioning as a coreceptor for Nodal signaling. For instance, Cripto may confer lability on signals from the visceral endoderm, as suggested previously by others (Shawlot et al. 1999). The patterning defects of *FoxH1*$^{-/-}$ mutants are less severe than are those of embryos completely lacking Nodal. Thus, the extraembryonic tissues are highly abnormal in *nodal*$^{-/-}$ mutants, whereas those tissues are relatively normal in type III *FoxH1* mutants. The phenotype of *FoxH1*$^{-/-}$ mutants is also less severe than that of *Smad2* mutants. In the absence of Smad2, embryos fail to establish P-D polarity properly, and the entire epiblast adopts an extraembryonic mesodermal fate (Waldrip et al. 1998; Heyer et al. 1999). In contrast, *FoxH1*$^{-/-}$ embryos establish P-D polarity. These phenotypic differences among *nodal*, *Smad2*, and *FoxH1* mutants suggest that Nodal signals act through both FoxH1-dependent and FoxH1-independent pathways. The actions of Nodal in A-P patterning and in patterning and elongation of the primitive streak are FoxH1 dependent, whereas those in mesoderm induction are FoxH1 independent.

Nodal signaling is also implicated in left-right patterning at a later stage of development (Schier and Shen 2000), and FoxH1 may play a role in mediating Nodal signals during this process. However, the early death of *FoxH1* mutant mice prevented us from studying the role of this transcription factor in left-right asymmetry. FoxH1 also may mediate signaling by TGF-β and related factors at later stages of development. Clarification of the roles of FoxH1 at these later stages will require conditional deletion of the gene.

Materials and methods

Generation of FoxH1-deficient mice

Genomic *FoxH1* clones were isolated from a genomic DNA library constructed from E14 ES cells. A targeting vector was constructed by subcloning the 5′ flanking region (the 3-kb *Sal*I–*Sac*II fragment), the exon 1–intron 1 region (the 2.3-kb *Sac*II–*Sma*I fragment), and the region containing the other exons and intron as well as the 3′ flanking region (the 7.8-kb *Sma*I–*Xba*I fragment) of *FoxH1* into a modified pMC1-DTpA vector (Taniguchi et al. 1997). A loxP fragment containing a *Bam*HI site was inserted between exon 1 and exon 2, and a loxP-Frt-*neo*-Frt cassette (Meyers et al. 1998) was inserted into the *Sac*II site in the 5′ flanking region. Gene targeting was performed as described (Sawai et al. 1991). The targeting vector was linearized with *Not*I before introduction into R1 ES cells by electroporation.

Of 140 G418-resistant ES clones, two clones (F94, F128) were shown to have undergone homologous recombination, as confirmed by Southern blot analysis with various probes, including a 5′ probe, a 3′ probe, and a *neo* probe. To generate a flox allele, we subjected F128 cells to electroporation with a Flp expression vector (pCAGGS-Flpe-IRES-puro; kindly provided by F. Stewart and S. Dymecki) followed by selection with puromycin (1 μg/mL; Sigma). Flp-mediated deletion was verified by PCR and Southern blot analyses. PCR was performed with the primers P1 (5′-ATCCTCGCCATGGCAACGCGA) and P2 (5′-AGTACCA CAGAATAGAGCACG); wild-type and flox alleles yield fragments of 252 and 361 bp, respectively. One clone (F128-10) that was shown to have lost *neo* was used in the present study. F94 or F128-10 cells were injected into blastocysts of C57BL/6Cr × BDF_1 mice (SLC, Shizuoka Japan), resulting in the birth of chimeric animals. Male chimeras derived from each ES cell line were bred with C57BL/6Cr females, yielding heterozygous F_1 offspring (C57BL/6Cr × 129 background). To generate a null allele (*FoxH1*$^{-}$), we crossed male chimeras with CAG-*Cre* transgenic mice (Sakai and Miyazaki 1997) to excise the loxP cassette. The resulting F_1 offspring were verified by Southern hybridization and PCR analysis with primers P1, P2, and P3 (5′-GACTGGGTGGCTGATAAGGCT); wild-type and excised alleles yield fragments of 252 and 592 bp, respectively. The F_1 heterozygotes were crossed with each other, producing *FoxH1*$^{neo/neo}$, *FoxH1*$^{flox/flox}$, and *FoxH1*$^{-/-}$ mice. For RT-PCR analysis, total RNA was prepared from E7.75 embryos with guanidine isocianate, and was reverse transcribed with oligo (dT). For detecting *FoxH1* mRNA, cDNA was subjected to PCR with the primers 5′-ATCCGTCAGGTCCAGGCAGTG-3′ and 5′-CTTGGCGAAAGCTCTGTG-3′. To detect *Hprt* mRNA as a control, the same cDNA was amplified with the primers 5′-AGCGATGATGAACCAGGTTA-3′ and 5′-GTTGAGAGAT CATCTCCACC-3′.

In situ hybridization and histology

Mouse embryos were staged on the basis of their morphology (Downs and Davies 1993). Whole-mount in situ hybridization was performed according to standard procedures (Wilkinson 1992). Wild-type and mutant embryos were processed in the same tube. Embryos were genotyped by PCR analysis of yolk sac DNA with primers P1 and P2 for the wild-type *FoxH1* allele, and with primers P1 and P3 for the *FoxH1* null allele. For histology, embryos were fixed with Bouin's solution, embedded in paraffin, and sectioned at a thickness of 8 μm. Sections were stained with hematoxylin and eosin.

Analysis of genetic interaction between FoxH1 *and* nodal

Mice that contain an *IRES-lacZ* cassette in the second exon of *nodal* have been described previously (Collignon et al. 1996). We crossed *nodal*$^{lacZ/+}$ mice with *FoxH1*$^{+/-}$ mice to obtain

double heterozygotes. Embryos obtained by intercrossing of the double heterozygotes or by crossing the double heterozygotes with *FoxH1*$^{+/-}$ animals were analyzed. The genotype of each embryo was determined by PCR. The expression of *nodal* in these embryos was monitored by staining with X-Gal.

Whole-embryo culture

E7.5 embryos were cultured for 24 h in 50-mL disposable tubes containing 2 mL of 50% Dulbecco's modified Eagle's medium supplemented with 50% rat serum, as described (Lawson et al. 1986); this volume of medium was sufficient for culturing four embryos (Sturm and Tam 1993). The tubes were filled with a mixture of 5% CO_2, 5% O_2, and 90% N_2 and were rotated at 30 rpm on a roller apparatus in an incubator.

Epiblast-specific deletion of FoxH1

The *lefty2-Cre* transgene was constructed by ligating the 5.5-kb upstream region of *lefty2* to a *Cre* cassette derived from pBS-Cre (kindly provided by H. Kondoh). Several mouse lines containing this transgene were established. To examine the specificity of *Cre* expression, we crossed each line with transgenic mice that harbor a *lacZ* gene that can be expressed only after Cre-mediated excision. Embryos were genotyped and stained with X-Gal. One transgenic line (21B) that shows epiblast-specific expression of *Cre* was used in this study. Line 21B animals were crossed with *FoxH1*$^{+/-}$ mice to obtain heterozygotes harboring the *Cre* transgene; these *FoxH1*$^{+/-}$,*lefty2-Cre* mice were mated with *FoxH1*$^{flox/flox}$ animals, and the resulting embryos were analyzed at E7.0, E8.5, and E10.5. The genotype of each embryo was determined by PCR analysis with primers P1, P2, and P3; wild-type, null, and flox *FoxH1* alleles yield fragments of 252, 592, and 361 bp, respectively. The *lefty2-Cre* transgene was detected by PCR with a pair of primers specific for *Cre* as described (Sakai and Miyazaki 1997).

Generation and analysis of chimera embryos

Chimeras were generated by blastocyst injection as described (Bradley 1987). Blastocysts were collected from intercross between *FoxH1*$^{+/-}$ animals and were injected with wild-type ES (ROSA26) cells at a ratio of 2:14 ES cells/blastocyst. Chimeric embryos were recovered at E8.5, fixed and processed for β-galactosidase staining with X-Gal (5-bromo-4-chloro-3-indoyl-β-D-galactoside). The genotype of the host blastocyst was determined retrospectively with extraembryonic tissues. Briefly, individual visceral yolk sacs were dissected from conceptuses, washed in phosphate-buffered saline (PBS), and the endoderm layer were isolated following digestion with pancreatic tyrosine as described (Hogan et al. 1994). DNA samples prepared from the endodermal layer were genotyped with respect to the *FoxH1* locus by PCR using primers P1, P2, and P3.

Acknowledgments

We thank A. Shimono and H. Kondoh for introducing us to ES cell–mediated gene targeting; E.J. Robertson for *nodal*^{lacZ} mice; J. Miyazaki for CAG-Cre mice; S. Aizawa, R. Beddington, E. De Robertis, P. Gruss, B. Hermann, B. Hogan, G. Martin, I. Matsuo, Y. Saga, H. Sasaki, and C. Wright for sharing reagents used in this study; and H. Hashiguchi, A. Hirao, S. Ohishi, K. Yamashita, M. Nishijima, Y. Masaoka, K. Miyama, and T. Tanabe for technical assistance. ROSA26 ES cells were provided by S. Aizawa with permissions from P. Soriano and E. Robertson. This work was supported by a grant from CREST (Core Research for Evolutional Science and Technology) of the Japan Science and Technology Corporation (to H.H.), grants from the Ministry of Education, Science, Sports, and Culture of Japan (to C.M., Y. Saijoh, and H.H.), and a grant from the Uehara Memorial Foundation (to Y. Saijoh).

The publication costs of this article were defrayed in part by payment of page charges. This article must therefore be hereby marked "advertisement" in accordance with 18 USC section 1734 solely to indicate this fact.

References

Acampora, D., Mazan, S., Lallemand, Y., Avantaggiato, V., Maury, M., Simeone, A., and Brulet, P. 1995. Forebrain and midbrain regions are deleted in *Otx2*$^{-/-}$ mutants due to a defective anterior neuroectoderm specification during gastrulation. *Development* **121:** 3279–3290.

Adachi, H., Saijoh, Y., Mochida, K., Ohishi, S., Hashiguchi, H., Hirao, A., and Hamada, H. 1999. Determination of left-right asymmetric expression of *nodal* by a left side-specific enhancer with sequence similarity to a *lefty-2* enhancer. *Genes & Dev.* **13:** 1589–1600.

Ang, S.-L. and Rossant, J. 1994. HNF3β is essential for node and notochord formation in mouse development. *Cell* **78:** 561–574.

Ang, S.-L., Conlon, R.A., Jin, O., and Rossant, J. 1994. Positive and negative signals from mesoderm regulate the expression of mouse *Otx2* in ectoderm explants. *Development* **120:** 2979–2989.

Ang, S.-L., Jin, O., Rhinn, M., Daigle, N., Stevenson, L., and Rossant, J. 1998. A targeted mouse *Otx2* mutation leads to severe defects in gastrulation and formation of axial mesoderm and to deletion of rostral brain. *Development* **122:** 243–252.

Beddington, R. and Robertson, E.J. 1998. Anterior patterning. *Trends Genet.* **14:** 277–284.

———. 1999. Axis development and early asymmetry in mammals. *Cell* **96:** 195–209.

Bradley, A. 1987. Production and analysis of chimeric mice. In *Teratocarcinomas and embryonic stem cells: A practical approach* (ed. E.J. Robertson), pp. 131–151. IRL Press, Oxford, UK.

Chen, X., Rubock, M.J., and Whitman, M. 1996. A transcriptional partner for Mad proteins in TGFβ signaling. *Nature* **383:** 691–696.

Chen, X., Weisberg, E., Fridmacher, V., Watanabe, M., Naco, G., and Whitman, M. 1997. Smad4 and FAST-1 in the assembly of activin-response factor. *Nature* **389:** 85–89.

Collignon, J., Varlet, I., and Robertson, E.J. 1996. Relationship between asymmetric *nodal* expression and the direction of embryonic turning. *Nature* **381:** 155–158.

Conlon, F.L., Lyons, K.M., Takaesu, N., Barth, K.S., Kispert, A.K., Herrmann, B., and Robertson, E.J. 1994. A primary requirement of *nodal* in the formation and maintenance of the primitive streak in mouse. *Development* **120:** 1919–1928.

Crossley, P.H. and Martin, G.R. 1995. The mouse *Fgf8* gene encodes a family of polypeptides and is expressed in regions that direct outgrowth and patterning in the developing embryo. *Development* **121:** 439–451.

Ding, J., Yang, L., Yan, Y.-T., Chen, A., Desai, N., Wynshaw-Boris, A., and Shen, M.M. 1998. *Cripto* is required for correct orientation of the anterior-posterior axis in the mouse embryo. *Nature* **395:** 702–707.

Downs, K.M. and Davies, T. 1993. Staging of gastrulating mouse embryos by morphological landmarks in the dissecting microscope. *Development* **118:** 1255–1266.

Gritsman, K., Zhang, J., Cheng, S., Heckscher, E., Talbot, W.S., and Schier, A.F. 1999. The EGF-CFC protein one-eyed pinhead is essential for Nodal signaling. *Cell* **97:** 121–132.

Gu, Z., Nomura, M., Simpson, B.B., Lei, H., Feijen, A., Van den Eijnden-van Raaij, J., Donahoe, P.K., and Li, E. 1998. The type III activin receptor ActRIB is required for egg cylinder organization and gastrulation in the mouse. *Genes & Dev.* **12:** 844–857.

Harland, R. and Gerhart, J. 1997. Formation and function of Spemann's organizer. *Annu. Rev. Cell. Dev. Biol.* **13:** 611–667.

Heyer, J., Escalante-Alcade, D., Lia, M., Boettinger, E., Edelman, W., Stewart, C., and Kucherlapati, R. 1999. Postgastrulation Smad2-deficient embryos show defects in embryo turning and anterior morphogenesis. *Proc. Natl. Acad. Sci.* **96:** 12595–12600.

Hogan, B., Beddington, R., Costantini, F. and Lacy, E. 1994. *Manipulating the mouse embryo: A laboratory manual.* Cold Spring Harbor Laboratory Press, Cold Spring Harbor NY.

Hoodless, P., Pye, M., Chaxaud, C., Labbe, E., Attisano, L., Rossant, J., and Wrana, J.L. 2001. *Fast* functions to specify the anterior primitive streak in the mouse. *Gene & Dev.* **15:** 1257–1271.

Kimura, C., Yoshinaga, K., Tian, E., Suzuki, M., Aizawa, S., and Matsuo, I. 2000. Visceral endoderm mediates forebrain development by suppressing posteriorizing signals. *Dev. Biol.* **225:** 304–321.

Kispert, A. and Herrmann, B.G. 1994. Immunohistochemical analysis of the Brachyury protein in wild-type IIInd mutant mouse embryos. *Dev. Biol.* **161:** 179–193.

Labbe, E., Silvestri, C., Hoodless, P.A., Wrana, J.L., and Attisano, L. 1998. Smad2 and Smad3 positively and negatively regulate TGFβ-dependent transcription through the forkhead DNA-binding protein FAST2. *Mol. Cell* **2:** 109–120.

Lawson, K.A., Meneses, J.J., and Pedersen, R.A. 1986. Cell fate and lineage in the endoderm of the presomite mouse embryo, studied with an intercellular tracer. *Dev. Biol.* **115:** 325–339.

Liu, B., Dou, C.L., Prabhu, L., and Lai, E. 1999. FAST2 is a mammalian winged-helix protein which mediates TGFβ signals. *Mol. Cell. Biol.* **19:** 424–430.

Massague, J. 1998. TGFβ signal transduction. *Annu. Rev. Biochem.* **67:** 753–791.

Matsuo, I., Kuratani, S., Kimura, C., Takeda, N., and Aizawa, S. 1995. Mouse *Otx2* functions in the formation and patterning of rostral head. *Genes & Dev.* **9:** 2646–2658.

Meno, C., Ito, Y., Saijoh, Y., Matsuda, Y., Tashiro, K., and Hamada, H. 1997. Two closely related left-right asymmetrically expressed genes, *lefty-1* and *lefty-2*: Their distinct expression domains, chromosomal linkage and direct neuralizing activity in *Xenopus* embryos. *Genes Cells* **2:** 513–524.

Meno, C., Gritmann, K., Ohfuji, Y., Heckscher, E., Ohishi, S., Mochida, K., Shimono, A., Kondoh, H., Talbot, W., Robertson, E.J., et al. 1999. Mouse Lefty2 and zebrafish Antivin are feedback inhibitors of Nodal signaling during vertebrate gastrulation. *Mol. Cell* **4:** 287–298.

Meyers, E.N., Lewandoski, M., and Martin, G.R. 1998. An *Fgf8* mutant allelic series generated by Cre- and Flp-mediated recombination. *Nature Genet.* **18:** 136–141.

Nomura, M. and Li, E. 1998. Smad2 role in mesoderm formation, left-right patterning and craniofacial development. *Nature* **393:** 786–790.

Norris, D.P. and Robertson, E.J. 1999. Node-specific and asymmetric *nodal* expression patterns are controlled by two distinct *cis*-acting regulatory elements. *Genes & Dev.* **13:** 1575–1589.

Osada, S., Saijoh, Y., Frisch, A., Yeo, C.-Y., Adachi, H., Watanabe, M., Whitman, M., Hamada, H., and Wright, C.V. 2000. Activin/Nodal responsiveness and asymmetric expression of *Xenopus nodal*-related gene converge on a FAST-regulated module in intron 1. *Development* **127:** 2503–2514.

Piccolo, S., Agius, E., Leyns, L., Bhattacharyya, S., Grunz, H., Boumeester, T., and De Robertis, E.M. 1999. The head inducer Cerberus is a multifunctional antagonist of Nodal, BMP, and Wnt signals. *Nature* **397:** 707–710.

Pogoda, H.-M., Solnica-Krezel, L. Driever, W., and Meyer, D. 2000. The zebrafish forkhead transcription factor FoxH1/Fast1 is a modulator of Nodal signaling required for organizer formation. *Curr. Biol.* **10:** 1041–1049.

Rhinn, M., Dierich, A., Shawlot, W., Behringer, R.R., Le Meur, M., and Ang, S.L. 1998. Sequential roles for Otx2 in visceral endoderm and neuroectoderm for forebrain and midbrain induction and specification. *Development* **125:** 845–856.

Saijoh, Y., Adachi, H., Mochida, K., Ohishi, S., Hirao, A., and Hamada, H. 1999. Distinct transcriptional regulatory mechanisms underlie left-right asymmetric expression of *lefty-1* and *lefty-2*. *Genes & Dev.* **13:** 259–269.

Saijoh, Y., Adachi, H., Sakuma, R., Yeo, C.-Y., Yashiro, K., Watanabe, M., Hashiguchi, H., Yashiro, K., Kawabata, M., Miyazono, K., et al. 2000. Left-right asymmetric expression of *lefty2* and *nodal* is induced by a signaling pathway that includes a transcription factor FAST2. *Mol. Cell* **5:** 35–47.

Sakai, K. and Miyazaki, J. 1997. A transgenic mouse line that retains Cre recombinase activity in mature oocytes irrespective of the *Cre* transgene transmission. *Biochem. Biophys. Res. Commun.* **237:** 318–324.

Sasaki, H. and Hogan, B.L.M. 1993. Differential expression of multiple fork head related genes during gastrulation and axial pattern formation in the mouse embryo. *Development* **118:** 47–59.

Sawai, S., Shimono, A., Hanaoka, K., and Kondoh, H. 1991. Embryonic lethality resulting from disruption of both *N-myc* alleles in mouse zygotes. *New Biologist* **9:** 861–869.

Schier, A.F. and Shen, M.M. 2000. Nodal signaling in vertebrate development. *Nature* **403:** 385–389.

Shawlot, W. and Behringer, R.R. 1995. Requirement for *Lim1* in head organizer function. *Nature* **374:** 425–430.

Shawlot, W., Wakamiya, M., Kwan, K.M., Kania, A., Jessel, T., and Behringer, R.R. 1999. Lim1 is required in both primitive streak-derived tissues and visceral endoderm for head formation in the mouse. *Development* **126:** 4925–4932.

Sirotkin, H.I., Gates, M.A., Kelley, P.D., Schier, A.F., and Talbot, W.S. 2000. *Fast1* is required for the development of dorsal axial structures in zebrafish. *Curr. Biol.* **10:** 1051–1054.

Song, J., Oh, S.P., Schrewe, H., Nomura, M., Lei, H., Okano, H., Gridley, T., and Li, E. 1999. The type II activin receptors are essential for egg cylinder growth, gastrulation, and rostral head development in mice. *Dev. Biol.* **213:** 157–169.

Sturm, K. and Tam, P.P.L. 1993. Isolation and culture of whole postimplantation embryos and germ layer derivatives. In *Guide to techniques in mouse development* (eds. P.M. Wassarman and M.L. DePamphilis), pp. 164–190. Academic Press, San Diego, CA.

Tam, P.P.L. and Beddington, R.S.P. 1987. The formation of mesodermal tissues in the mouse embryo during gastrulation and early organogenesis. *Development* **99:** 109–126.

Tam, P.P.L. and Steiner, K.A. 1999. Anterior patterning by synergistic interaction of the early gastrula organizer and the anterior germ layer tissues of the mouse embryo. *Develop-*

ment **126:** 5171–5179.

Taniguchi, M., Yuasa, S., Fujisawa, H., Naruse, I., Saga, S., Mishima, M., and Yagi, T. 1997. Disruption of *Semaphorin III/D* gene causes severe abnormality in peripheral nerve projection. *Neuron* **19:** 519–530.

Thomas, P. and Beddington, R. 1996 Anterior primitive endoderm may be responsible for patterning the anterior neural plate in the mouse embryo. *Curr. Biol.* **6:** 1487–1496.

Thomas, P.Q., Brown, A., and Beddington, R.S. 1998. *Hex*: A homeobox gene revealing peri-implantation asymmetry in the mouse embryo and an early transient marker of endothelial cell precursors. *Development* **125:** 85–94.

Toyama, R., O'Connell, M.L., Wright, C.V., Kuehn, M.R., and Dawid, I.B. 1995. Nodal induces ectopic *goosecoid* and *lim1* expression and axis duplication in zebrafish. *Development* **121:** 383–391.

Tremblay, K.D., Hoodless, P.A., Bikoff, E.K., and Robertson, E.J. 2000. Formation of the definitive endoderm in mouse is a Smad2-dependent process. *Development* **127:** 3079–3090.

Varlet, I., Collignon, J., and Robertson, E.J. 1997. *nodal* expression in the primitive endoderm is required for the specification of the anterior axis during mouse gastrulation. *Development* **124:** 1033–1044.

Waldrip, W.R., Bikoff, E.K., Hoodless, P.A., Wrana, J.L., and Robertson, E.J. 1998. Smad2 signaling in extraembryonic tissues determines anterior-posterior polarity of the early mouse embryo. *Cell* **92:** 797–808.

Watanabe, M. and Whitman, M. 1999. FAST-1 is a key maternal effector of mesoderm inducers in the early *Xenopus* embryo. *Development* **126:** 5621–5634.

Weinstein, D.C., Ruiz i Altaba, A., Chen, W.S., Hoodless, P., Prezioso, V.R., Jessel, T.M., and Darnell, J.E., Jr. 1994. The winged-helix transcription factor HNF3β is required for notochord development in the mouse embryo. *Cell* **78:** 575–588.

Weisberg, E., Winner, G.E., Chen, X., Farnsworth, C., Hogan, B.L.M., and Whitman, M. 1998. A mouse homologue of FAST-1 transduces TGFβ superfamily signals and is expressed during early embryogenesis. *Mech. Dev.* **79:** 17–27.

Whitman, M. 1998. Smads and early developmental signaling by the TGFβ superfamily. *Genes & Dev.* **12:** 2445–2462.

Wilkinson, D.G. 1992. Whole mount in situ hybridization of vertebrate embryos. In *In situ hybridization: a practical approach* (ed. D.G. Wilkinson), pp. 75–84. IRL Press, Oxford, UK.

Zhou, S., Zawel, L., Lengauer, C., Kinzler, K.W., and Vogelstein, B. 1998. Characterization of human FAST-1, a TGFβ and activin signal transducer. *Mol. Cell* **2:** 121–127.

Zhou, X., Sasaki, H., Lowe, L., Hogan, B.L., and Kuehn, M.R. 1993. Nodal is a novel TGF-β–like gene expressed in the mouse node during gastrulation. *Nature* **361:** 543–547.

Development 130, 1795-1804

doi:10.1242/dev.00408

Nodal signaling induces the midline barrier by activating *Nodal* expression in the lateral plate

Masamichi Yamamoto, Naoki Mine, Kyoko Mochida, Yasuo Sakai*, Yukio Saijoh, Chikara Meno and Hiroshi Hamada†

Developmental Genetics Group, Graduate School of Frontier Biosciences, Osaka University, and CREST, Japan Science and Technology Corporation (JST), 1-3 Yamada-oka, Suita, Osaka 565-0871, Japan

*Present address: E. Kennedy Shriver Center, Division of Developmental Neuroscience, 200 Trapelo Rd, Waltham, MA 02254, USA

†Author for correspondence (e-mail: hamada@fbs.osaka-u.ac.jp)

Accepted 13 January 2003

SUMMARY

The transcription factor Foxh1 mediates Nodal signaling. The role of Foxh1 in left-right (LR) patterning was examined with mutant mice that lack this protein in lateral plate mesoderm (LPM). The mutant mice failed to express *Nodal*, *Lefty2* and *Pitx2* on the left side during embryogenesis and exhibited right isomerism. Ectopic introduction of Nodal into right LPM, by transplantation of left LPM or by electroporation of a *Nodal* vector, induced *Nodal* expression in wild-type embryos but not in the mutant. Ectopic *Nodal* expression in right LPM also induced *Lefty1* expression in the floor plate. Nodal signaling thus initiates asymmetric *Nodal* expression in LPM and induces *Lefty1* at the midline. Monitoring of Nodal activity in wild-type and *Foxh1* mutant embryos suggested that Nodal activity travels from the node to left LPM, and from left LPM to the midline.

Key words: Foxh1, Left-right asymmetry, Midline, Nodal, Mouse

INTRODUCTION

The establishment of three axes (anteroposterior, dorsoventral and left-right) is a fundamental aspect of the development of a body plan. Substantial insight has recently been achieved at the genetic and molecular levels into the generation of left-right (LR) asymmetry in vertebrate embryos (Beddington and Robertson, 1999; Capdevila et al., 2000; Wright, 2001; Hamada et al., 2002). The establishment of LR asymmetry is thought to be achieved in four distinct steps: (1) the breaking of LR symmetry in or near the node, (2) transfer of LR-biased signals from the node to the lateral plate, (3) asymmetric expression of signaling molecules such as Nodal and Lefty on the left side of the lateral plate and (4) the induction by these signaling molecules of LR asymmetric morphogenesis of visceral organs. In addition, the midline barrier must be established to separate the two sides of a developing embryo.

Nodal and Lefty (Ebaf – Mouse Genome Informatics), both of which are members of the transforming growth factor β (TGFβ) family of proteins, play important roles in several embryonic patterning events (Schier and Shen, 2000; Brennan et al., 2001; Juan and Hamada, 2001). Lefty antagonizes Nodal signaling by acting as a feedback inhibitor (Meno et al., 1999; Cheng et al., 2000; Sakuma et al., 2002). In LR patterning, genetic evidence suggests that Nodal expressed on the left side of the lateral plate acts as a left-side determinant and induces left side-specific morphogenesis of visceral organs (Oh and Li, 1997; Yan et al., 1999; Lowe et al., 2001), whereas Lefty2 (Leftb – Mouse Genome Informatics), which is induced by Nodal in the left lateral plate, restricts the timing and the region of Nodal activity (Meno et al., 2001). Nodal and Lefty have similar roles among vertebrates from the zebrafish to mouse (Sampath et al., 1997; Rebagliati et al., 1998; Bisgrove et al., 1999; Thisse and Thisse, 1999).

Despite the recent progress in our understanding of LR patterning, many important questions remain unanswered. One such question concerns the mechanism by which symmetry is broken in the first place. Breaking of symmetry in mammals appears to involve nodal flow, the leftward flow of extra-embryonic fluid in the node generated by the vortical movement of nodal cilia (Nonaka et al., 1998). Thus, nodal flow is impaired in mutant mice in which LR patterning is randomized (Okada et al., 1999). Indeed, many of the genes whose mutation results in LR patterning defects encode proteins required for the formation or motility of cilia. Furthermore, imposition of an artificial flow was able to direct LR patterning in early mouse embryos (Nonaka et al., 2002). The mechanism by which Nodal flow achieves this effect, however, has remained unclear. It is possible that the flow transports a LR determination factor toward the left side, but the identity of such a factor is unknown.

The mechanism of signal transfer from the node to the lateral plate is also unknown. Both the identity of the signal (or signals) transported from the node to the lateral plate mesoderm (LPM) and whether the signal is transferred directly from the node to the lateral plate or is first relayed to an intermediate region such as the paraxial mesoderm remain to be determined.

Another important and related question concerns the mechanism by which the expression of *Nodal* is initiated in left LPM. Although an autoregulatory mechanism involving signaling by Nodal and the transcription factor Foxh1 (previously known as Fast2) is responsible for amplification of *Nodal* expression in left LPM (Saijoh et al., 2000; Norris et al., 2002), it is not known how *Nodal* expression is initiated. Ectopic expression of Nodal in right LPM of chick embryos was not able to induce *Nodal* expression (M. Levin, PhD thesis, Harvard University, 1996), suggesting that an unknown factor other than Nodal initiates *Nodal* expression in left LPM. Bone morphogenetic protein (BMP) signaling has been proposed to regulate *Nodal* expression negatively in the chick, and a BMP antagonist such as Caronte may initiate *Nodal* expression by inhibiting BMP activity on the left side (Rodriguez Esteban et al., 1999; Yokouchi et al., 1999). However, recent evidence has suggested that BMP signaling positively regulates *Nodal* expression by inducing an EGF-CFC factor in LPM (Schlange et al., 2001; Schlange et al., 2002; Piedra and Ros, 2002). The factor responsible for the initiation of asymmetric *Nodal* expression in LPM thus remains elusive. Finally, the midline structures serve as a barrier that prevents the diffusion of asymmetric signals (Danos and Yost, 1996; Lohr et al., 1997; Meno et al., 1998), but it is unclear how the midline barrier is established and precisely how it functions. Analysis of *Lefty1* mutant mice has shown that Lefty1, a Nodal antagonist expressed on the left side of the prospective floor plate (PFP), contributes to midline barrier function (Meno et al., 1998). However, it is unknown how *Lefty1* expression is induced at the midline.

We have now studied the role of Nodal-Foxh1 signaling in LR patterning by analyzing *Foxh1* conditional mutant mice. We have also examined Nodal function by developing transplantation and electroporation systems for use with mouse embryos and applying these systems to the *Foxh1* mutant mice. Unexpectedly, Nodal-Foxh1 signaling was shown to be able to initiate *Nodal* expression in LPM and to induce *Lefty1* expression at the midline. Our results indicate that the left-sided expression of *Nodal* in LPM is initiated by Nodal produced in the node, and that *Lefty1* expression at the midline is induced by Nodal produced in left LPM. We propose that Nodal activity travels from the node to left LPM, and from left LPM to the midline.

MATERIALS AND METHODS

LPM-specific deletion of *Foxh1*

The *Lefty2-3.0 Cre* transgene was constructed by ligating the 3.0-kb upstream region of mouse *Lefty2* to a *Cre* cassette derived from pBS-Cre (kindly provided by H. Kondoh). Several transgenic lines harboring this transgene were established. To examine the specificity of *Cre* expression, we crossed each line with Cre-reporter mice harboring a *lacZ* gene that is expressed only after Cre-mediated excision (Sakai and Miyazaki, 1997). Embryos were genotyped and stained with X-gal. One transgenic line (77b) that exhibited bilateral Cre expression in the lateral plate was used in this study. Line 77b animals were crossed with $Foxh1^{+/-}$ mice to obtain heterozygotes harboring the *Cre* transgene; these $Foxh1^{+/-}$, *Lefty2-3.0 Cre* mice were then mated with $Foxh1^{flox/flox}$ animals (Yamamoto et al., 2001), and the resulting embryos were analyzed at E8.2, E9.5 and E10.5.

In situ hybridization and histology

Mouse embryos were staged on the basis of their morphology (Downs and Davies, 1993). Whole-mount in situ hybridization was performed according to standard procedures (Wilkinson, 1992). Wild-type and mutant embryos were processed in the same tube. Embryos were genotyped by PCR analysis of yolk sac DNA.

Transplantation of LPM

Fragments of tissue (containing ~20 cells) were isolated for transplantation from the left LPM of mouse embryos at the four-somite stage. For use as recipients, mouse embryos were recovered at the two-somite stage, dissected free of decidual tissues and Reichert's membrane, and maintained in culture until manipulation. Cell clumps from donor embryos were grafted to the right LPM, left paraxial mesoderm or left LPM of the host embryos with the use of tungsten needles. The transplanted embryos were cultured for 3 hours at 37°C in 35 mm disposable dishes containing 4 ml of 50% Dulbecco's modified Eagle's medium supplemented with 50% rat serum (Lawson et al., 1986); this volume of medium was sufficient for culture of eight embryos (Sturm and Tam, 1993). A transplant remained as a mass after the culture, showed distinct density and thickness, and was easily distinguished from the host tissues.

Electroporation of a *Nodal* expression vector into LPM

The full-length cDNAs of mouse Nodal, constitutive active human ALK4 (caALK4), *lacZ* and EGFP were subcloned into the eucaryotic expression vectors pEF-BOS (Mizushima and Nagata, 1990), pcDNA3, pEF and pCX, respectively. Each plasmid was suspended in phosphate-buffered saline at a concentration of 5 mg/ml. Mouse embryos at the two-somite stage were dissected free of decidual tissues and Reichert's membrane and maintained in culture until electroporation. Electroporation was performed with a CUY21 electroporator and a pulse monitor (BTX, Tokyo). Platinum electrodes were used as an anode and a cathode and were positioned near the posterior and anterior regions of the embryo, respectively. Electric pulses were applied (14 V for 129 ms, five times) while the DNA solution (1 μl) was injected into the anterior region of left or right LPM. The electroporated embryos were cultured for 6 hours in a 50 ml disposable tube containing 4 ml of 50% Dulbecco's modified Eagle's medium supplemented with 50% rat serum (Lawrence and Struhl, 1996), a volume sufficient for the culture of eight embryos (Sturm and Tam, 1993). The tubes were rotated at 30 rpm on a roller apparatus placed in a 37°C incubator containing 5% CO_2. This culture condition is optimized for normal LR development so that left-sided *Nodal* expression in LPM is preserved in >95% of the cultured embryos. A Nodal or *caALK4* expression vector was introduced together with an EGFP expression vector by electroporation, and regions that received the vectors were confirmed by the presence of EGFP fluorescence.

RESULTS

Conditional deletion of *Foxh1* in the lateral plate

Foxh1 null mutants exhibit defects in anteroposterior patterning and in node formation (Hoodless et al., 2001; Yamamoto et al., 2001). The early mortality of the null mutants, however, has impeded characterization of the role of Foxh1 at later stages of development. We have now examined the contribution of Foxh1 to LR patterning by generating conditional mutant mice. Mutant mice harboring a flox allele of *Foxh1* ($Foxh1^{flox}$) have been described (Yamamoto et al., 2001), and, in the present study, we aimed to delete *Foxh1* in the lateral plate with the use of transgenic mice expressing the Cre recombinase in this tissue. The Cre-expressing transgene

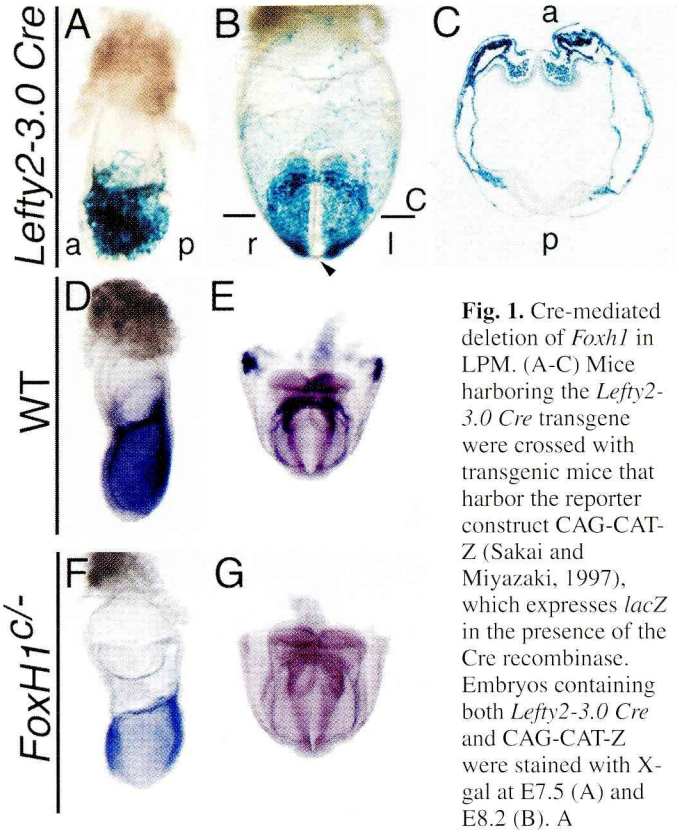

Fig. 1. Cre-mediated deletion of *Foxh1* in LPM. (A-C) Mice harboring the *Lefty2-3.0 Cre* transgene were crossed with transgenic mice that harbor the reporter construct CAG-CAT-Z (Sakai and Miyazaki, 1997), which expresses *lacZ* in the presence of the Cre recombinase. Embryos containing both *Lefty2-3.0 Cre* and CAG-CAT-Z were stained with X-gal at E7.5 (A) and E8.2 (B). A transverse section at the plane indicated in B is shown in C. At E7.5, most of the mesoderm exhibited X-gal staining whereas the ectoderm and endoderm did not. At E8.2, the anterior region of LPM, paraxial mesoderm and the heart were positive for staining, whereas the posterior portion of LPM and midline structures (arrowhead in B), including the PFP, were negative. a, anterior; p, posterior; l, left; r, right. (D-G) Whole-mount in situ hybridization analysis of *Foxh1* transcripts. Lateral views are shown for wild-type (WT) (D) and *Foxh1*$^{c/-}$ (F) embryos at E7.5 and anterior views for wild-type (E) and *Foxh1*$^{c/-}$ (G) embryos at E8.2. In the *Foxh1*$^{c/-}$ embryos, Foxh1 mRNA was not detected in the regions that were positive for X-gal staining in A-C.

Lefty2-3.0 Cre contains a 3 kb fragment of the mouse *Lefty2* promoter that directs gene expression in nascent mesoderm (Saijoh et al., 1999). One of the transgenic lines (77b) harboring this transgene was used in this study.

To confirm the expression pattern of the *Cre* transgene in 77b mice, we crossed the animals with Cre-reporter mice that express *lacZ* in response to Cre activity (Sakai and Miyazaki, 1997). Embryos harboring both *Lefty2-3.0 Cre* and the Cre-reporter *lacZ* transgene were recovered at various stages and stained for β-galactosidase activity with the substrate X-gal. Staining was first evident at embryonic day 6.75 (E6.75) in the nascent mesoderm. At E7.5, most of the embryonic region of the mesoderm exhibited staining, whereas the primitive streak, ectoderm and endoderm were negative (Fig. 1A). Mesoderm-specific staining remained evident at E8.2; however, the midline structures, including the axial mesoderm, lacked Cre activity (Fig. 1B). At this stage, the pattern of Cre activity differed between the anterior and posterior regions of the embryo (Fig. 1C). In the anterior region, X-gal staining was complete in the LPM, paraxial mesoderm, definitive endoderm and heart. In the region posterior to the node, however, Cre activity was detected only in the most lateral region of LPM. About 30 to 50% of the extra-embryonic mesoderm cells in the yolk sac and amnion were also positive for X-gal staining. At E9.5, mesoderm-derived cells in the anterior region were positive whereas the mesoderm in the posterior region was negative (data not shown). Thus, at stages later than the early somite stage, Cre activity was mostly restricted to the mesoderm of the anterior region of the embryo.

Foxh1$^{flox/flox}$ mice were then mated with *Foxh1*$^{+/-}$, *Lefty2-3.0 Cre* mice to obtain *Foxh1*$^{flox/-}$, *Lefty2-3.0 Cre* mice (for simplicity, these conditional mutant mice are referred to as *Foxh1*$^{c/-}$). Cre-mediated deletion of *Foxh1* in the *Foxh1*$^{c/-}$ embryos was confirmed by examining *Foxh1* expression. Whereas Foxh1 mRNA is abundant in all three germ layers of gastrulating wild-type embryos (Fig. 1D,E), *Foxh1* expression was absent in the mesoderm of *Foxh1*$^{c/-}$ embryos (Fig. 1F,G).

Right isomerism in *Foxh1* conditional mutant embryos

We first examined LR patterning in the *Foxh1*$^{c/-}$ embryos by analyzing the transcription of asymmetrically expressed genes such as *Nodal*, *Lefty1*, *Lefty2* and *Pitx2*. In wild-type embryos, *Nodal* is expressed in two domains at the early somite stage: the node and left LPM (Fig. 2A,B). In most *Foxh1*$^{c/-}$ embryos examined (31/37, 84%), however, left-sided expression of *Nodal* in left LPM was absent (Fig. 2C); in the remaining embryos (6/37, 16%), a low level of *Nodal* expression was detected in a small region of left LPM adjacent to the node (Fig. 2D,E), probably because a Nodal-positive loop was operative in this region before deletion of *Foxh1* was complete. *Nodal* expression in the node was maintained in all (37/37) *Foxh1*$^{c/-}$ embryos (insets in Fig. 2C,D). The expression of *Lefty2* apparent in left LPM of wild-type embryos (Fig. 2F) was abolished in all (16/16) *Foxh1*$^{c/-}$ embryos examined (Fig. 2G). The expression of *Lefty1* observed in the PFP of wild-type embryos (Fig. 2F) was also lost in all (16/16) *Foxh1*$^{c/-}$ embryos (Fig. 2G) (in some *Foxh1*$^{c/-}$ embryos, *Lefty1* expression was detected in a small region of PFP adjacent to the node at the two-somite stage but this expression disappeared at four-somite stage). This latter effect was unexpected given that *Foxh1* is preserved in midline structures including the PFP (Fig. 1B). The expression of *Lefty1* apparent in the node of wild-type embryos was maintained in the mutant embryos (inset of Fig. 2G). The asymmetric expression of *Pitx2* apparent in wild-type embryos (Fig. 2H,I,N-P) was abolished in two-thirds (29/43) of *Foxh1*$^{c/-}$ embryos at E8.2 (Fig. 2J) and in ~70% (18/26) of the mutant embryos between E9.0 and E10.5 (Fig. 2K,Q-S), whereas bilateral *Pitx2* expression in the branchial arch was maintained in all *Foxh1*$^{c/-}$ embryos. In the remaining mutant embryos, a reduced level of left-sided *Pitx2* expression was detected both in LPM at E8.2 (Fig. 2L) and in several organs and other structures, including the common atrial chamber, lung bud, sinus venosus, vitelline vein, common cardinal vein and gut, at later stages (Fig. 2M,T-V).

Foxh1$^{c/-}$ mice were carried to term but died within several days after birth. Examination of the visceral organs of *Foxh1*$^{c/-}$ neonates revealed various LR defects with right isomerism as the major phenotype (Fig. 3). Although the lungs of wild-type mice contain one and four lobes on the left and right sides, respectively (Fig. 3A), the lungs of most (40/45, 89%) of the

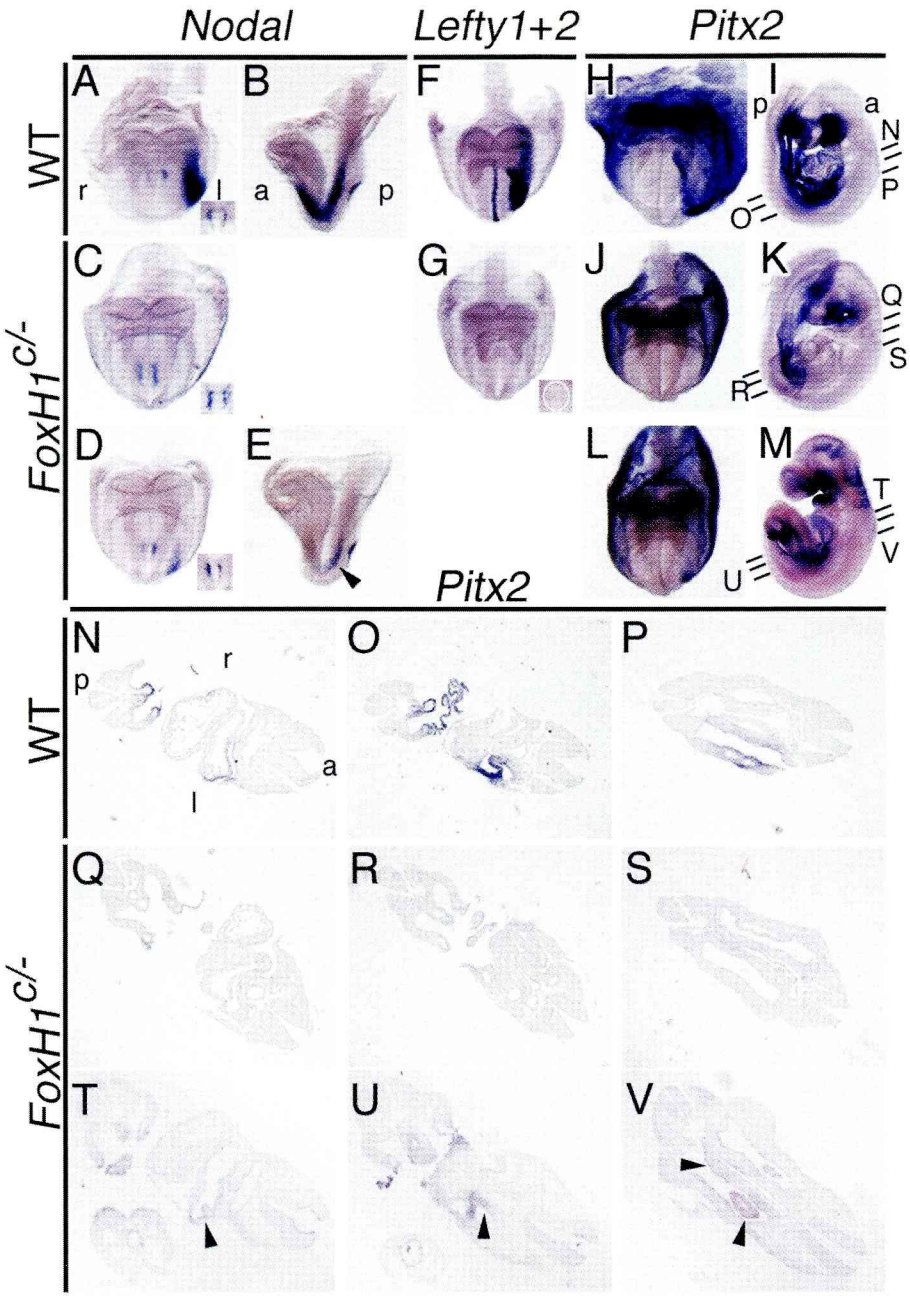

Fig. 2. Aberrant expression of *Nodal*, *Lefty1*, *Lefty2* and *Pitx2* in *Foxh1*$^{c/-}$ embryos. The expression of *Nodal* (A-E), *Lefty1* plus *Lefty2* (F,G) and *Pitx2* (H-V) in wild-type (WT) and *Foxh1*$^{c/-}$ embryos was examined by whole-mount in situ hybridization. Embryos shown in A-H,J,L are at E8.2, whereas the others are at E9.5. Transverse sections at the planes indicated in I, K and M are shown in N-P, Q-S and T-V, respectively. All E8.2 embryos are anterior views, with the exception that left lateral views are shown for B and E. The insets in A, C, D and G show the node in posterior view of the embryos. The white line in the inset of G indicates the location of the node. Most *Foxh1*$^{c/-}$ embryos fail to exhibit left-sided gene expression, although some retain *Nodal* expression in a small region of left LPM adjacent to the node (arrowhead in E) and a low level of left-sided *Pitx2* expression in various organs (arrowheads in T-V). a, anterior; p, posterior; l, left; r, right.

Foxh1$^{c/-}$ mice examined manifested right isomerism, having four lobes on both sides (Fig. 3B). A small proportion (3/45, 7%) of *Foxh1*$^{c/-}$ mice exhibited partial right isomerism, having two or three lobes on the left side and four lobes on the right side. Abnormal positioning of the great arteries, either arterial transposition (9/41, 22%) (Fig. 3P,S) or double-outlet right ventricle (31/41, 76%) (Fig. 3Q,T), was also frequently observed in *Foxh1*$^{c/-}$ mice. The position of the heart apex was reversed (toward the right; 15/41, 37%) (Fig. 3K), ambiguous (in the middle; 7/41, 17%) (Fig. 3J) or normal (toward the left; 19/41, 46%) in *Foxh1*$^{c/-}$ mice. Additional heart malformations, including ventricular septal defect without valve defects (VSD; 25/41, 61%) (Fig. 3T), atrial septal defect without valve defects (ASD; 30/41, 73%) (Fig. 3Q) and endocardial cushion defect (common atrioventricular valve plus ASD and VSD; 10/41, 24%) (data not shown), were also observed. The external morphology of the atrium was also affected, showing right isomerism (11/43, 26%) or LR inversion (13/43, 30%). The azygos vein, which is normally located on the left side (Fig. 3C), was reversed (13/43, 30%) (Fig. 3D), bilateral (14/43, 33%) or normal (16/43, 37%) in *Foxh1*$^{c/-}$ mice. Additional defects included hypoplasia of the spleen (21/40, 53%) (Fig. 3F) and the presence of the stomach on the right side (8/43, 19%) (Fig. 3H). The relative positions of left and right renal veins were reversed (14/44, 32%) or the two veins were located at the same level (12/44, 27%) (Fig. 3M). The portal vein, which normally passes dorsally to the duodenum, passed ventrally to the duodenum in *Foxh1*$^{c/-}$ mice (12/38, 32%) (Fig. 3N). These morphological defects resemble those observed with cryptic mutant mice (Yan et al., 1999), and are, in general, consistent with a lack of Nodal, the left-side determinant, in left LPM. The phenotype of *Foxh1*$^{c/-}$ mice also resemble that of the zebrafish mutant lacking Foxh1 (Chen et al., 1997; Bisgrove, 2000).

Induction of *Nodal* expression in the lateral plate requires Foxh1

Asymmetric *Nodal* expression in left LPM begins in a region adjacent to the node and expands along the anteroposterior axis. It is currently unknown how *Nodal* expression is initiated in left LPM; it may involve a positive autoregulatory mechanism, but direct evidence is lacking. To study the mechanism of *Nodal* induction, we developed a system for cell transplantation into LPM. A piece of tissue was dissected from the left LPM of a donor embryo at the four-somite stage (*Nodal* is already expressed in the entire left LPM at this stage) and was

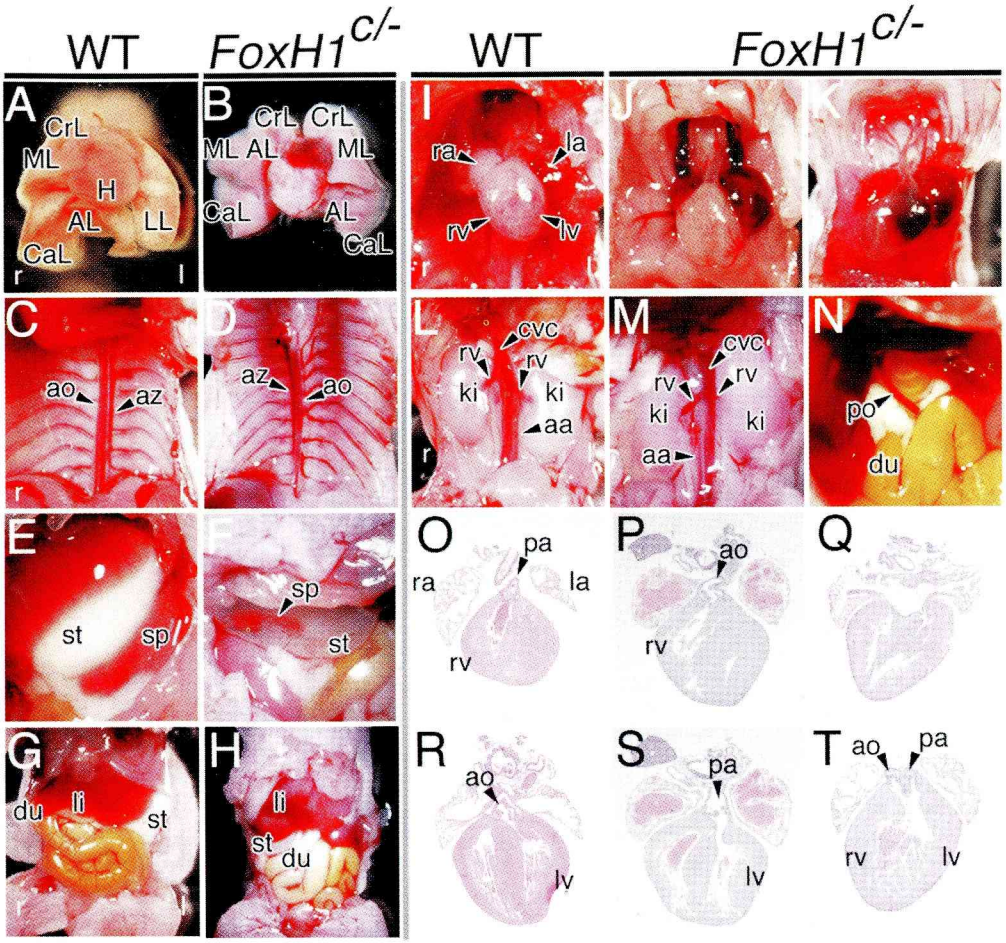

Fig. 3. LR defects in the visceral organs of *Foxh1*$^{c/-}$ mice. Visceral organs and heart sections of wild-type (WT) and *Foxh1*$^{c/-}$ neonates are shown. Genotype is indicated at the top of each column. (A,B) Lobation of the lung. In the wild-type mouse (A), the left and right lungs have one and four lobes, respectively. In most *Foxh1*$^{c/-}$ mice (B), both left and right lungs have four lobes. AL, accessory lobe; CaL, caudal lobe; CrL, cranial lobe; ML, medial lobe; H, heart; LL, left lobe. (C,D) The azygos vein (az) of the wild-type mouse is located on the left side (C). In most *Foxh1*$^{c/-}$ mice, the azygos vein is located on the right side (D) or both sides. ao, aorta. (E,F) Hypoplasia of the spleen (sp) in the *Foxh1*$^{c/-}$ mouse (F). st, stomach. (G,H) Visceral organs including the stomach are reversed in many *Foxh1*$^{c/-}$ mice (H). du, duodenum; li, liver. (I-K) The heart apex is located on the left side of the wild-type mouse (I), but is either in the middle (J) or on the right side (K) of *Foxh1*$^{c/-}$ mice. la, left atrium; lv, left ventricle; ra, right atrium; rv, right ventricle. (L,M) The right renal vein is located anteriorly to the left renal vein in the wild-type mouse (L). In *Foxh1*$^{c/-}$ mice, the relative positions of left and right renal veins are reversed or the two veins are located at the same level (M). cvc, caudal vena cava; ki, kidney; rv, renal vein; aa, abdominal aorta. (N) Aberrant positioning of the portal vein (po) in the *Foxh1*$^{c/-}$ mouse. (O-T) Frontal sections of the heart. In most *Foxh1*$^{c/-}$ mice, the heart manifests severe malformations, including transposition of the great arteries (P,S) and double outlet of the right ventricle (Q,T). pa, pulmonary artery.

transplanted into the right LPM of a recipient embryo at the two-somite stage (*Nodal* expression is initiated but not expanded in left LPM at this stage) (Fig. 4A). When the *Foxh1*$^{c/-}$ embryo was used as a recipient, a donor LPM was transplanted into the left LPM. We then examined whether the transplanted left LPM was able to induce *Nodal* expression in the right LPM of the recipient embryo. Indeed, the transplanted left LPM induced *Nodal* expression in the recipient right LPM (3/3). Thus, *Nodal* expression in right LPM was not only apparent in the region adjacent to the transplanted left LPM but expanded along the anteroposterior axis (Fig. 4B). In most instances, the induced *Nodal* expression did not extend over the entire area of right LPM, possibly as a result of its premature termination by Lefty2 present in the transplanted left LPM (exogenous *Nodal* expression alone in the right LPM induced *Nodal* expression throughout the entire region of right LPM, as shown below). By contrast, transplantation of right LPM into the right LPM of a host embryo failed to induce *Nodal* expression in the recipient right LPM (3/3, data not shown).

We performed similar transplantation experiments with *Foxh1*$^{c/-}$ embryos. Left LPM obtained from a wild-type embryo was thus transplanted to the anterior region of left LPM of *Foxh1*$^{c/-}$ embryos. Such manipulation failed to induce *Nodal* expression in the left LPM of the host embryo (10/10) (Fig. 4F,G), indicating that the induction of *Nodal* expression in LPM requires Foxh1.

Initiation by Nodal of *Nodal* expression in the lateral plate

Our results suggested that an unknown factor derived from left LPM is able to initiate *Nodal* expression in right LPM. An obvious candidate for this factor was Nodal itself present in left LPM. To test this possibility, we introduced a *Nodal* expression vector and an EGFP expression vector into embryos at the early somite stage by electroporation. The embryos were first examined for fluorescence to locate the cells that received the vectors (Fig. 5A), and were subjected to in situ hybridization. Introduction of the *Nodal* vector into right LPM of wild-type embryos resulted in the induction of endogenous *Nodal* expression (Fig. 5B,C). *Nodal* expression induced in right LPM expanded along the anteroposterior axis and extended throughout the entire region of the right LPM (25/25) (arrowheads in Fig. 5C). Electroporation of an EGFP expression vector alone into right LPM of wild-type embryos did not give rise to such expanded *Nodal* expression except in one (1/20) case. By contrast, introduction of the

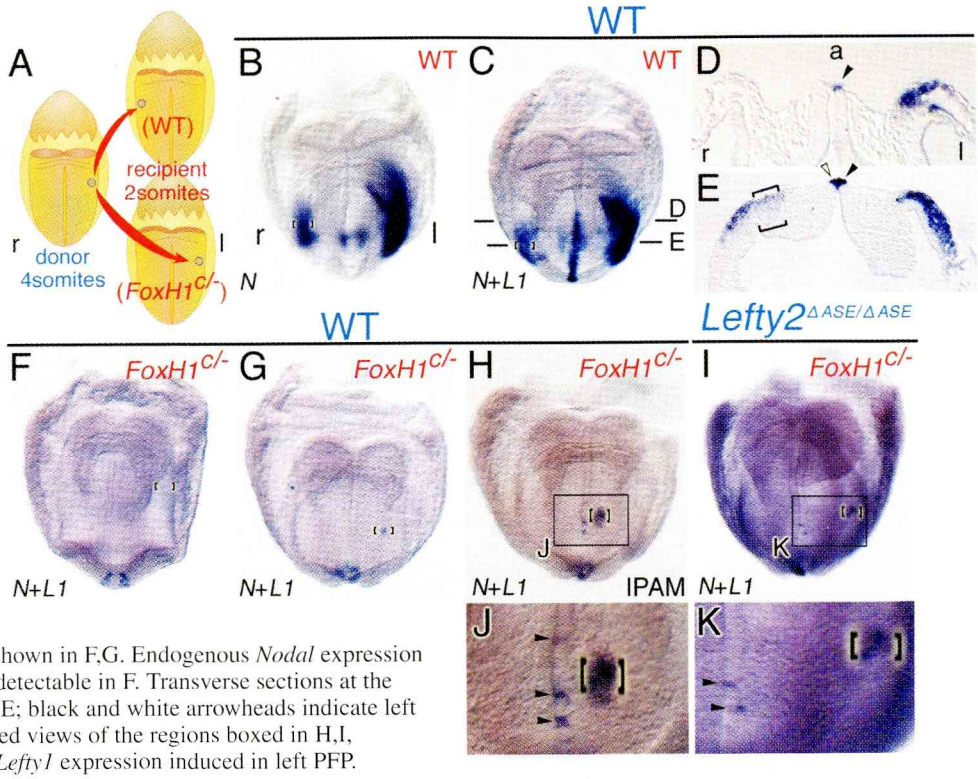

Fig. 4. Induction of *Nodal* and *Lefty1* by transplanted left LPM.
(A) Schematic representation of the tissue transplantation system.
(B-K) Expression of *Nodal* (*N* in B) and *Nodal* plus *Lefty1* (*N+L1* in C-K) was examined by whole-mount in situ hybridization 3 hours after the indicated type of transplantation. Genotypes of the recipients and donors are shown in red and blue, respectively, at the top of each panel. Donor tissue was derived from left LPM of the indicated embryos. The transplant sites in the host embryos are indicated by square brackets (B,C,E-K). Donor tissue was transplanted to the anterior region of LPM in host embryos, with the exception of the embryo shown in H,J, which received the transplant in the paraxial mesoderm (IPAM). Two representative *Foxh1*$^{c/-}$ embryos that received a transplant derived from the left LPM of wild-type (WT) embryo are shown in F,G. Endogenous *Nodal* expression in the transplant is detectable in G but undetectable in F. Transverse sections at the planes indicated in C are shown in D and E; black and white arrowheads indicate left and right PFP, respectively. (J,K) Magnified views of the regions boxed in H,I, respectively. Arrowheads in J,K indicate *Lefty1* expression induced in left PFP.

Nodal expression vector into the left or right LPM of *Foxh1*$^{c/-}$ embryos failed to induce *Nodal* (Fig. 5F). Thus, ectopic Nodal is able to induce *Nodal* expression in right LPM, but this induction requires the presence of Foxh1 in LPM.

Induction of *Lefty1* expression at the midline by Nodal produced in the left lateral plate

Lefty1 plays an essential role as the midline barrier (Meno et al., 1998). In *Foxh1*$^{c/-}$ embryos, *Lefty1* expression in the floor plate was lost (Fig. 2G) despite the fact that *Foxh1* was not deleted in the PFP (Fig. 1B). Furthermore, both *Nodal* (Fig. 2C) and *Lefty1* (Fig. 2G) expression was preserved in the node. These observations suggested that *Lefty1* expression in the floor plate might be induced by Nodal produced in left LPM. Consistent with this notion, previous studies (Chen and Schier, 2001; Meno et al., 2001) have suggested that Nodal is able to act over a long distance. We therefore tested this possibility with the use of our transplantation and electroporation systems.

Lefty1 is expressed in the PFP on the left side of wild-type embryos (Meno et al., 1997). A piece of left LPM transplanted to the right LPM of wild-type embryos was able to induce not only *Nodal* in the right LPM but also *Lefty1* in the right PFP (3/3) (Fig. 4C). Thus, *Lefty1* expression in the PFP became bilateral only at the levels where *Nodal* was ectopically expressed in right LPM (Fig. 4D,E), supporting the idea that Nodal produced in LPM induces *Lefty1* expression in the PFP. Similar experiments were performed with *Foxh1*$^{c/-}$ embryos, which retain *Foxh1* in the PFP but lack *Lefty1* expression in this region. Transplantation of left LPM from wild-type embryos to the left LPM of *Foxh1*$^{c/-}$ embryos did not result in the induction of *Lefty1* expression in the PFP (0/10) (Fig. 4F,G). However, transplantation of the left LPM to the paraxial mesoderm, a site closer to the PFP, resulted in the induction of *Lefty1* (3/4) (Fig. 4H,J). Furthermore, left LPM obtained from *Lefty2*$^{\Delta ASE/\Delta ASE}$ embryos, in which Nodal activity is increased as a result of the lack of Lefty2 (Meno et al., 2001), induced *Lefty1* expression in the PFP even when transplanted to the left LPM of *Foxh1*$^{c/-}$ embryos (4/5) (Fig. 4I,K).

Introduction of the *Nodal* expression vector into the right LPM of wild-type embryos also induced *Lefty1* expression in the PFP (18/25) (Fig. 5D,E). The spatial level of ectopic *Lefty1* expression along the anteroposterior axis of the PFP corresponded to that of ectopic *Nodal* expression in the right LPM. In most instances, *Lefty1* expression was bilateral throughout the entire PFP, while ectopically induced *Nodal* expression extended throughout the entire region of right LPM (Fig. 5E). Furthermore, introduction of the *Nodal* expression vector into the left LPM of *Foxh1*$^{c/-}$ embryos also induced *Lefty1* expression in the PFP (6/8) (Fig. 5G,H), making it unlikely that *Lefty1* was induced by secondary signals produced by the Nodal-Foxh1 pathway. In these various experiments, *Nodal* expression was never induced in the PFP either by the transplanted left LPM or by introduction of the *Nodal* expression vector into right LPM (Fig. 4B, Fig. 5B).

These results suggest that *Lefty1* expression in PFP is directly induced by Nodal produced in LPM but do not exclude an alternative possibility that it is induced by secondary factor(s) produced in LPM by a Nodal-dependent yet Foxh1-independent pathway. To test the latter possibility, we examined the effects of constitutive active ALK4 (caALK4). As expected, caALK4 was able to induce *Nodal* in the right LPM of the wild-type embryos (5/5) (Fig. 5I). However, introduction of the caALK4 expression vector into the left LPM of *Foxh1*$^{c/-}$ embryos failed to induce *Lefty1* expression in the PFP (11/11) (Fig. 5J). These results now demonstrate

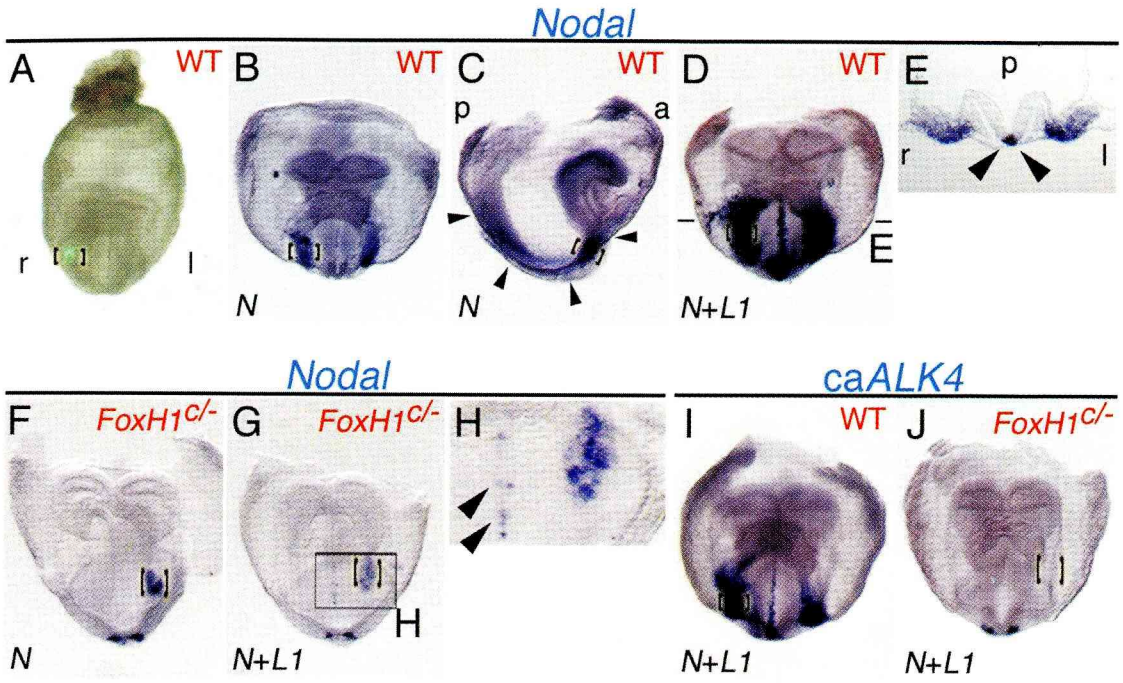

Fig. 5. Induction of *Nodal* and *Lefty1* by a *Nodal* expression vector. Expression vectors for Nodal plus EGFP (enhanced green fluorescent protein) (A-H) or those for caALK4 plus EGFP (I,J) were introduced by electroporation into the anterior region of right LPM of a wild-type (WT) embryo (A-E,I) or into the anterior region of left LPM of a *Foxh1*$^{c/-}$ embryo (F-H,J). Electroporated expression vectors are shown in blue, while genotypes of the recipient embryos are shown in red. Six hours after electroporation, expression of *Nodal* (*N* in B,C,F) or *Nodal* plus *Lefty1* (*N+L1* in D,E,G-J) was examined by whole-mount in situ hybridization. Electroporated regions, which were confirmed by the presence of EGFP fluorescence (A), are indicated by the square brackets. Anterior views are shown in (A,B,D,F-J), whereas right lateral view is shown in C. A transverse section at the plane indicated in D is shown in E. A magnified view of the boxed region indicated in G is shown in H. Arrowheads indicate *Nodal* expression in the right LPM (C) and *Lefty1* expression (E,H) induced by the *Nodal* expression vector.

that Nodal activity produced in LPM directly induces *Lefty1* expression in PFP.

Nodal activity travels from left LPM to the PFP

Our results suggest that Nodal ectopically produced in LPM may diffuse over the relatively long distance to the PFP and there induce *Lefty1* expression. We next examined whether the PFP indeed receives Nodal signals from left LPM with the use of a *lacZ* transgene whose expression is strictly dependent on Nodal signaling. This transgene, *(n2)7-lacZ*, contains seven tandem repeats of a Foxh1 binding site and its expression is induced by the Nodal-Foxh1 pathway (Saijoh et al., 2000; Sakuma et al., 2002). X-gal staining of transgenic embryos harboring *(n2)7-lacZ* revealed *lacZ* expression in the PFP predominantly on the left side as well as in left LPM (Fig. 6A,B). Given that *Nodal* is not expressed in the PFP, Nodal produced elsewhere (either in left LPM or the node) must have traveled to the PFP. By contrast, X-gal staining of *Foxh1*$^{c/-}$

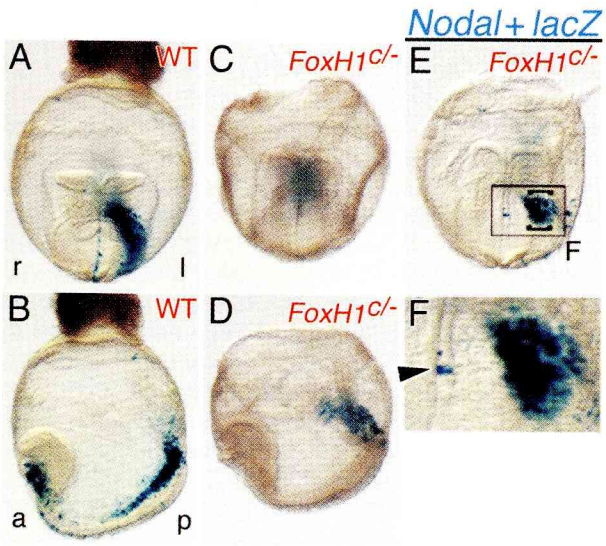

Fig. 6. Monitoring of Nodal activity in mouse embryos with a Nodal-responsive transgene. Expression of the Nodal-responsive transgene *(n2)7-lacZ* was examined in wild-type (WT) (A,B) and *Foxh1*$^{c/-}$ (C,D) embryos. In the *Foxh1*$^{c/-}$ embryo, X-gal staining in left LPM and PFP is lost whereas that in the allantois remains (C,D). Expression vectors for *Nodal*, *EGFP* and *lacZ* were also introduced into the left LPM of a *Foxh1*$^{c/-}$ embryo harboring the *(n2)7-lacZ* transgene and, 6 hours later, the embryo was stained with X-gal (E,F). The region that received the expression vectors is apparent from the EGFP fluorescence and X-gal staining in left LPM (indicated by the square brackets). X-gal-positive region in left LPM failed to expand due to the absence of Foxh1 in LPM. A magnified view of the boxed region indicated in E is shown in F. The arrowhead in F indicates X-gal staining in the PFP that was induced by Nodal. Anterior views are shown in A,C,E, whereas left lateral views are shown in B,D.

embryos harboring the *(n2)7-lacZ* transgene revealed that *lacZ* expression was abolished in the left LPM and PFP, although staining in the allantois and at the base of the allantois remained (10/10) (Fig. 6C,D). Similarly, another Nodal-responsive *lacZ* reporter gene, *Lefty2 ASE-lacZ*, that contains the asymmetric enhancer (ASE) of *Lefty2* also gave rise to X-gal staining in the PFP in addition to the left LPM of wild-type embryos (Saijoh et al., 1999); however, this transgene was inactive in the PFP of *Foxh1*$^{c/-}$ embryos (11/11) (data not shown). *Foxh1*$^{c/-}$ mice lack *Nodal* expression in left LPM but that in the node is unaffected (Fig. 2C-E). Furthermore, they retain *Foxh1* in the PFP (Fig. 1B,C). Finally, introduction of the *Nodal* expression vector into left LPM of *Foxh1*$^{c/-}$ embryos harboring the *(n2)7-lacZ* (7/7) (Fig. 6E,F) or *Lefty2 ASE-lacZ* (2/2) (data not shown) transgene resulted in expression of *lacZ* in the PFP. Together, these results suggest that Nodal synthesized in left LPM, not Nodal produced in the node, travels to the PFP and activates the Nodal-responsive *lacZ* transgenes.

DISCUSSION

Our results indicate that Nodal signaling induces the initiation and expansion of asymmetric *Nodal* expression in LPM as well as initiates *Lefty1* expression at the midline. They also provide insight into the mechanism by which asymmetric signals are transferred between structures during LR patterning. On the basis of the present and previous data, we propose the following scenario (Fig. 7). First, Nodal produced in the node travels from the node to left LPM, where it initiates asymmetric *Nodal* expression (alternatively, Nodal may act on left LPM indirectly). Second, Nodal protein produced in the small region of left LPM adjacent to the node diffuses along the anteroposterior axis, resulting in the expansion of *Nodal* expression within left LPM. Third, Nodal produced in left LPM also travels toward the midline, where it induces the expression of *Lefty1*, the product of which is crucial for midline barrier function. Thus, according to this scenario, two critical events of LR patterning, asymmetric expression of *Nodal* in LPM and *Lefty1* expression at the midline, are established by diffusion of Nodal followed by Nodal signaling. Foxh1 is required at least for the induction of *Nodal* in left LPM.

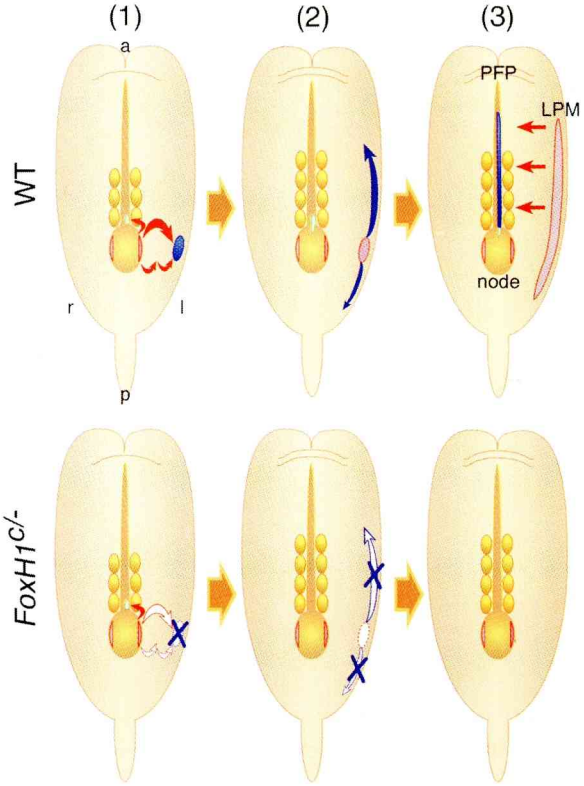

Fig. 7. Model for the movement of Nodal activity during LR patterning. Three events involving Nodal are illustrated. Blue represents the domains that receive Nodal signals and in which Foxh1 is active. Red indicates the domains in which *Nodal* is expressed. Arrows indicate the directions of signal transfer. In the wild-type embryo (top row), Nodal produced in the node travels to left LPM and initiates *Nodal* expression in a small region adjacent to the node (1). At this stage, *Lefty1* is expressed in a small region of PFP adjacent to the node (green). *Lefty1* expression in this domain may be induced by Nodal produced in the node. (2) Nodal produced in the small region of left LPM diffuses along the anteroposterior axis in left LPM and thereby induces the expansion of *Nodal* expression. (3) Nodal produced in left LPM travels to the entire PFP region along the AP axis (blue), where it induces *Lefty1* expression. In *Foxh1*$^{c/-}$ embryos (bottom row), Nodal produced in the node is unable to initiate *Nodal* expression in left LPM because of the absence of Foxh1 in LPM. As a result, *Nodal* expression in left LPM and *Lefty1* expression in PFP are absent.

Nodal produced in the node may initiate *Nodal* expression in left LPM

How is asymmetric *Nodal* expression initiated in LPM? Our transplantation and electroporation experiments with mouse embryos revealed that ectopically expressed Nodal induced endogenous *Nodal* expression in right LPM. Nodal is thus able to initiate *Nodal* expression in LPM, suggesting the possibility that Nodal produced in the node travels to left LPM and there initiates *Nodal* expression. Previous observations are also consistent with this idea. First, *Nodal* expression in the node (the perinodal region) begins earlier than that in left LPM (Collignon et al., 1996). Second, asymmetric *Nodal* expression in left LPM begins in a small region adjacent to the node. Third, asymmetric *Nodal* expression in left LPM is controlled by a left side-specific enhancer designated ASE (Adachi et al., 1999; Norris et al., 2002; Norris and Robertson, 1999), the most critical elements of which are two Foxh1-binding sites (Adachi et al., 1999; Saijoh et al., 2000). These Foxh1-binding sites act as a Nodal-responsive element, suggesting that *Nodal* is regulated by a positive autoregulatory mechanism. Fourth, components required to mediate Nodal signaling (such as ALK4, ActRII, Cryptic, Smads and Foxh1) are all expressed in LPM on both sides. Fifth, in various mutant mice with LR defects, asymmetric *Nodal* expression in LPM is always absent when *Nodal* expression in the node is abolished (Lowe et al., 2001; Saijoh et al., 2003). Finally, the role of Nodal produced in the node has been more convincingly demonstrated by Brennan et al. (Brennan et al., 2002). Thus, mutant mice specifically lacking Nodal in the node fail to initiate asymmetric *Nodal* expression in LPM, revealing that *Nodal* expression in the node is indeed essential for asymmetric gene expression in left LPM (Brennan et al., 2002). Nonetheless, it

remains to be seen whether Nodal coming from the node directly acts on left LPM to initiate *Nodal* expression. Other factors such as GDF1 may also be involved in signal transfer from the node to LPM, as GDF1 is expressed in the node and the lack of GDF1 results in the loss asymmetric *Nodal* expression in LPM (Rankin et al., 2000).

Foxh1 is expressed bilaterally in LPM at the early somite stage when *Nodal* is expressed in left LPM (Saijoh et al., 2000), and may function in both the initiation and amplification of *Nodal* expression in left LPM. Although it is difficult to distinguish these two processes experimentally, Foxh1 is implicated in both by our observation that the transplantation of left LPM to *Foxh1*$^{c/-}$ embryos failed to induce *Nodal* expression even in the cells adjacent to the transplant site.

If Nodal synthesized in the node acts on left LPM, what might prevent Nodal activity from traveling toward the right side? Nodal flow, the leftward flow of extra-embryonic fluid in the node generated by vortical movement of the cilia (Nonaka et al., 1998), may transport Nodal preferentially toward the left side. Indeed, the role of nodal flow in LR patterning was recently demonstrated by testing the effects of artificial fluid flow in embryos (Nonaka et al., 2002). Although ciliated cells can be found in the organizer region of non-mammals, including the chick (Essner et al., 2002), fluid flow may not be generated there. Coincidentally, ectopic introduction of Nodal into the right LPM failed to induce endogenous *Nodal* expression (M. Levin, PhD thesis, Harvard University, 1996). Thus, a different mechanism may operate in the chick for the transfer of asymmetric signals from the node to left LPM.

Nodal protein produced in left LPM induces *Lefty1* expression at the midline

The midline structures, including the floor plate and notochord, are required to separate the two sides of the embryo (Danos and Yost, 1996), with Lefty1 being critical for midline barrier function (Meno et al., 1998). Our observations now suggest that *Lefty1* expression in the PFP is induced by Nodal produced in left LPM. First, *Foxh1*$^{c/-}$ embryos, which lack *Nodal* expression in left LPM but retain it in the node, fail to express *Lefty1* in the PFP, suggesting that Nodal produced in the node is unable to induce *Lefty1* expression in the PFP. Second, and more importantly, transplanted left LPM or a *Nodal* expression vector introduced into right LPM induced *Lefty1* expression in the PFP of wild-type embryos but not in that of *Foxh1*$^{c/-}$ embryos. Third, introduction of constitutively active ALK4 into the left LPM of *Foxh1*$^{c/-}$ embryos was unable to induce *Lefty1* expression in PFP, excluding a possibility that an unknown factor produced by a Nodal-dependent yet Foxh1-independent pathway induces *Lefty1*. The idea that *Lefty1* expression is induced by LPM-derived Nodal is also consistent with previous observations. Comparison of the kinetics of *Lefty1* and *Nodal* expression thus revealed that *Lefty1* expression in the PFP is preceded by *Nodal* expression in left LPM (C. M. et al., unpublished data). Furthermore, *Nodal* is not expressed in the PFP. Finally, mutant mice lacking a component of the Nodal signaling pathway, such as the co-receptor Cryptic, fail to express *Lefty1* in the PFP as well as *Nodal* in left LPM (Yan et al., 1999).

After Nodal produced in left LPM travels to the midline and induces *Lefty1* expression, Lefty1, which is also able to travel over long distances (Sakuma et al., 2002), might then be expected to diffuse toward the LPM. Lefty1 that reaches the right LPM would render it incompetent for Nodal signaling and prevent *Nodal* expression there. Lefty1 that reaches left LPM, together with Lefty2 produced in the left LPM, may contribute to rapid repression of *Nodal* expression in this region. Midline barrier function is abolished in mutant mice that lack Lefty1, resulting in bilateral expression of *Nodal* and *Lefty2* (Meno et al., 1998). We previously suggested that, in the absence of Lefty1, an unknown left-side determinant travels across the midline and reaches the right LPM, where it induces the expression of *Nodal* and *Lefty2* (Meno et al., 1998). Our data now suggest that this left-side determinant is most likely Nodal.

Although our results indicate that *Lefty1* expression at the midline is induced by Nodal produced in left LPM, it is not clear whether this expression depends on Foxh1. *Lefty1* expression is lost even in the least severe type of *Foxh1*-null mutant (Yamamoto et al., 2001). However, this effect may be secondary to misspecification of the midline cells in the absence of Foxh1 (Hoodless et al., 2001; Yamamoto et al., 2001). Our previous analysis of the transcriptional regulatory elements of *Lefty1* by transgenic approaches (Saijoh et al., 1999) suggested that the 1.2 kb region immediately upstream of *Lefty1* is sufficient for its asymmetric expression in the PFP. Although this 1.2 kb region contains three potential binding sites for Foxh1, mutation of these sequences did not impair the PFP-specific expression of *Lefty1* (Y.S. and H.H., unpublished). Nodal signaling that induces *Lefty1* in the PFP therefore may not involve Foxh1.

Overall, our results obtained with *Foxh1*$^{c/-}$ mice suggest that Nodal activity travels from the node to left LPM, and from left LPM to the midline. A direct test of this conclusion will require visualization of the behavior of Nodal in mouse embryos.

We thank anonymous reviewers for many constructive comments; Yayoi Ikawa and Sachiko Ohishi for technical assistance; Jun Takeuchi and Toshihiko Ogura for introducing us to electroporation; Kohei Miyazono for a caALK4 expression vector; and Masaru Okabe for pCX-EGFP. This work was supported by a grant from CREST (Core Research for Evolutional Science and Technology) of the Japan Science and Technology Corporation (to H.H.), and by a grant from the Ministry of Education, Science, Sports, and Culture of Japan (to C.M.). M.Y. is a recipient of a fellowship from the Japan Society for the Promotion of Science for Japanese Junior Scientists.

REFERENCES

Adachi, H., Saijoh, Y., Mochida, K., Ohishi, S., Hashiguchi, H., Hirao, A. and Hamada, H. (1999). Determination of left/right asymmetric expression of *nodal* by a left side-specific enhancer with sequence similarity to a *lefty-2* enhancer. *Genes Dev.* **13**, 1589-1600.

Beddington, R. S. and Robertson, E. J. (1999). Axis development and early asymmetry in mammals. *Cell* **96**, 195-209.

Bisgrove, B. W., Essner, J. J. and Yost, H. J. (1999). Regulation of midline development by antagonism of lefty and nodal signaling. *Development* **126**, 3253-3262.

Bisgrove, B. W., Essner, J. L. and Yost, H. J. (2000). Multiple pathways in the midline regulate concordant brain, heart and gut left-right asymmetry. *Development* **127**, 3567-3579.

Brennan, J., Lu, C. C., Norris, D. P., Rodriguez, T. A., Beddington, R. S. and Robertson, E. J. (2001). Nodal signalling in the epiblast patterns the early mouse embryo. *Nature* **411**, 965-969.

Brennan, J., Norris, D. P. and Robertson, E. J. (2002). Nodal activity in the node governs left-right asymmetry in the mouse. *Genes Dev.* **16**, 2339-2344.

Capdevila, J., Vogan, K. J., Tabin, C. J. and Izpisua Belmonte, J. C. (2000). Mechanisms of left-right determination in vertebrates. *Cell* **101**, 9-21.

Chen, J. N., van Eeden, F. J., Warren, K. S., Chin, A., Nusslein-Volhard, C., Haffter, P. and Fishman, M. C. (1997). Left-right pattern of cardiac BMP4 may drive asymmetry of the heart in zebrafish. *Development* **124**, 4373-4382.

Chen, Y. and Schier, A. F. (2001). The zebrafish Nodal signal *Squint* functions as a morphogen. *Nature* **411**, 607-610.

Cheng, A. M., Thisse, B., Thisse, C. and Wright, C. V. (2000). The lefty-related factor Xatv acts as a feedback inhibitor of nodal signaling in mesoderm induction and L-R axis development in Xenopus. *Development* **127**, 1049-1061.

Collignon, J., Varlet, I. and Robertson, E. J. (1996). Relationship between asymmetric *nodal* expression and the direction of embryonic turning. *Nature* **381**, 155-158.

Danos, M. C. and Yost, H. J. (1996). Role of notochord in specification of cardiac left-right orientation in zebrafish and Xenopus. *Dev. Biol.* **177**, 96-103.

Downs, K. M. and Davies, T. (1993). Staging of gastrulating mouse embryos by morphological landmarks in the dissecting microscope. *Development* **118**, 1255-1266.

Essner, J. J., Vogan, K. J., Wagner, M. K., Tabin, C. J., Yost, H. J. and Brueckner, M. (2002). Conserved function for embryonic node cilia. *Nature* **418**, 37-38.

Hamada, H., Meno, C., Watanabe, D. and Saijoh, Y. (2002). Establishment of vertebrate left-right asymmetry. *Nat. Rev. Genet.* **3**, 103-113.

Hoodless, P. A., Pye, M., Chazaud, C., Labbe, E., Attisano, L., Rossant, J. and Wrana, J. L. (2001). FoxH1 (Fast) functions to specify the anterior primitive streak in the mouse. *Genes Dev.* **15**, 1257-1271.

Juan, H. and Hamada, H. (2001). Roles of *nodal-lefty* regulatory loops in embryonic patterning of vertebrates. *Genes Cells* **6**, 923-930.

Lawrence, P. A. and Struhl, G. (1996). Morphogens, compartments, and pattern: lessons from Drosophila? *Cell* **85**, 951-961.

Lawson, K. A., Meneses, J. J. and Pedersen, R. A. (1986). Cell fate and cell lineage in the endoderm of the presomite mouse embryo, studied with an intracellular tracer. *Dev. Biol.* **115**, 325-339.

Lohr, J. L., Danos, M. C. and Yost, H. J. (1997). Left-right asymmetry of a nodal-related gene is regulated by dorsoanterior midline structures during *Xenopus* development. *Development* **124**, 1465-1472.

Lowe, L. A., Yamada, S. and Kuehn, M. R. (2001). Genetic dissection of *nodal* function in patterning the mouse embryo. *Development* **128**, 1831-1843.

Meno, C., Gritmann, K., Ohfuji, Y., Heckscher, E., Ohishi, S., Mochida, K., Shimono, A., Kondoh, H., Talbot, W., Robertson, E. J., Schier, A. F. and Hamada, H. (1999). Mouse Lefty2 and zebrafish Antivin are feedback inhibitors of Nodal signaling during vertebrate gastrulation. *Mol. Cell* **4**, 287-298.

Meno, C., Ito, Y., Saijoh, Y., Matsuda, Y., Tashiro, K., Kuhara, S. and Hamada, H. (1997). Two closely-related left-right asymmetrically expressed genes, *lefty-1* and *lefty-2*: their distinct expression domains, chromosomal linkage and direct neuralizing activity in Xenopus embryos. *Genes Cells* **2**, 513-524.

Meno, C., Shimono, A., Saijoh, Y., Yashiro, K., Mochida, K., Ohishi, S., Noji, S., Kondoh, H. and Hamada, H. (1998). *lefty-1* is required for left-right determination as a regulator of *lefty-2* and *nodal*. *Cell* **94**, 287-297.

Meno, C., Takeuchi, J., Sakuma, R., Koshiba-Takeuchi, K., Ohishi, S., Saijoh, Y., Miyazaki, J., ten Dijke, P., Ogura, T. and Hamada, H. (2001). Diffusion of Nodal signaling activity in the absence of the feedback inhibitor Lefty2. *Dev. Cell* **1**, 127-138.

Mizushima, S. and Nagata, S. (1990). pEF-BOS, a powerful mammalian expression vector. *Nucleic Acids Res.* **18**, 5322.

Nonaka, S., Tanaka, Y., Okada, Y., Takeda, S., Harada, A., Kanai, Y., Kido, M. and Hirokawa, N. (1998). Randomization of left-right asymmetry due to loss of nodal cilia generating leftward flow of extraembryonic fluid in mice lacking KIF3B motor protein. *Cell* **95**, 829-837.

Nonaka, S., Shiratori, H., Saijoh, Y. and Hamada, H. (2002). Determination of left-right patterning of the mouse embryo by artificial nodal flow. *Nature* **418**, 96-99.

Norris, D. P., Brennan, J., Bikoff, E. K. and Robertson, E. J. (2002). The Foxh1-dependent autoregulatory enhancer controls the level of Nodal signals in the mouse embryo. *Development* **129**, 3455-3468.

Norris, D. P. and Robertson, E. J. (1999). Asymmetric and node-specific *nodal* expression patterns are controlled by two distinct cis-acting regulatory elements. *Genes Dev.* **13**, 1575-1588.

Oh, S. P. and Li, E. (1997). The signaling pathway mediated by the type II activin receptor controls axial patterning and lateral asymmetry in the mouse. *Genes Dev.* **11**, 1812-1826.

Okada, Y., Nonaka, S., Tanaka, Y., Saijoh, Y., Hamada, H. and Hirokawa, N. (1999). Abnormal nodal flow precedes situs inversus in *iv* and *inv* mice. *Mol. Cell* **4**, 459-468.

Piedra, M. E. and Ros, M. A. (2002). *BMP* signaling positively regulates *Nodal* expression during left right specification in the chick embryo. *Development* **129**, 3431-3440.

Rankin, C. T., Bunton, T. B., Lawler, A. M. and Lee, S.-J. (2000). Regulation of left-right patterning in mice by growth/differentiation factor-1. *Nat. Genet.* **24**, 262-265.

Rebagliati, M. R., Toyama, R., Fricke, C., Haffter, P. and Dawid, I. B. (1998). Zebrafish nodal-related genes are implicated in axial patterning and establishing left-right asymmetry. *Dev. Biol.* **199**, 261-272.

Rodriguez Esteban, C., Capdevila, J., Economides, A. N., Pascual, J., Ortiz, A. and Izpisua Belmonte, J. C. (1999). The novel Cer-like protein Caronte mediates the establishment of embryonic left-right asymmetry. *Nature* **401**, 243-251.

Saijoh, Y., Adachi, H., Mochida, K., Ohishi, S., Hirao, A. and Hamada, H. (1999). Distinct transcriptional regulatory mechanisms underlie left-right asymmetric expression of *lefty-1* and *lefty-2*. *Genes Dev.* **13**, 259-269.

Saijoh, Y., Adachi, H., Sakuma, R., Yeo, C. Y., Yashiro, K., Watanabe, M., Hashiguchi, H., Mochida, K., Ohishi, S., Kawabata, M., Miyazono, K., Whitman, M. and Hamada, H. (2000). Left-right asymmetric expression of *lefty2* and *nodal* is induced by a signaling pathway that includes the transcription factor FAST2. *Mol. Cell* **5**, 35-47.

Saijoh, Y., Oki, M., Ohishi, S. and Hamada, H. (2003). Left-right patterning of the mouse lateral plate requires Nodal produced in the node. *Dev. Biol.* (in press).

Sakai, K. and Miyazaki, J. (1997). A transgenic mouse line that retains *Cre* recombinase activity in mature oocytes irrespective of the *cre* transgene transmission. *Biochem. Biophys. Res. Commun.* **237**, 318-324.

Sakuma, R., Ohnishi Yi, Y., Meno, C., Fujii, H., Juan, H., Takeuchi, J., Ogura, T., Li, E., Miyazono, K. and Hamada, H. (2002). Inhibition of Nodal signalling by Lefty mediated through interaction with common receptors and efficient diffusion. *Genes Cells* **7**, 401-412.

Sampath, K., Cheng, A. M., Frisch, A. and Wright, C. V. (1997). Functional differences among Xenopus nodal-related genes in left-right axis determination. *Development* **124**, 3293-3302.

Schier, A. F. and Shen, M. M. (2000). Nodal signalling in vertebrate development. *Nature* **403**, 385-389.

Schlange, T., Schnipkoweit, I., Andree, B., Ebert, A., Zile, M. H., Arnold, H. H. and Brand, T. (2001). Chick CFC controls *Lefty1* expression in the embryonic midline and *nodal* expression in the lateral plate. *Dev. Biol.* **234**, 376-389.

Schlange, T., Arnold, H. H. and Brand, T. (2002). BMP2 is a positive regulator of Nodal signaling during left-right axis formation in the chicken embryo. *Development* **129**, 3421-3429.

Sturm, K. and Tam, P. P. (1993). Isolation and culture of whole postimplantation embryos and germ layer derivatives. *Methods Enzymol.* **225**, 164-190.

Thisse, C. and Thisse, B. (1999). Antivin, a novel and divergent member of the TGFβ superfamily, negatively regulates mesoderm induction. *Development* **126**, 229-240.

Wilkinson, D. G. (1992). Whole mount in situ hybridization of vertebrate embryos. In *In Situ Hybridization: A Practical Approach* (ed. D. G. Wilkinson), pp. 75-84. Oxford: IRL Press.

Wright, C. V. (2001). Mechanisms of left-right asymmetry: what's right and what's left? *Dev. Cell* **1**, 179-186.

Yamamoto, M., Meno, C., Sakai, Y., Shiratori, H., Mochida, K., Ikawa, Y., Saijoh, Y. and Hamada, H. (2001). The transcription factor FoxH1 (FAST) mediates Nodal signaling during anterior-posterior patterning and node formation in the mouse. *Genes Dev.* **15**, 1242-1256.

Yan, Y. T., Gritsman, K., Ding, J., Burdine, R. D., Corrales, J. D., Price, S. M., Talbot, W. S., Schier, A. F. and Shen, M. M. (1999). Conserved requirement for EGF-CFC genes in vertebrate left-right axis formation. *Genes Dev.* **13**, 2527-2537.

Yokouchi, Y., Vogan, K. J., Pearse, R. V., II and Tabin, C. J. (1999). Antagonistic signaling by Caronte, a novel Cerberus-related gene, establishes left-right asymmetric gene expression. *Cell* **98**, 573-583.